



**Department of Earth & Environmental Sciences**

# **Wyoming Field Guide**



**DEES Graduate Student Field Trip**

**June-July 2011**

Department of Earth and Environmental Sciences, Columbia University 2011

Prepared and edited by Natalia Zakharova and Jason Jweda

Front page photo: Elephant Rock, WY

# Table of Content:

|   |            |
|---|------------|
| <b>PREFACE .....</b>  | <b>4</b>   |
| <b>TRIP ITINERARY .....</b>   | <b>5</b>   |
| <b>INTRODUCTION TO WYOMING .....</b>                                      | <b>7</b>   |
| <b>REGIONAL GEOLOGY .....</b>   | <b>8</b>   |
| OVERVIEW OF OROGENIC EVENTS IN THE ROCKIES .....                          | 8          |
| STRATIGRAPHIC EXPRESSION OF ANCESTRAL ROCKIES AND LARAMIDE UPLIFTS .....  | 10         |
| LARAMIDE DEFORMATION.....   | 13         |
| WYOMING-IDAHO THRUST BELT.....  | 17         |
| TETON MOUNTAIN UPLIFT HISTORY .....                                       | 20         |
| BASIN AND RANGE NORMAL FAULTING.....                                      | 22         |
| GEOLOGIC HISTORY OF BOULDER AREA, COLORADO.....                           | 25         |
| <b>YELLOWSTONE HOTSPOT .....</b>  | <b>30</b>  |
| VOLCANISM ASSOCIATED WITH YELLOWSTONE HOTSPOT (SNAKE RIVER PLAIN).....    | 30         |
| VOLCANISM OF YELLOWSTONE NATIONAL PARK .....                              | 32         |
| THERMAL AND MECHANICAL EFFECTS OF THE YELLOWSTONE HOTSPOT.....            | 36         |
| SEISMICITY AND TOMOGRAPHY OF THE YELLOWSTONE REGION .....                 | 39         |
| INSAR MEASUREMENTS OF YELLOWSTONE CALDERA.....                            | 42         |
| HYDROLOGY OF YELLOWSTONE NATIONAL PARK .....                              | 44         |
| MICROBIOLOGY OF THE YELLOWSTONE HOT-SPRINGS .....                         | 47         |
| <b>OTHER GEOLOGIC FEATURES OF INTEREST.....</b>                           | <b>52</b>  |
| STILLWATER COMPLEX .....  | 52         |
| HEART MOUNTAIN LANDSLIDE .....  | 55         |
| GLACIAL DEPOSITS.....   | 58         |
| <b>DETAILED ITINERARY AND DESCRIPTION OF VISITED SITES.....</b>           | <b>60</b>  |
| DAY 1 (JUNE 25, 2011) – BOULDER, CO .....                                 | 60         |
| DAY 2 (JUNE 26, 2011) – WYOMING STRATIGRAPHY .....                        | 63         |
| DAY 3 (JUNE 27, 2011) – WYOMING-IDAHO THRUST BELT.....                    | 68         |
| DAY 4 (JUNE 28, 2011) – TETON NATIONAL PARK.....                          | 75         |
| DAY 5 (JUNE 29, 2011) – YELLOWSTONE HOTSPOT VOLCANICS.....                | 79         |
| DAY 6 (JUNE 30, 2011) – YELLOWSTONE NATIONAL PARK .....                   | 86         |
| DAY 7 (JULY 1, 2011) – STILLWATER MINE AND HEART MOUNTAIN DETACHMENT..... | 90         |
| DAY 8 (JULY 2, 2011) – HEART MOUNTAIN DETACHMENT.....                     | 93         |
| DAY 9 (JULY 3, 2011) – SHELL FALLS AND RED GULCH DINOSAUR TRACKS .....    | 102        |
| <b>ACKNOWLEDGMENTS.....</b>   | <b>105</b> |
| <b>APPENDIX 1. TRIP PARTICIPANTS.....</b>                                 | <b>106</b> |
| <b>APPENDIX 2. TRIP COSTS.....</b>  | <b>107</b> |

## Preface

This guide is based on the Columbia University graduate student field trip to Wyoming in summer 2011, made possible by the Stroke Memorial Fund at Lamont-Doherty Earth Observatory. In nine days, the group visited four states and covered well over 1000 miles of Rocky Mountain geology. The group started in Denver, Colorado and traversed parts of Wyoming, Idaho, and Montana. Of the many geological attractions of Wyoming, Yellowstone National Park located over Yellowstone Hotspot is possibly the crown jewel. Yellowstone is the largest volcanic system in North America and the associated geothermal activity produces the largest active geysers in the world, as well as thousands of other fascinating geothermal features. In addition to Yellowstone National Park, Wyoming also offers opportunities to observe characteristic geologic features of the Western United States: manifestation of Sevier and Laramide orogenies, Basin and Range extensional features, regional stratigraphic units, dinosaur tracks, catastrophic landslides, effects of Yellowstone hotspot volcanism, and much more. This guide describes a number of convenient locations to observe and explore these features, and provides background information about major geologic processes that shaped this region over time.

## Trip Itinerary

### **DAY 1 - June 25<sup>th</sup>, 2011:**

- Flew to Denver, CO
- Explored Flagstaff Mountain by NCAR in Boulder, CO
- Stayed in Greeley, CO

### **DAY 2 - June 26<sup>th</sup>, 2011:**

- Drove to Lander, WY, observing the stratigraphic section (Archean-Jurassic) and effects of Laramide thrust faulting
- Drove to Pinedale, WY examining glacial deposits
- Camped at Pinedale camp

### **DAY 3 - June 27<sup>th</sup>, 2011:**

- Studied glacial deposits at Fremont Lake
- Drove through the Wyoming-Idaho thrust belt, stopping to examine structures
- Drove to Grand Teton National Park, examining the uplift history of the Teton Range
- Camped at the University of Michigan's Camp Davis

### **DAY 4 - June 28<sup>h</sup>, 2011:**

- Rode the Teton Village tram to the top of Rendezvous Mountain, hiked the snowy Tetons while observing Paleozoic stratigraphy
- Drove through the Snake River Canyon, observing Sevier-aged thrust faulting and active fault scarps
- Camped in Alpine, WY

### **DAY 5 - June 29<sup>th</sup>, 2011:**

- Drove north along Grand Valley into Swan Valley and then across the Snake River Plain to Yellowstone National Park, examining pyroclastic formations associated with Yellowstone volcanism
- Stopped to study the 1959 Hebgen Lake Earthquake catastrophic landslide and fault scarp
- Arrived in Yellowstone and observed Old Faithful geyser
- Camped in Grant Village campground in the park

### **DAY 6 – June 30<sup>th</sup>, 2011:**

- Explored the Yellowstone Park: mud volcanoes and fumaroles, the Grand Canyon of the Yellowstone, Obsidian Cliffs, Mammoth Hot Springs (travertine terraces), and Tower Falls (columnar basalt)
- Drove northeast, stopping to look at Heart Mountain Detachment (the largest terrestrial landslide on Earth)
- Camped at Hunter Peak campground

**DAY 7 – July 1<sup>st</sup>, 2011:**

- Drove over Beartooth Pass, stopping to examine Heart Mountain Detachment at Pilot Peak Overlook
- Explored the Stillwater mine and layered intrusion (Nye, MT)
- Camped at Hunter Peak campground

**DAY 8 – July 2<sup>nd</sup>, 2011:**

- Drove through Sunlight Basin observing the Heart Mountain Detachment, Cathedral Cliffs, White Mountains, and Dead Indian Pass
- Drove to the Bighorn Mountains
- Camped at Shell Canyon campground

**DAY 9 – July 3<sup>rd</sup>, 2011:**

- Drove out of the Bighorn Mountains stopping at Shell Falls and Red Gulch Dinosaur Track site
- Traveled through Wind River Canyon stopping for lunch at Boysen Reservoir
- Stayed in Greeley

**DAY 10 – July 4<sup>th</sup>, 2011:**

- Returned rental vehicles
- Flew back to New York

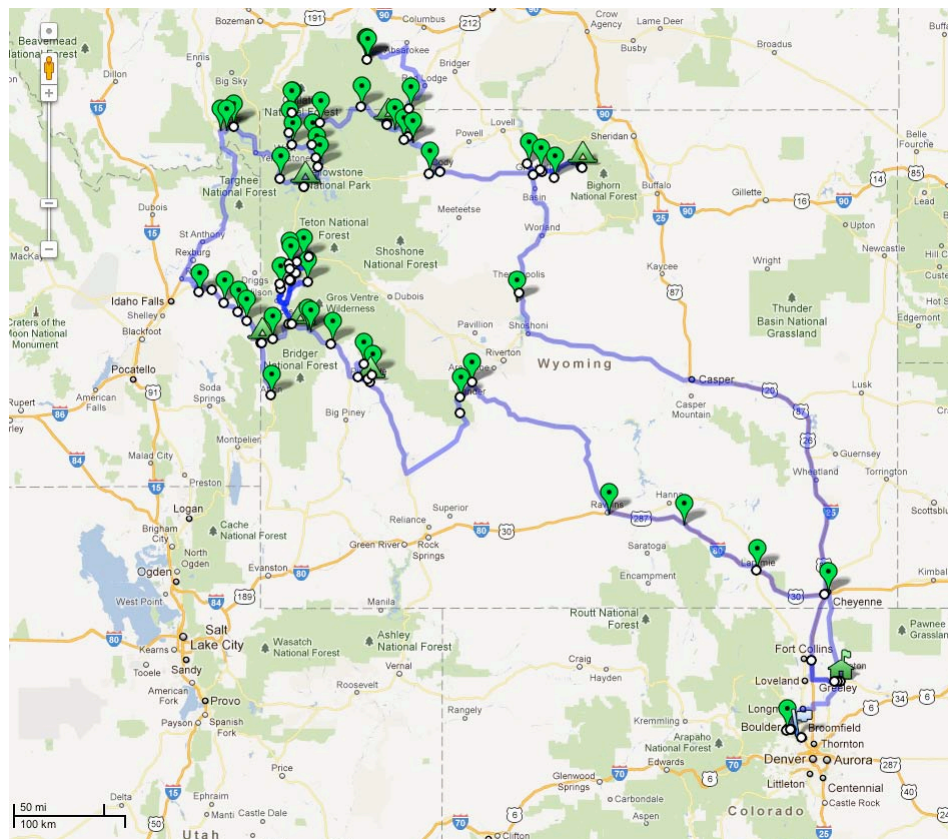


Figure 1. Schematic route of the trip and major visited sites.

## Introduction to Wyoming

*Contributed by Alexander Lloyd*

Though some might consider the “Cowboy State” to be pretty average in most regards, the state of Wyoming has many distinctions. The state borders are defined by lines of latitude (41°N and 45°N) and longitude (104°3'W and 111°3'W). These unseen boundaries make Wyoming one of only three U.S. states to have all of its borders delineated by straight latitudinal and longitudinal lines rather than natural landmarks. The longitudinal boundary is not a round number because when the state boundaries were first defined, the U.S. Geologic Survey measured longitude from the Washington Meridian, which ran through the old Naval Observatory, so the state border was initially defined as 27°W and 34°W. Though Wyoming is the tenth largest state by area, it is the least populated state in the entire U.S. With this combination of area and people, one would expect that a population density of 5.4 (per square mile) should qualify Wyoming as the least densely populated state as well, but Alaska owns this category with a population density of 1.2 (per square mile).

The physiographic provinces of the Great Plains and Rocky Mountains split Wyoming. Our field trip focused primarily on the geology of the Rocky Mountains, as the High Plains region of Wyoming is not very distinctive. On the route outlined in this field trip guide, it is possible to get a glimpse of all of the mountain ranges in Wyoming, except the Black Hills in the northeast region of the state. In the northwest are the Absaroka, Owl Creek, Gros Ventre, Wind River and Teton ranges. In the north central are the Bighorn Mountains; and in the southern region the Laramie, Snowy, and Sierra Madre ranges. The Continental Divide runs north-south through the state and splits around the Great Divide Basin. The eastern portion of the state is part of the Missouri River Basin and drains into the Gulf of Mexico. The western half is split between the Snake River, which drains into the Columbia River, and the Green River, which drains into the Colorado River. The U.S. government owns about 48% of the land in the state, which puts Wyoming in the top six states for both percentage and total area of government-owned land. Most of the land owned by the federal government is administered by the Bureau of Land Management and the U.S. Forest Service. The national parks visited on this trip (Yellowstone and Grand Teton) account for approximately 8% of this land (which is high compared to most states).

The climate of any area in Wyoming is defined by its latitude, altitude, and local topography. Since there is a wide range of physiographic characteristics, a statewide summary of the climate is difficult to describe. While on the topic of climate, Wyomingites distinguish themselves as emitting more carbon dioxide per person than any other U.S. state or any other country because coal supplies nearly all of the state’s electrical power.

The economy of Wyoming today is mainly driven by tourism and mineral extraction industries, while agriculture has declined in importance since the founding of the state. The largest airport in the state is the Jackson Hole Airport, which serves the Grand Teton and Yellowstone crowds. This is a testament to the importance of tourism in the state as the city of Jackson has 1/6th the population of Cheyenne, the capital and most populous city. Wyoming distinguishes itself by being the top producer of coal in the U.S. Wyoming also has the largest known reserves of trona in the world. Trona is a primary source of sodium carbonate and is utilized for both industrial applications (e.g. glass manufacturing) and domestic uses (water softener). The trona near Green River, Wyoming lies in layered evaporite deposits from 800 to 1,600 feet (240 to 490 m) below ground, where the trona was deposited in lacustrine conditions during the Paleogene period.

(Source: [www.wikipedia.org](http://www.wikipedia.org))

## Regional Geology

### Overview of Orogenic Events in the Rockies

*Contributed by Claire Bendersky*

North America has had not one, but two Rocky Mountain belts. The Ancestral and modern Rockies were formed by subduction in nearly the same location. Both Rocky Mountain belts call into question how a mountain belt can be uplifted in the interior of a stable craton at a far distance from contemporary subduction. Here we consider the tectonic environment at the time of the Ancestral Rocky uplift.

In the Devonian, North America was part of a larger continental block, called Laurentia (Figure 2). Oceanic crust was subducted under the western and eastern margins of Laurentia while sea level was on average >120m higher than it is today (Haq & Schutter, 2008).

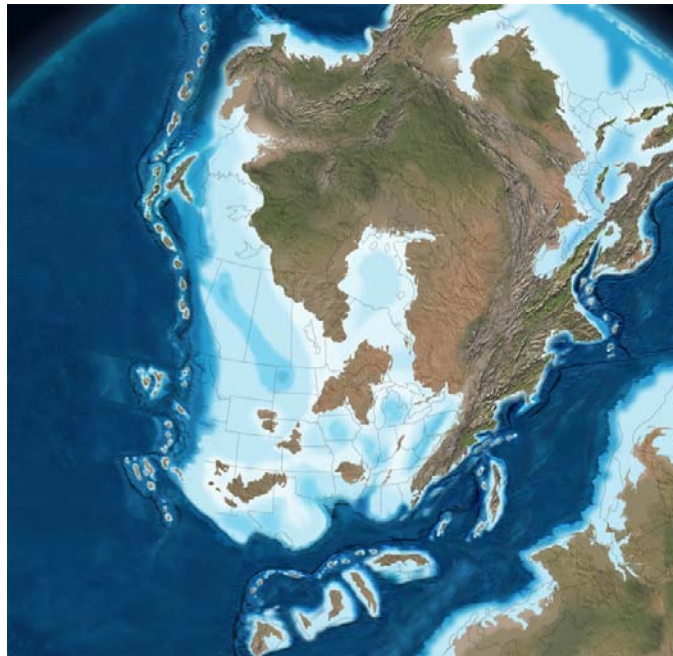


Figure 2. North America in the Late Devonian (360 Ma), from <http://cpgeosystems.com/>

Subduction under the western margin of Laurentia occurred in two discrete events between the Devonian and Triassic. The Antler Orogeny spanned ~25 million years of the Devonian-Mississippian. About 110 million years later, the Sonoma Orogeny spanned another ~25 million years over the Permian-Triassic (Dickinson, 2004). Evidence of these ancient subduction events is found as allochthons in the Great Basin.

Oceanic crust was subducted under the eastern margin of Laurentia as Gondwana, the southern supercontinent, approached. Laurentia and Gondwana converged during Carboniferous time to form the Appalachian Mountains as part of the Alleghenian Orogeny (Figure 3).

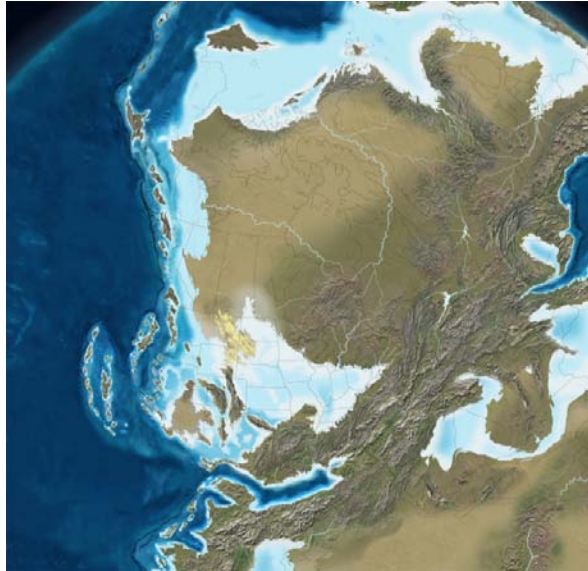


Figure 3. North America in the Late Pennsylvanian (300 Ma), modified after <http://cpgeosystems.com/>

The cause of Ancestral Rockies uplift remains unclear as the mountains and much of the evidence for them have eroded. Pieces of the Ancestral Rockies are mostly found as sediments preserved in basins. The North American craton has been overprinted with younger tectonic events, including the Laramide and Sevier Orogenies. During the rise of the Ancestral Rockies the western margin was passive, tectonically quiescent between the Antler and Sonoma Orogenies. The eastern margin was actively deforming, creating the Appalachian Mountains equal in magnitude to the Himalayas. Yet this was far from the Ancestral Rockies. Thus we find multiple theories explaining the rise of the Ancestral Rockies.

In the Pennsylvanian, part of Gondwana converged with *southeastern* Laurentia during the Ouachita Orogeny. This marks the final stage in the assembly of Pangea and resulted in the modern day Ouachita Mountains in Oklahoma and Arkansas. The stresses involved could have propagated northwest and reactivated a pre-existing zone of weakness to form the Ancestral Rockies (Kluth and Coney, 1981; Burchfiel et al., 1992).

The period of quiescence along the western-margin of Laurentia may have been a transform boundary, similar to modern day California. This force along with north-south compression, brought on by pre-existing zones of weakness in the craton, combined to raise the Ancestral Rockies (Sevenson and Baars, 1986; Johnson et al, 1991).

Contrary to the notion of a passive western margin, igneous rocks in northeastern Mexico indicate contemporary subduction under *southwestern* Laurentia. Compression from subduction may have propagated northeastward uplifting the Ancestral Rockies. (Handschy et al, 1987; McKee et al, 1988; Ye et al., 1996)

These ideas strive to explain the enigmatic occurrence of an ancient intra-cratonic mountain belt. The site of the modern Rockies is equally curious. They formed during the Laramide Orogeny as the Farallon plate was subducted at a shallow angle under the west coast of North America. The low angle slab moved the focus of melting and mountain building much farther inland than the normal 200 to 300 miles associated with arc volcanism observed at subduction zones today (USGS online document, 2004). Read further along in the guidebook to learn about the modern Rocky Mountains.

## References:

- Burchfiel, B.C., D.S. Cowan, and G.A. Davis (1992), "Tectonic overview of the Cordilleran orogen in the western United States", in B.C. Burchfiel, P.W. Lipman, and M.L. Zoback, eds., *The Cordilleran orogene*, GSA v. G-3.
- Dickinson (2004) "Evolution of the North American Cordillera". *Annu. Rev. Earth Planet. Sci.* 2004. 32:13–45
- Handschy, J.W., G.R. Keller, and K.J. Smith, (1987). "The Ouachita system in northern Mexico", *Tectonics*, v. 6, no. 3, p. 323-330.
- Haq, B. U.; Schutter, SR (2008). "A Chronology of Paleozoic Sea-Level Changes". *Science* 322 (5898): 64–68.
- Johnson, S.Y., M.A. Chan, and E.A. Konopka, (1991). Pennsylvanian and early Permian paleogeography of the Uinta-Piceance basin region, northwestern Colorado and northeastern Utah, USGS Bulletin 1787.
- Kluth, C.F. and P.J. Coney, (1981). "Plate tectonics of the Ancestral Rocky Mountains". *Geology*, v. 9, p. 10-15.
- McKee, J.W., N.W. Jones, and T.H. Anderson, (1988). Las Dalias basin: A record of late Paleozoic arc volcanism in northeastern Mexico, *Geology*, v. 16, p. 37-40.
- Stevenson, G.M. and D.L. Baars, (1986). The Paradox: A pull-apart basin of Pennsylvanian age, in J.A. Peterson, ed., *Paleotectonics and sedimentation in the Rocky Mountain region*: AAPG Memoir 41, p. 513-539.
- USGS online document, 2004. "Geologic Provinces of the United States: Rocky Mountains."  
<http://geomaps.wr.usgs.gov/parks/province/rockymtn.html>
- Ye, H., L. Royden, C. Burchfiel, and M. Schuepbach, (1996). Late Paleozoic deformation of interior North America: The greater Ancestral Rocky Mountains, *AAPG Bulletin*, v. 80, no. 9, p. 1397-1432.

## Stratigraphic Expression of Ancestral Rockies and Laramide Uplifts

*Contributed by Julius Busecke*

The Ancestral Rocky Mountains (ARM) are a feature of late Mississippian to early Permian origin (320 – 270 Ma), situated in the mid-western to southern US. The uplifts were mainly oriented in a N-NW to S-SE direction. The actual uplifts have been eroded away, but the stratigraphy and sediment records still prove their existence. Herein I will present 4 theories on why these features formed in the middle of the North American continent (main supporters are indicated in parentheses).

### **Ouichita-Marathon Orogeny (Kluth, Burchfield)**

This group argues that the Ouichita-Marathon Orogeny is the source of stress to the North American plate, which caused the ARM to form. The argument is based on the assumption that the Western margin of the North American plate was in a state of relative quiescence during the formation of the ARM. Kluth (1986) argues that the Mississippian Antler Orogeny had ceased, and the Mesozoic Sonoma Orogeny had not yet begun. Therefore the stresses responsible for the uplift had to originate from either the south or east. Kluth (1986) discounted the Alleghenian Orogeny, which formed the Appalachian Mountains during that time, based on the distance to the ARM – the stress needed to form the ARM could not be provided from an event this far away. This leaves the Ouichita-Marathon Orogeny as a source for the stress. It is argued that the stresses could have been transmitted via preexisting weaknesses, which then determined the location and orientation of the ARM.

### **Wichita Megashear (Budnik)**

Budnik (1986) introduces the theory that the ARM formed along another preexisting zone of weakness – the 'Wichita Megashear' – he bases his argument on the sense of displacement along the Wichita Megashear. He presents structural analysis, which indicate a left lateral shear that contradicts the right lateral shear needed to support the Ouichita-Marathon Orogeny model. He proposes the Appalachian as the main suturing zone between Gondwana and Laurussia

instead of the Ouichitas. To support his argument he invokes the different shortening of the plate due to both the Ouichita-Marathon Orogeny and the Alleghenian Orogeny. Where the latter produced a significantly bigger amount of shortening.



Figure 4. Late Paleozoic geography and tectonics of western North America, showing the intracratonic Ancestral Rocky Mountains (dashed pattern) in relation to contemporaneous structures and events. The Ouachita Orogenic Belt is dashed where present in the subsurface only. Other rock units include: ophiolites (black); miogeoclinal rocks (light gray); off-shelf rocks (dark gray); CA, Chilliwack arc; CC, Cache Creek assemblage; ELAF, eastern limit of Antler foredeep; EP, El Paso Mountains; H, Hermosillo; IN, Independence Mountains; NA, Nicola arc; NC, northern Cascade Mountains; OB, Oquirrh basin; OG, Osgood Mountains; PR, Peninsular Ranges; SB, San Bernadino Mountains; SJ, San Juan Islands; SM, Slide Mountain; UU Uinta uplift; UB, Uinta basin; WB, Williston basin; WISZ, future location of West Idaho suture zone; W-SD, Wallowa-Seven Devils arc. From Burchfiel, Lipman and Zoback, 1992).

### Subduction (Ye et al.)

Ye et al. (1996) argue that the general orientation of the ARM does not agree with the models introduced above. Rather a NE-SW direction of compression is needed to form the ARM. A model of a flat NE-dipping subducting plate is introduced. The theory is based on evidence for a volcanic arc found by (McKee, Jones, and Anderson, 1988). Two analogous cases are presented:

- The late Cretaceous-early Cenozoic Laramide Orogeny that created the modern Rocky Mountains of the western United States
- The Cenozoic shortening along the east side of the Sierra Pampeanas in the Argentine Andes

Both involve intraplate shortening as far as 500 km from the subduction boundary as well as a very shallow angle for the downgoing slab.

### Transtension (Stevenson and Baars)

The last theory invokes two big preexisting weaknesses in the North American craton. The Olympic-Wichita Linement (1675-1460 Ma) and the Colorado Linement (1700 Ma). The small difference in the timing suggests that these two formed together as an expression of North-South compression of the craton. (Stevenson and Baars, 1986) find that the ARM formed as one of multiple reactivations of the preexisting weaknesses.

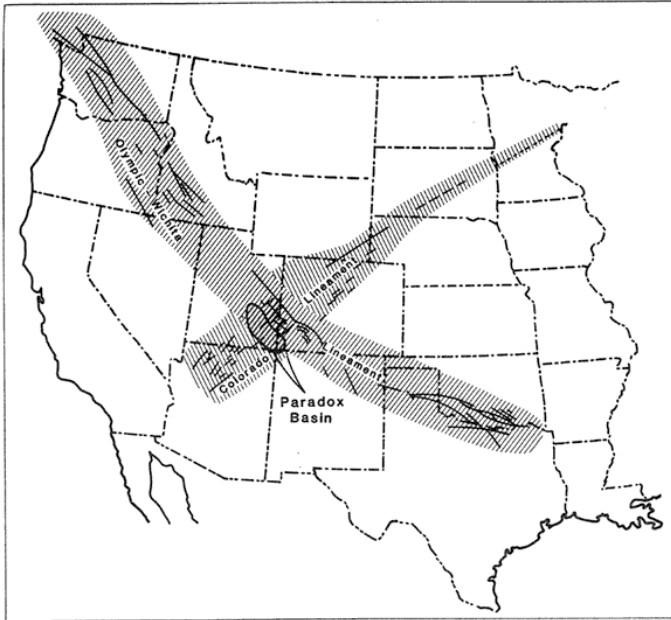


Figure 5. Proterozoic basement lineament of the western United States, with the Paradox basin at their intersection. From Stevenson and Baars (1986).

### References

- Kluth, C.F., 1986. Plate tectonics of the Ancestral Rocky Mountains, in J.A. Peterson, ed., *Paleotectonics and sedimentation in the Rocky Mountain region*: AAPG Memoir 41, p. 353-369.
- Burchfiel, B.C., D.S. Cowan, and G.A. Davis, Tectonic overview of the Cordilleran orogen in the western United States, in B.C. Burchfiel, P.W. Lipman, and M.L. Zoback, eds., *The Cordilleran orogene*, GSA v. G-3.
- Budnik, R.T., 1986. Left-lateral intraplate deformation along the Ancestral Rocky Mountains: implications for late Paleozoic plate motions, *Tectonophysics*, 132, p. 195-214.
- McKee, J.W., N.W. Jones, and T.H. Anderson, 1988. Las Dalias basin: A record of late Paleozoic arc volcanism in northeastern Mexico, *Geology*, v. 16, p. 37-40.
- Stevenson, G.M. and D.L. Baars, 1986. The Paradox: A pull-apart basin of Pennsylvanian age, in J.A. Peterson, ed., *Paleotectonics and sedimentation in the Rocky Mountain region*: AAPG Memoir 41, p. 513-539.
- Ye, H., L. Royden, C. Burchfiel, and M. Schuepbach, 1996. Late Paleozoic deformation of interior North America: The greater Ancestral Rocky Mountains, *AAPG Bulletin*, v. 80, no. 9, p. 1397-1432.
- <http://www.colorado.edu/GeolSci/Resources/WUSTectonics/AncestralRockies/index>

## Laramide Deformation

*Contributed by Anna Foster*

The western US has experienced several periods of compressional deformation from the late Paleozoic throughout the early Cenozoic. Although the last of these episodes was a period of continuous subduction beneath the west coast, it is divided into two overlapping orogenic events because of the difference in character of the resulting uplifts: the Sevier Orogeny (140-60 Ma) and the Laramide Orogeny (70-35 Ma). The Laramide orogeny was the tectonic event that formed the Rocky Mountains.

The Sevier and Laramide orogenies are distinctive in both the area affected and the type of deformation. Sevier deformation was characterized by thin-skinned flat-ramp thrusting, and occurred closer to the plate boundary. The Sevier Orogeny is discussed in the following section of this field guide. Laramide uplifts, on the other hand, are found in the interior of the North American plate more than 1,600 kilometers from the subduction zone and concentrated in present-day Montana, Wyoming, and Colorado (Figure 4). Laramide uplifts are examples of thick-skinned deformation, meaning that they are basement-cored structures. These crystalline basement uplifts are generally NW-SE trending, but with many variations. This orientation and the specific locations of the uplifts are thought to be due to the reactivation of old faults created in the assembly of the continent, as well as the orogeny responsible for the Ancestral Rockies (1.1 Ga and 330 Ma) (Karlstrom and Humphreys, 1998).

While it is recognized that pre-existing weaknesses may have influenced the Laramide deformation, the questions of how and why this type of deformation occurred remain. On a crustal scale, the view has evolved over time. The first model for basement-cored deformation was the Block Uplift model (Thom, 1923; Chamberlain, 1945). In this model, motion occurs on a nearly vertical fault, and the hanging wall may flop over after being exposed (Figure 7a). However, COCORP, a large active-source seismology study, revealed that most fault planes in the area were low-angle throughout the crust (Brewer et al., 1982). Additionally, horizontal displacements of approximately 9 miles were observed. Both of these pieces of evidence rule out the original block uplift model. These observations in conjunction with observations of folded Precambrian crystalline rocks and an overturned and deformed sequence of mostly Paleozoic rocks underlying the Precambrian thrust mass (Figure 6) led to the Fold-Thrust Uplift model (Berg, 1962), in which displacement on a low-angle fault at depth causes deformation near the surface in the form of a fault-propagation fold. Eventually, the fold may overturn, and as the displacement accumulates, the fault may break through the fold (Figure 7c). This model is widely accepted today, and applies to both thick- and thin-skinned deformation.

Fold-thrust uplift explains the mechanism for deformation, but not the driving force. The change from thin- to thick-skinned deformation has been explained by a change from normal, steep-slab subduction to flat-slab subduction of the Farallon plate. Several pieces of evidence support this hypothesis. First, deformation occurred far from the plate boundary, and it is hard to transmit stresses without these additional traction stresses along the base of the lithosphere. Second, the downgoing Farallon slab was decreasing in age (Engelbreton et al., 1988), and the subduction rate was thought to be increasing (Jerrard, 1986). Both of these factors contribute to an increase in buoyancy of the subducting slab. Third, prior to the Laramide orogeny, magmatism progressed west to east, with evidence for mantle melting, possibly resulting from slab shallowing (Coney and Reynolds, 1977). During the Laramide, magmatism in the Great Basin was from a purely crustal source (Patino-Douce et al, 1990), which indicates the lithosphere was refrigerated (Dumitru et al., 1991). Following the Laramide, there was an

ignimbrite flare-up event, injecting large amounts of basalt into the crust and indicating a change from cold to hot conditions in the lithosphere (Coney, 1980; Johnson, 1991; Perry et al., 1993). This could be the result of the removal of the Farallon plate from beneath the North American plate. Finally, the record of vertical motions shows that there was a period of pre-Laramide subsidence, followed by Laramide and post-Laramide uplift.

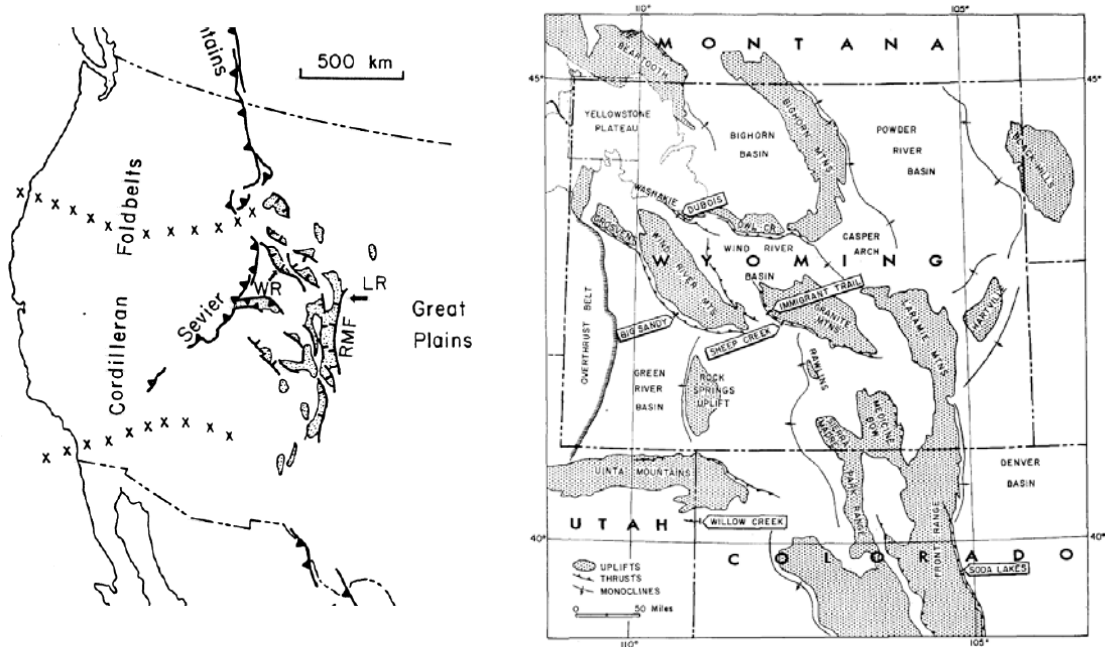


Figure 6. Map of Laramide-age crystalline basement uplifts in the western US, left, from Brewer et al. (1982), right, in the region of the field guide, from Berg (1962).

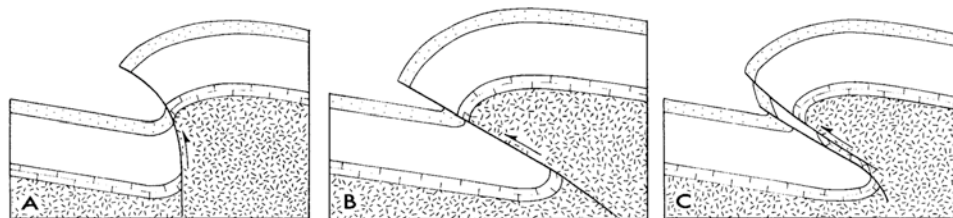


Figure 7. Models of thrusting. A- block uplift; B- thrust uplift; C- fold-thrust uplift. From Berg (1962).

There are several possible explanations for these vertical motions. The most likely explanation for the pre-Laramide subsidence is suction or “pull” from the slab at the base of the lithosphere (Mitrovica et al, 1989). The explanation for the uplift is less clear. Flat-slab subduction could have allowed mechanical removal of the lithosphere, making it more buoyant (Bird, 1988). However, this is not supported by lithospheric thickness studies (Humphreys et al., 2003). Another possibility is lower crustal flow, moving material from the crust thickened by the Sevier orogeny, in what is now the Basin and Range, into the Colorado Plateau, Rocky Mountains, and Great Plains (MacQuarry and Chase, 2000). This would have thickened the crust

and caused isostatic uplift. However, there is no observed tilting of the Colorado Plateau, the upper- and lower-crust isostatic measurements are correlated (Wendlandt et al., 1993; Selverstone et al., 1999), and the lower crust has been observed to support earthquakes (Wong and Humphrey, 1989), all of which argue against lower crustal flow. This leaves the hydration hypothesis, in which the addition of water promotes melt and creates hydrous mineral phases that reduce the density of the lithosphere and weaken it, allowing mantle shortening and crustal thrusting (Humphreys et al., 2003).

In summary, the Laramide orogeny is defined by fold-thrust deformation in the form of thrust-bounded basement-cored uplifts. The inboard location of deformation and volcanism was caused by flat-slab subduction, and the location of uplifts was influenced by pre-existing Precambrian structures. Hydration of the lithosphere likely played an important role in allowing shortening, magmatism, and uplift. In this field guide, there are several examples of Laramide uplifts including Rattlesnake Mountain, Sheep Mountain, the Gros Ventre Range, the Wind River Mountains, Laramie Mountains, Beartooth Mountains, Owl Creek Mountains, and the Bighorn Mountains.

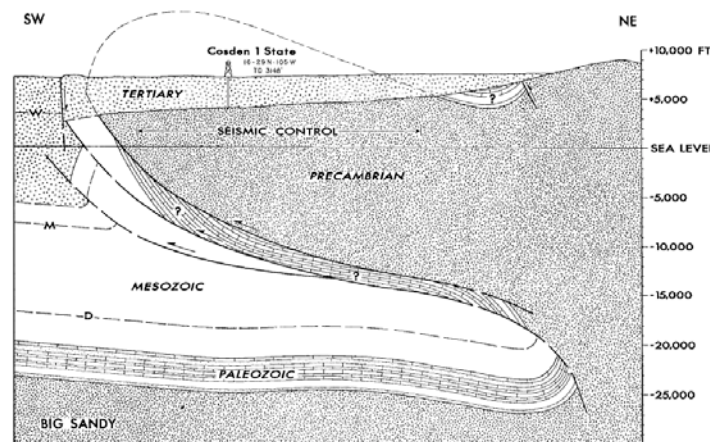


Figure 8. Example of structural evidence for fold-thrust uplift from the Wind River thrust, showing overturned layers, from Berg (1962).

## References

- Berg, R., 1962, Mountain flank thrusting in Rocky Mountain foreland, Wyoming and Colorado: Bull. Am. Assoc. Petroleum Geologists, v. 46, n. 11, p. 2019-2032.
- Bird, P., 1988, Formation of the Rocky Mountains, western United States: A continuum computer model: Science, v. 239, p. 1501-1507.
- Brewer, J.A., Allmendinger, R.W., Brown, L.D., Oliver, J.E., Kaufman, S., 1982, COCORP profiling across the Mountain Front in southern Wyoming, Part 1: Laramide structure: Geol. Soc. Am. Bull., v. 93, p. 1242-1252.
- Chamberlin, R.T., 1945, Basement control in Rocky Mountain deformation: Am. Jour. Sci., v. 243-A, p. 98-116.
- Coney, P. J., and Reynolds, S. J., 1977, Flattening of the Farallon slab: Nature, v. 270, p. 403-406.
- Coney, P. J., 1980, Cordillerian metamorphic core complexes: An overview, in Crittendon, M. D., Coney, P. J., and Davis, G. H., eds., Cordillerian metamorphic core complexes: Geological Society of America Memoir 153, p. 7-31.

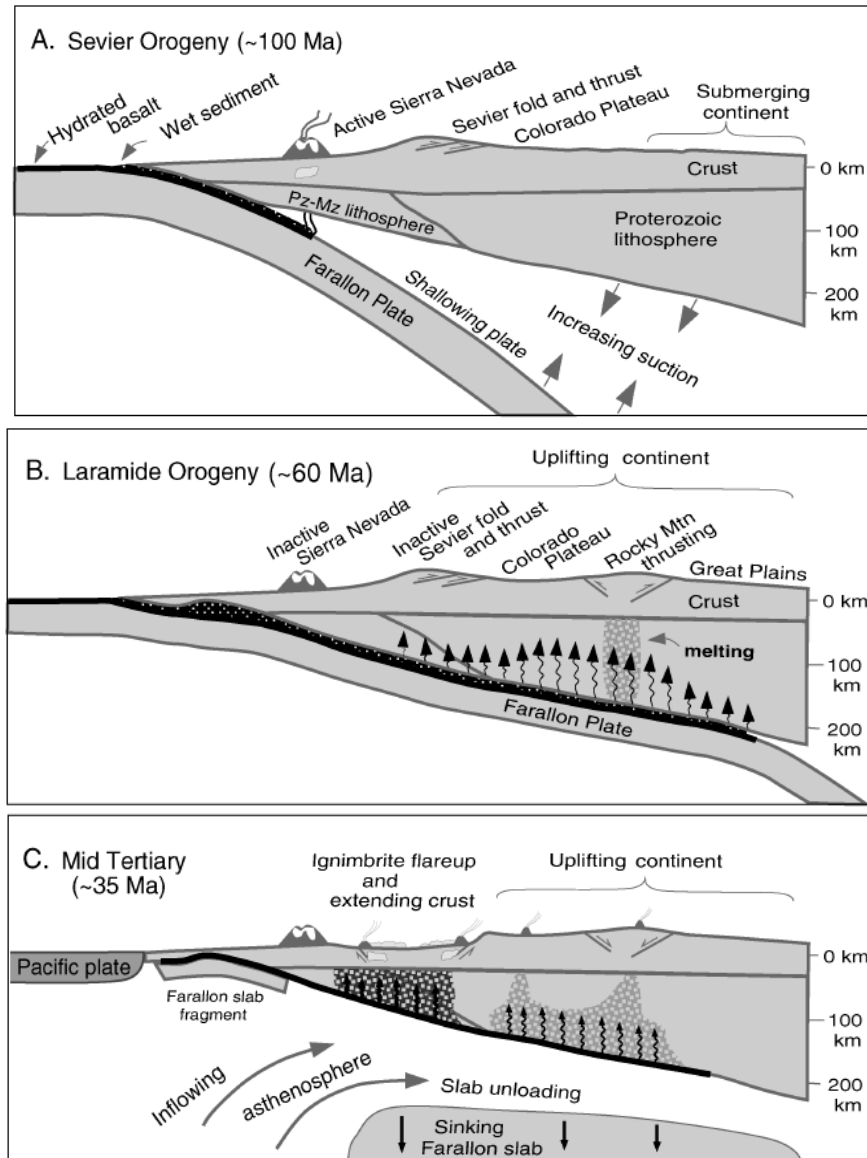


Figure 9. Progression of steep slab subduction during the Sevier orogeny. (A) to flat-slab, hydrated- and refrigerated-lithosphere conditions during the Laramide Orogeny (B), to post-Laramide lithospheric warming (C). From Humphreys et al. (2003).

Dumitru, T. A., Gans, P. B., Foster, D. A., and Miller, E. L., 1991, Refrigeration of the western Cordilleran lithosphere during Laramide shallow-angle subduction: *Geology*, v. 19, p. 1145–1148.

Engelbreton, D. C., Cox, A., and Gordon, R. G., 1988, Relative motions between oceanic and continental plates in the Pacific Basin: Geological Society of America, Special Paper no. 206, 59 p.

Humphreys, E., Hessler, E., Dueker, K., Farmer, G. Lang, Erslev, E., Atwater, T., 2003, How Laramide-age hydration of North American lithosphere by the Farallon slab controlled subsequent activity in the western United States: *International Geology Review*, v. 45, n. 7, p. 575-595.

Jerrard, R. D., 1986, Relations among subduction parameters: *Reviews of Geophysics*, v. 24, p. 217–284.

- Johnson, C. M., 1991, Large-scale crust formation and lithosphere modification beneath middle to late Cenozoic calderas and volcanic fields, western North America: *Journal of Geophysical Research*, v. 96, p. 13,485–13,507.
- Karlstrom, K. E., and Humphreys, E. D., 1998, Persistent influence of Proterozoic accretionary boundaries in the tectonic evolution of southwestern North America: Interaction of cratonic grain and mantle modification events: *Rocky Mountain Geology*, v. 33, p. 161–179.
- MacQuarrie, N., and Chase, C. G., 2000, Raising the Colorado Plateau: *Geology*, v. 28, p. 91–94.
- Mitrovica, J. X., Beaumont, C., and Jarvis, G. T., 1989, Tilting of continental interiors by dynamical effects of subduction: *Tectonics*, v. 8, p. 1079–1094.
- Patino-Douce, A. E., Humphreys, E. D., and Johnston, A. D., 1990, Anatexis and metamorphism in tectonically thickened continental crust exemplified by the Sevier Hinterland, western North America: *Earth and Planetary Science Letters*, v. 97, p. 290–315.
- Perry, F. V., DePaolo, D. J., and Baldrige, W. S., 1993, Neodymium isotopic evidence for decreasing crustal contributions to Cenozoic ignimbrites of the western United States: Implications for the thermal evolution of the Cordillerian crust: *Geological Society of America Bulletin*, v. 105, p. 872–882.
- Silverstone, J., Pun, A., and Condie, K., 1999, Xenolithic evidence for Proterozoic crustal evolution beneath the Colorado Plateau: *Geological Society of America Bulletin*, v. 111, p. 590–606.
- Thom, W.T., Jr., 1923, The relation of deep-seated faults to the surface structural features of central Montana: *Am. Assoc. Petroleum Geologists Bull.*, v. 7, p. 1-13.
- Wendlandt, E., DePaolo, D. J., and Baldrige, W. S., 1993, Nd and Sr isotope chronostratigraphy of Colorado Plateau lithosphere: Implications for magmatic and tectonic underplating of the continental crust: *Earth and Planetary Science Letters*, v. 116, p. 23–43.
- Wong, I. G., and Humphrey, J. R., 1989, Contemporary seismicity, faulting, and the state of stress in the Colorado Plateau: *Geological Society of America Bulletin*, v. 101, p. 1127–1146.

## Wyoming-Idaho Thrust Belt

*Contributed by Marc Vankeuren*

The Sevier orogenic belt consists of a narrow zone of continuous structural disturbances that runs along the length of the U.S Cordillera (Figure 10). The Idaho-Wyoming-Utah thrust belt is part of the Cordilleran foreland thrust belt, which stretches from Alaska to Mexico. The Sevier orogenic belt was originally named for the Sevier arch in western Utah. Armstrong (1968) redefined the style and extent of deformation and referred to it as the Sevier orogenic belt (Heller et al., 1986). The classic Sevier belt is characterized by (1) thrusts with west-dipping, listric geometry, soling into a major basal detachment of Archaen or Proterozoic age at the western side of the thrust belt; (2) a minimum of 50% shortening of supracrustal strata perpendicular to the belt without the development of mylonites or significant metamorphism; and (3) younging (progression of decreasing age) of major thrusts from west to east with deformation spanning from latest Jurassic into the earliest Eocene (Allmendinger and Jordan, 1981).

The Cordilleran thrust belt in Wyoming, northern Utah, and eastern Idaho is composed of 5 major thrust fault systems and is one of the first places where major “thin-skinned” thrust sheets was recognized as a distinct tectonic style. The major thrusts, from west to east, are the: Paris-Willard; Meade-Laketown; Crawford; Absaroska; Darby; and Prospect. The thrust fault systems are arranged in an eastward overlapping array with younging of major motion from west to east. Thrusting in Wyoming and the adjacent regions was quasi-continuous during at least a 70

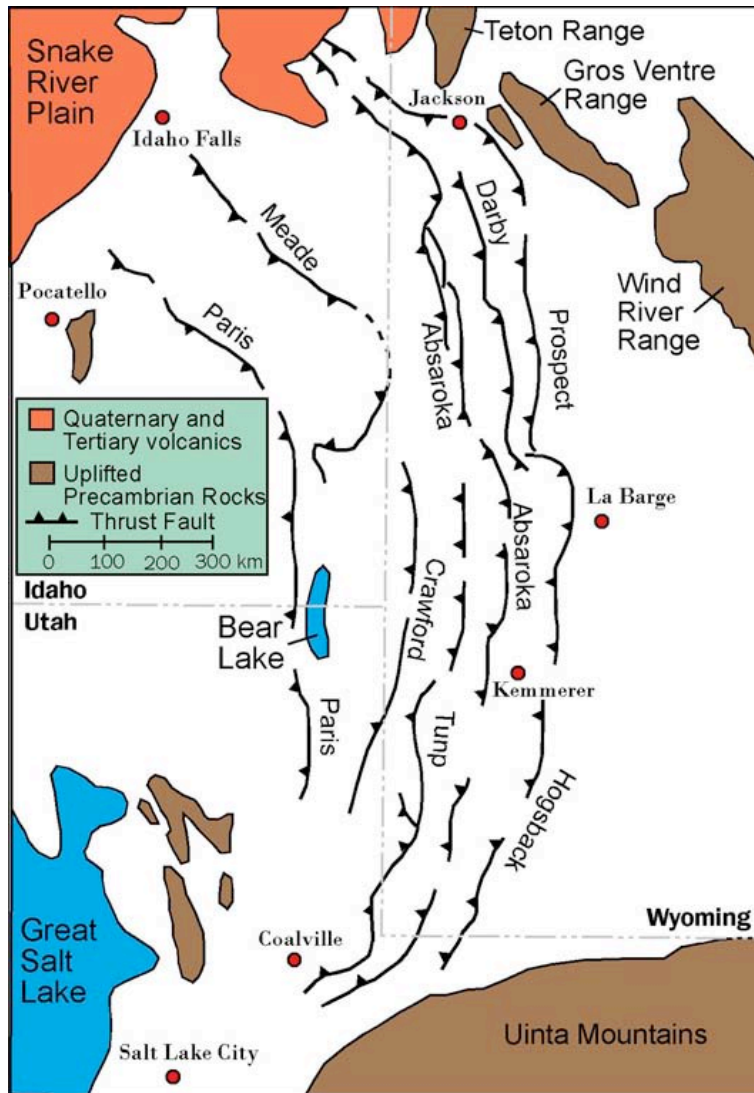


Figure 10. The major thrust faults of the Idaho-Wyoming-Utah salient and the time intervals of major displacement: Paris thrust (middle-Early Cretaceous 120-113 Ma); Meade thrust (late-Early Cretaceous 113-98 Ma); Crawford thrust (late Cretaceous 87-84 Ma); Absaroka thrust (late Cretaceous 84-74 Ma); and Hogsback (Darby) thrust (Paleocene 63-57 Ma). From Armstrong and Oriel, 1986.

million year time period from the Cretaceous until the middle Eocene. A wedge of westward thickening shallow-marine sediments of Proterozoic through Jurassic ages was thrust eastward on the major thrust fault systems. This orogenic process created clastic debris that was shed eastward from the rising thrust sheets into the adjacent subsiding basins causing it to be incorporated into the younger thrust sheets and subsequently recycled into younger basins as thrusting proceeded eastwards (Royse, 1993).

Each of these thrust systems contain more than one significant thrust fault. Although major thrust displacement progressed in time toward the east, parts of each system were reactivated or imbricated by younger thrusts. Older thrust sheets became integral parts of younger ones and consequently underwent uplift and deformation even after their major



displacement. The eastward younging of major displacement and minor subsequent reactivations are the consequence of the continuous maintenance of the eastward tapering wedge shape of the thrust section. Maximum displacement of the whole system is estimated to be ~165km and the total displacement on individual thrust faults is as much as 64 km, according to this interpretation (Royse, 1993).

Thrust fault surfaces have a ramp-flat geometry. The fault configuration is controlled by stratification and by lithologic thickness changes in the sediments. Structurally weak layers such as Cambrian shale, Triassic and Jurassic evaporates, and Cretaceous shale contain extensive flats, whereas ramps form in the more competent rocks such as Paleozoic carbonate and Jurassic sandstones. Transport of the nearly flat beds over these ramps created folds and promoted imbrication within the thrust plates (Figure 11). Extensive flats are the sites of “piggyback” basins such as the Fossil Basin.

The thrust plates have been cut by numerous, mostly west-dipping normal (extensional) faults of post early Eocene to Holocene age, such as the Hoback and Grand Valley faults. These faults have accommodated a significant amount of east-west horizontal extension, ~10 km or so to the entire thrust belt. Many of these normal faults are known to merge with or terminate against the older faults, thus reactivating them as normal faults.

## References

- Allmendinger, R.W., Jordan, T.E., 1981, Mesozoic evolution, hinterland of the Sevier orogenic belt, *Geology*, v. 9, p. 308-313.
- Heller, P.L., Bowdler, S.S., Chambers, H.P., Hagen, E.S., Shuster, M.W., Winslow, N.S., Time of initial thrusting in the Sevier orogenic belt, Idaho-Wyoming and Utah, *Geology*. V. 14, p. 388-391.
- Royse, Frank, Jr., 1993, An overview of the geologic structure of the thrust belt in Wyoming, northern Utah, and Eastern Idaho, in Snoke, A.W., Steidtmann, J.R., and Roberts, S.M., editors, *Geology of Wyoming: Geological Survey of Wyoming Memoir No. 5*, p. 273-311.

## Teton Mountain Uplift History

*Contributed by Cathleen Doherty*

Northwestern Wyoming and southwestern Montana are characterized by Cenozoic volcanism, Neogene extensional structures, and faulting associated with the Laramide orogeny [1]. The Teton Range of western Wyoming is the product of these events. The Teton Range sits at the eastern terminus of the Snake River Plain, and is bordered by the Plio-Pleistocene Yellowstone rhyolitic plateau to the north [1]. The Teton Range is a subrange of the Rocky Mountains, with Grand Teton as the highest peak at an elevation of ~4,200 m () [2]. The range extends 70 km in length and is 20 km wide and it is recognized by its snow-capped jagged peaks and its abrupt relief relative to the Jackson Hole valley [2].

The Tetons are comprised of ~2 Ga Precambrian gneiss and granite, making them well suited for fission track analysis (which can be used to determine uplift rate) [1, 3]. Above the Precambrian basement rocks lies the Precambrian-Cambrian unconformity, which is characterized by its dome shape. During the Paleozoic, the Precambrian Tetons were overlain by 1.5 km of strata, which persisted throughout the Mesozoic [1]. The late Cretaceous Laramide orogeny resulted in deformation of the Teton Range and thrust faulting through the southern portion of the range. Normal faulting during the late Cenozoic along the length of the Teton

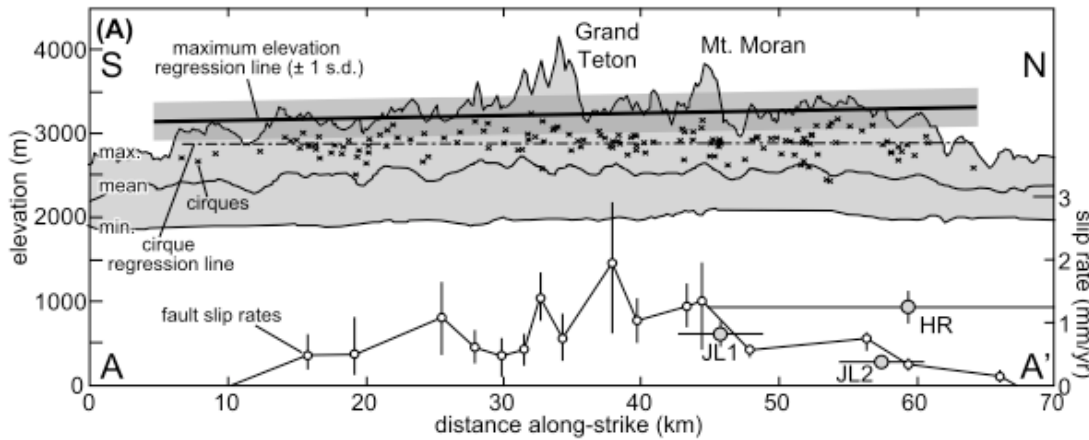


Figure 12. Topographic profile showing the elevation of the Teton Range. The shaded area shows the maximum, minimum, and mean elevations. Fault slip rates [from Machette et al., 2001; O'Connell et al., 2003]. From Foster et al., 2010.

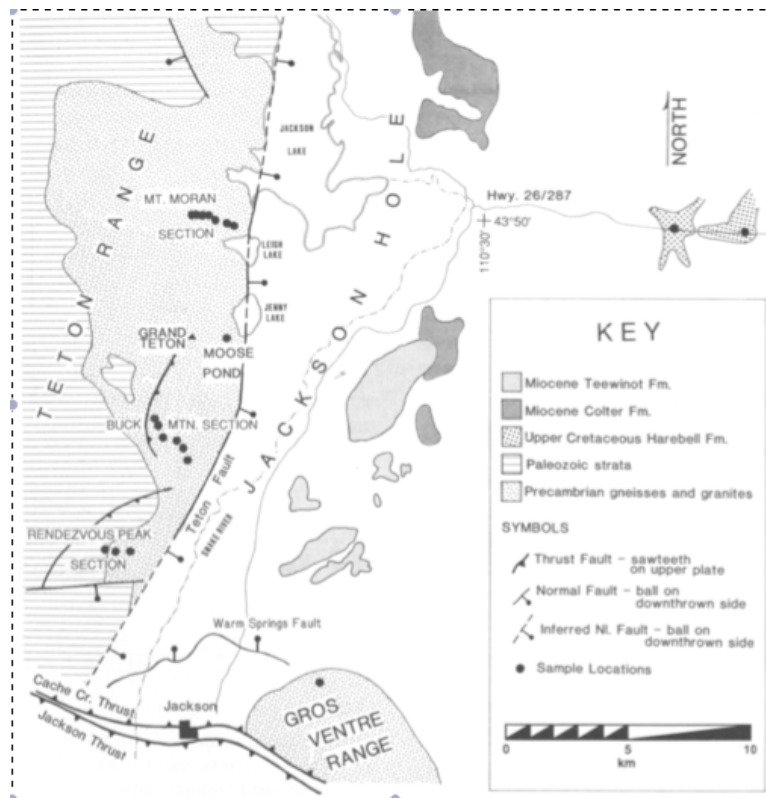


Figure 13. Geologic map of the Teton Range. From Roberts and Burbank, 1993

Range (reactivated Laramide faults) has resulted in it's >2 km of elevation above it's neighboring valley (Foster, 2010). The Teton normal fault is east dipping, with Jackson Hole as the hanging wall and the Teton Range dipping toward the west (Figure 13).

Recent studies suggest that the Teton Fault has slip rates amongst the fastest recorded United States at ~2.2 mm/yr in the last 2 Myr [4, 5]. The uplift of the Teton Range began at ~ 9

Ma, exposing the Precambrian rocks we see today [6]. The Precambrian basement rocks show Late Cenozoic subsidence of the Jackson Hole valley by ~5 km. Geophysical and stratigraphic data suggest footwall uplift of the Teton Range ~2 km higher than surface at present day [1, 7]. This is supported by structural offsets of stratigraphic units and a visible fault scarp running along the boundary between the Jackson Hole valley and the Teton Range. These include offsets in the 4 Ma Conant Creek Tuff and the 2.05 Ma Huckleberry Ridge Tuff, which are offset by 1520 m and 1220 m, respectively [1, 6].

Fission track dating of apatites in the Precambrian core of the Teton Range reveal variance in ages of samples taken from the northern and southern sections. This would suggest that the Precambrian-Cambrian unconformity was folded in the Cretaceous and dipped toward the north, displacing the range front by an additional ~2 km with an uplift rate of 0.1-0.2 mm/yr in the Late Cretaceous [1]. Structural evidence for rapid uplift includes the absence of footwalls, the straight east face of the Tetons, the asymmetry of the range, and the fault scarp along the mountain front.

## References

1. Roberts, S.V., Burbank, D.W., 1993. Uplift and thermal history of the Teton Range (northwestern Wyoming) defined by apatite fission-track dating. *Earth Planet. Sci. Lett.*, 118: 295-309
2. Foster, D., 2010. Glacial-topographic interactions in the Teton Range, Wyoming. *J. Geophys. Res.* 115, F01007, doi: 10.1029/2008JF001135.
3. J.C. Reed, Jr. and R.E. Zartman, Geochronology of Pre- cambrian rocks of the Teton Range, Wyoming, *Geol. Soc. Am. Bull.* 84, 561-582, 1973.
4. Machette, M. N., K. L. Pierce, J. P. McCalpin, K. M. Haller, and R. L. Dart (2001), Map and data for Quaternary faults and folds in Wyoming, U.S. Geol. Surv. Open File Rep., 01-461.
5. O'Connell, D. R. H., C. K. Wood, D. A. Ostenaar, L. V. Block, and R. C. LaForge (2003), Ground motion evaluation for Jackson Lake Dam, Minidoka Project, Wyoming, Rep. 2003 – 2, p. 33, Bur. of Reclamation, Denver, Colo.
6. J.D. Love, Summary of upper Cretaceous and Cenozoic stratigraphy, and of tectonic and glacial events in Jackson Hole, northwest Wyoming, *Wyo. Geol. Assoc. Guidebook*, 29th Annu. Field Conf., pp. 585-593, 1977.
7. J.D. Love, J.C. Reed, Jr., R.L. Christiansen and J.R. Stacy, Geologic block diagram and tectonic history of the Teton Range, Wyoming-Idaho, *US Geol. Surv. Misc. Geol. Invest. Map* 1-730, 1973.

## Basin and Range Normal Faulting

*Contributed by Guleed Ali*

The Basin and Range Province is a region principally occupying the western US that is characterized by a unique range-basin-range topography. The Sierra Nevada microplate, Colorado Plateau and Rio Grande Rift, and the Columbia Plateau define the western, eastern, and northern tectonic boundaries, respectively. Although the Basin and Range is generally defined as an extensional tectonic province, it is comprised of multiple zones that exhibit unique tectonic deformation. From geodetic data (Bennett et al. 1999), the Basin and Range can be divided into a distinct northern and southern component at ~ 36°N (Bennett et al. 1999). North of this latitude, the Basin and Range accommodates 11-13 mm/yr (~20-25%) of North American-Pacific Plate motion (Bennett et al. 1999). Whereas south of this latitude, the Basin and Range does not accommodate significant plate motion (Bennett et al. 1999). A likely explanation for this observation is that most of the deformation associated with plate motion is instead captured to

the west by the adjacent San Andreas fault zone. In addition, the western and eastern portions of the region display transtension- and extension-dominated modes of deformation, respectively (Bennett et al. 1999).

The modern Basin and Range owes its genesis to the Late Cretaceous-Eocene Laramide Orogeny. During this time, crustal shortening formed the Nevadaplano- an extensive, low-relief, high orogenic plateau with a thick (~40-50 km) crust (Decelles 2004). This high plateau, which was centered over Nevada and western Utah, is analogous to the modern Andean Altiplano along the Pacific-South American subduction complex. Studies using stable isotopes in volcanic glasses as a proxy for paleoaltimetry (e.g., Cassell et al. 2009) provide evidence of the presence of this Late Cenozoic elevated plateau. Mix et al. 2011 used the same proxy to demonstrate that >3 km elevations were achieved during the Middle Eocene along the Canadian Cordillera. Also, Mix et al. 2011 argues for a high Nevadaplano during the Late Eocene-Oligocene (Figure 14), which is much later than previous authors estimated. Despite the differences in chronology, the existence of the Nevadaplano as an over-thickened and gravitationally unstable structure is an important initial condition that influenced the formation of the Basin and Range Province.

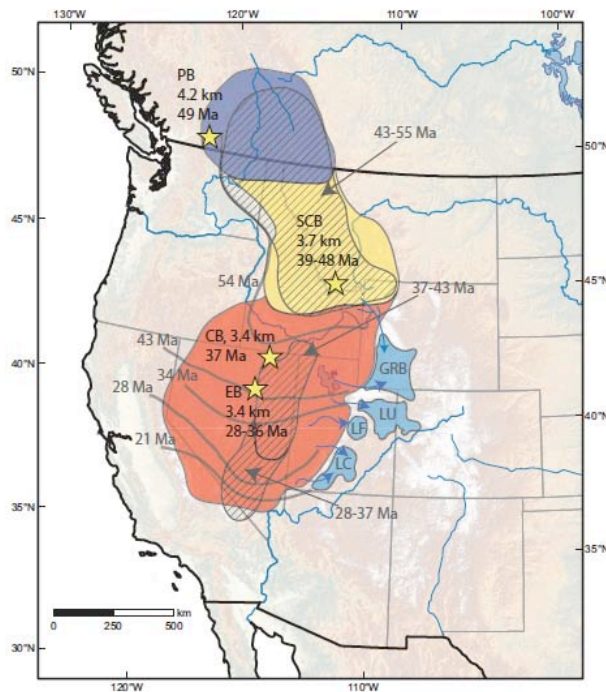


Figure 14. Correlation between magmatism, extension, and uplift in the Basin and Range Province. Regions of low  $d_{18O}$  (isotopic composition of paleo-precipitation) interpreted as elevations >3 km are shaded purple (by 49 Ma), yellow (by 39 Ma), and red (by 28 Ma). Lakes in Laramide foreland show capture of waters from highlands. From Mix et al., 2011.

Following a large pulse of Eocene magmatism, extension began in the western US around 16-17 Ma. This extension is coincident with the outpouring of the Columbia River Basalt, tearing and detachment of the underlying Farallon slab, and early Oregonian and Nevadan Yellowstone hotspot volcanics (Colgan and Henry 2009; Parsons et al. 1994). Colgan et al. 2004 tested Parsons et al. 1994's hypothesis for a Yellowstone hotspot-induced Basin and Range-style extension using apatite fission-track ages (which represent the cooling of a rock below  $100 \pm 20^\circ\text{C}$ ) from the Santa Rose Range in northwestern Nevada – a crustal block uplifted along a

westward-dipping normal fault. Using this thermochronometric system, Colgan et al. 2004 demonstrated that Basin and Range extension occurred in the Santa Rosa Range ~7.5-10 Ma (Figure 15), which is much younger than the known onset of Yellowstone volcanism. This result is further supported by other studies, which propose bimodal collapse of the Nevadaplano. First, extension began ~16-17 Ma within well-defined zones that were disconnected by predominantly undeformed zones (Ernst 2010). However, a much younger extensional period occurred at ~10 Ma, which we associate with range bounding, high-angle, Basin and Range-style normal faulting (Ernst 2010). To explain this difference, Colgan and Henry 2009 proposed a model invoking a change in Pacific-North American plate motion as the primary cause for the collapse of the Nevadaplano. This change was due to a westward-moving Mendocino triple junction. However, the authors also mention Farallon slab detachment may have enhanced or altered the mode of extension that would have occurred if the Pacific-North American plate motion was only changing.

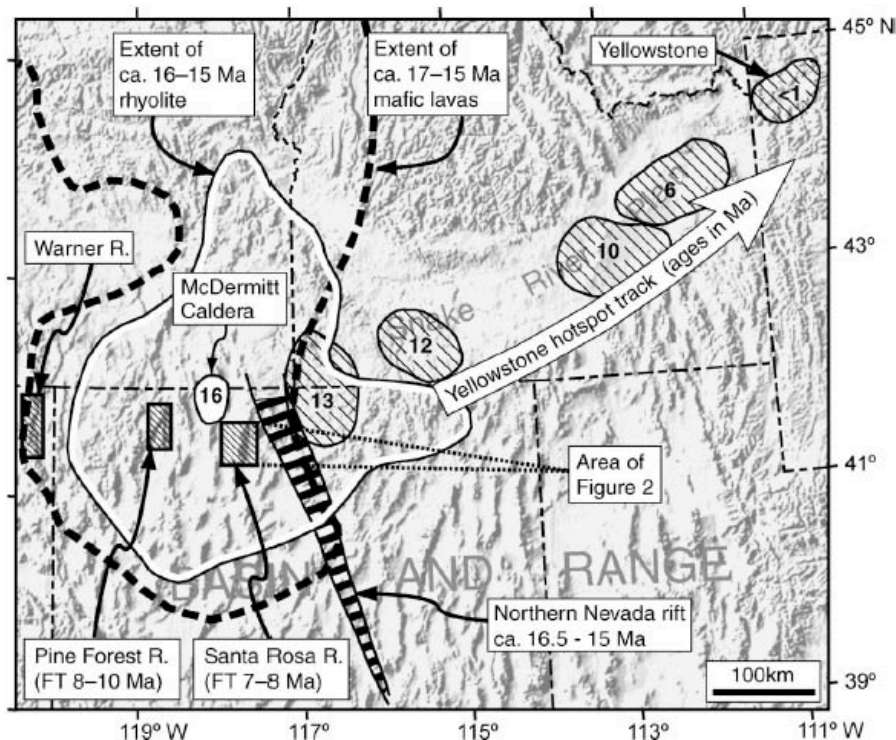


Figure 15. Shaded-relief map of the western US, showing location of Santa Rosa Range relative to the start of the Yellowstone hotspot track. Eruptive centers that define hotspot track, and their ages are from Pierce and Morgan (1992); extent of 15-17 Ma volcanic rocks is from Christiansen and Yeats (1992); From Colgan et al., 2004.

#### References:

- Bennett, R.A., Davis, J.L., and Wernicke, B.P., 1999, Present-day pattern of Cordilleran deformation in the western United States: *Geology*, v. 27, no. 4, p. 371–374, doi: 10.1130/0091-7613
- Cassel, E.J., Graham, S.A., and Chamberlain, C.P., 2009, Cenozoic tectonic and topographic evolution of the northern Sierra Nevada, California, through stable isotope paleoaltimetry in volcanic glass: *Geology*, v. 37, p. 547–550, doi: 10.1130/G25572A.1.
- Colgan, J.P., Dumitru, T.A., Miller, E.L., 2004. Diachroneity of Basin and Range extension and Yellowstone hotspot volcanism in northwestern Nevada. *Geology* 32, 121–124.
- Colgan, J.P., and Henry, C.D., 2009, Rapid middle Miocene collapse of the Mesozoic orogenic plateau in north-central Nevada: *International Geology Review*, v. 51, p. 920–961, doi:10.1080/00206810903056731.

- DeCelles, P.G., 2004, Late Jurassic to Eocene evolution of the Cordilleran thrust belt and foreland basin system, western U.S.A.: *American Journal of Science*, v. 304, p. 105–168, doi: 10.2475/ajs.304.2.105.
- Ernst, W.G., 2010, Young convergent margins, climate, and crustal thickness—A Late Cretaceous–Paleogene Nevadaplano in the American Southwest?: *Lithosphere*, v. 2, p. 67–75, doi: 10.1130/L84.1
- Mix, H.T., Mulch, A., Kent-Corson, M.L., and Chamberlain, C.P., 2011, Cenozoic migration of topography in the North American Cordillera: *Geology*, v. 39, p. 87-90, doi: [10.1130/G31450.1](https://doi.org/10.1130/G31450.1).
- Parsons, T., Thompson, G.A., and Sleep, N.H., 1994, Mantle plume influence on the Neogene uplift and extension of the U.S. western Cordillera?: *Geology*, v. 22p. 83-86.

## **Geologic History of Boulder Area, Colorado**

### **The rise and fall of Ancestral Rockies**

*Contributed by Rafael Almeida*

The oldest rocks in the Boulder area are Precambrian in age, and formed 1.7 billion Ga (Figure 16). The Precambrian rocks consist of granitic and metamorphic rocks. The predominant Precambrian granitic rock in the Boulder Canyon area is the Boulder Creek granodiorite, and it makes up the walls of Boulder Canyon. It also makes up the crest and west side of Flagstaff Mountain. There are no strata preserved in the Boulder area from before the Pennsylvanian. During the early part of the Pennsylvanian Period, about 300 million years ago, several mountain ranges were pushed up in central and western Colorado. These ranges are known as the Ancestral Rockies. The Ancestral Rocky Mountains are long gone, but might have been as high, or perhaps higher, than the current Rocky Mountains. In the uplift process, the miles of overlying rock were eroded away, exposing the granodiorite and pegmatites and submitting them to weathering. This chemical weathering formed a soil profile on the surface of the granodiorite, a process that is known as grussification. This can be observed along the Flagstaff Mountain road at the contact between the Boulder Granodiorite and the Fountain Formation at “Contact Corner”.

Erosion cut into these rocks and streams carried eroded sand and pebbles from the Ancestral Rockies, dumping the material in wide deposits of gravel. This debris was deposited as a mixture of coarse and fine fragments, forming the sandstones and shales that make up the Fountain Formation. The Fountain Formation crops out along the Front Range in Colorado. It forms the Flatirons west of Boulder as well as the Red Rocks near Morrison and the Garden of the Gods near Colorado Springs. Most of the Fountain Formation can be called an arkose, a coarse, feldspar-rich sandstone that is typically pink in color because of the abundant pink feldspar grains within it. It was deposited by alluvial fans and braided streams draining off a nearby mountain uplift, part of the Ancestral Rockies. Much of Central Colorado was uplifted during this mountain-building event, which occurred about 230 million years before the modern Rockies were raised. The Fountain Formation was deposited about 290-296 million years ago.

In some parts of the Fountain Formation you can easily see the channels and cross-beds (small dune-like forms) that indicate deposition by streams. Although most of the grains (both pink feldspar and buff to white quartz) are coarse sand size (around 2 mm and sometimes larger), you should be able to find extremely coarse individual clasts. Feldspar crystals an inch or more long may show perfectly flat cleavage (breakage) faces. Most of the pink color comes from feldspar, but in some zones a dark purplish color is probably imparted by hematite (iron oxide) cement. The Fountain Formation is pretty crumbly, which indicates that it is not very well

cemented. Together with its coarse grain size, this is evidence for a deposit that was laid down very near the source area. Further evidence for this is the presence of feldspar, which is unstable relative to quartz. In mature sandstones that have been transported great distances, most of the feldspar has weathered to clay and is gone, leaving only clean quartz in environments like beaches. Even more evidence for the proximity of the source of the Fountain sediments is the fact that in most areas of the Front Range, these rocks lie directly upon 1.7-billion-year-old Precambrian rocks. The surface between the Precambrian rocks and the Fountain Formation is called an unconformity, and it represents a time break of nearly one and one-half billion years for which there is no rock record. If any rocks were deposited during this interval, they were eroded during the uplift of the Ancestral Rockies. The Formation was originally laid down flat, but was steeply tilted during the uplift of the modern Rockies. The Flatirons, Red Rocks, and Sanitas Ridge, all directly west of Boulder, are composed of Fountain Formation.

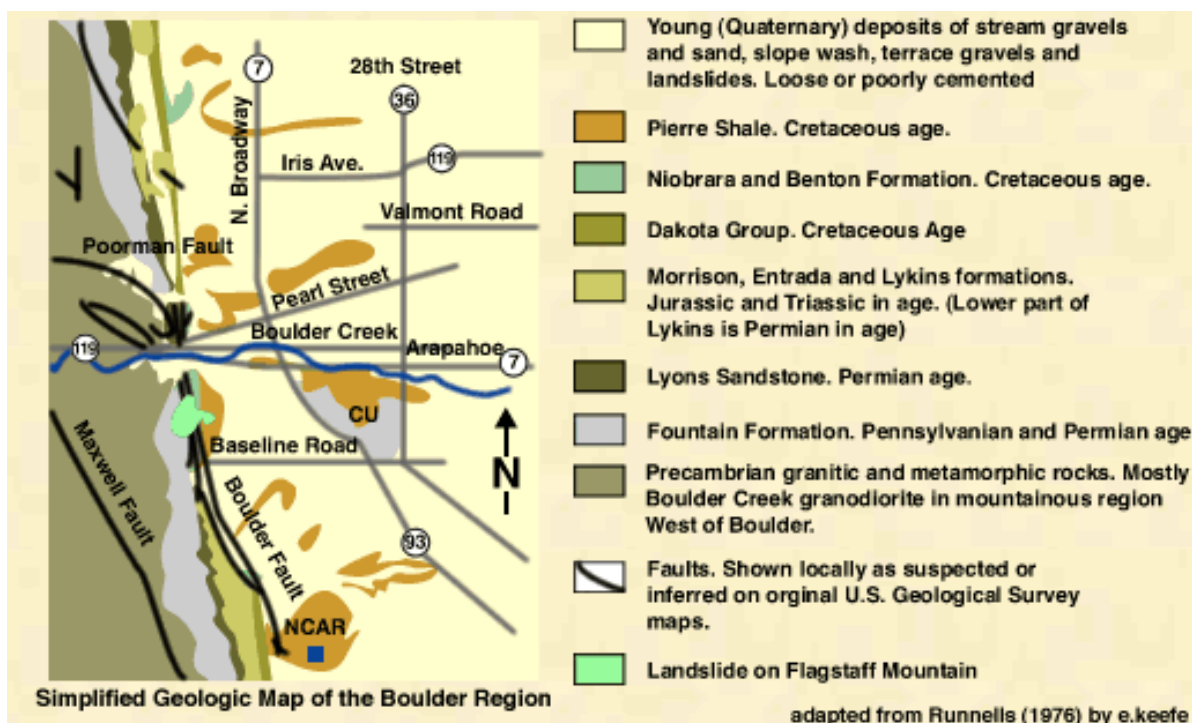


Figure 16. Geologic map of the Boulder area. From: <http://bcn.boulder.co.us/basin/natural/geology/geolmap.html>

During the Permian Period, about 260 million years ago, the sea began to creep in from the east. The climate on the land was that of a desert, with vast areas of sand dunes being blown about by the wind. These sands buried the older Fountain Formation to depths of at least 220 feet in this region, forming the Lyons Sandstone. The rock hardened from finely textured sediments that were deposited as the Ancestral Rocky Mountain Range continued to erode. Sand dunes and beach deposits formed here when Boulder was a hot, arid desert adjacent to a wide shallow sea to the east. The Lyons Sandstone is very hard, forming ridges (hogbacks) in most places along the Front Range. You will see the Lyons sandstone as flagstone sidewalks and patios throughout Colorado, as well as in buildings at the University of Colorado.

Around 250 million years ago erosion reduced the Ancestral Rockies to lowlands along the margin of the shallow sea. During the next 20 million years or so, during the end of the

Permian and part of the Triassic Period, the Boulder area was marked by broad, flat floodplains, with rivers flowing lazily to the east. Soft muds and silts were carried by the streams, to be deposited to a thickness of about 675 feet on top of the older, underlying Lyons sandstone. These deposits are preserved today as the bright red Lykins Formation. The Lykins formation is soft, consisting mostly of shale, sandstone, and siltstone. It forms the Lykins Valley, just west of the first hogback west of Boulder. The remainder of the Triassic period was marked by a continuation of the gentle uplift and erosion that had characterized earlier Permian time, and deposits of this time are absent in the Boulder area. Stromatolites, limestone fossils of slimy layered mounds of photosynthetic cyanobacteria (blue-green algae), also formed in the salty waters. On the Mallory Cave Trail, just west of the Mesa Trail, there is a large grey rock by the side of the trail. Close inspection will reveal the thin, onion-like layers of a stromatolite. Deposits are also absent for most of the Jurassic Period. But in late Jurassic time, about 150 million years ago, a desert environment and widespread sand dunes had again formed in western Colorado and eastern Utah. The thin eastern edge of this field of sand is preserved in the Boulder area in the form of light-colored, cross-bedded Entrada Sandstone, about 30 feet thick.

Late in Jurassic time, floodplain conditions again developed, and the Morrison Formation was deposited. The deposition of the Morrison Formation marks the complete erosion and burial of the Ancestral Rocky Mountains. The Morrison formation consists of about 300 feet of brown, green, red, and blue mud, volcanic ash, silt, and sand. The soft rocks of the Morrison Formation are famous for dinosaur fossils. Although not commonly seen in the Boulder area, dinosaur bones are abundant elsewhere in the Morrison Formation, particularly near the town of Morrison, at Dinosaur Ridge in Golden, and in Dinosaur National Monument. These sediments were carried across broad, swampy lowlands by rivers flowing eastward from highlands and volcanic areas far to the west in Utah and Nevada. The moist and hospitable climate supported an abundance of life, including dinosaurs.

At the start of the Cretaceous Period, about 135 million years ago, sands and gravels were carried eastward over the Boulder area from mountains rising to the west in Utah and Nevada. At about the same time, a massive invasion by the sea began in eastern Colorado. The sea entered the central U.S. from the north and south, laying down a deposit of beach sand along its edge, known as the lower part of the Dakota group. The group of formations, including some marine shales, is about 320 feet thick near Boulder. The lower sandstone of the Dakota is very hard and resistant to erosion, so that it stands in stark relief above the softer sediments above and below it, forming the first hogback west of Boulder. The Dakota hogback can be traced both to the north and south along the eastern side of the Front Range for hundreds of miles, all the way from Colorado Springs north to the Wyoming border. Extensive ripple marks are preserved in the Dakota sandstone. Besides being a major source of groundwater, Dakota Sandstone has been extensively mined for fire clay and contains a third of the state's oil and gas deposits in the Denver Basin. You can see this formation at Echo Rocks, and by the water tank just west of the National Center for Atmospheric Research (NCAR). You can also hike over Dakota Ridge on the NCAR Trail (west of NCAR), the Red Rocks trails north of Canyon Blvd., and the Dakota Ridge Trail in north Boulder.

The next 70 million years of Cretaceous time were marked by several advances and retreats of the sea. The deposits associated with these episodes of marine flooding consist of shale, sandstone, limestone, and some beds of coal. The environments suggested by the rocks include the deep sea, sandy beaches, and coast swamps. Names applied to the various formations are (from oldest to youngest): the Benton Shale, Niobrara Limestone, Pierre Shale, Fox Hills

Sandstone, and the Laramie Formation. Together these formations total over 10,000 feet of sediment. Fossils are abundant in many of these units. These strata are generally soft and easily eroded. The city of Boulder and the National Center of Atmospheric Research (NCAR) are built on the Pierre Shale. The fresh Pierre is gray, soft, and best seen in fresh roadcuts and ditches. At the end of Cretaceous time, about 70 million years ago, the sea slowly withdrew to the northeast. It left behind vast swamps, from which the coals of the Laramie Formation formed. The withdrawal of the sea took about 10 to 15 million years.

Between about 68 and 40 million years ago the present Laramide Rocky Mountains were uplifted. The 1.7 billion year old Boulder Creek Granodiorite and pegmatites that had been covered by younger rocks were uplifted once again, and the 10,000 feet of overlying sedimentary rock layers were tilted and eroded exposing the ancient igneous rocks. During this uplift, the Fountain Formation (which forms the Flatirons), the Dakota Ridge sandstone, and the other rock layers were tilted to their present position. During the Laramide uplift there were some igneous intrusions. An example of this is the prominent Valmont Dike, a nearly vertical igneous intrusion into the overlying Pierre Shale. Because igneous rock is harder than the surrounding sedimentary rock, it has resisted erosion and forms a visible landmark east of Boulder. Where the magma reached the surface of the earth, it spewed out in the form of volcanic eruptions. Only the scattered remains of lava flows can be seen in the Boulder area, such as on the tops of North and South Table Mountains near Golden. Active mountain building continued throughout the Paleocene and Eocene and to a lesser degree through the Quaternary. It is probable that the Rockies attained their greatest height in the early Tertiary Period, about 45 million years ago. Those peaks were later lowered by erosion.

As streams carried rock debris out of the mountains, coarse gravel and huge boulders covered the gently sloping surfaces along the mountain front. Over time, streams eroded and cut through these gravel- and boulder-covered surfaces, leaving a patchwork of higher, gravel-capped areas separated by lower erosion channels where streams cut through the soft older rock layers beneath. Looking southwestward from the city of Boulder toward the Flatirons, a series of these flat-topped mesas is visible. These mesas are remnants of erosional surfaces, called pediments, that developed during lulls in regional uplift. Throughout the history of mountain building, streams continued to erode and transport rock debris out onto the plains east of the mountain front, producing these flat surfaces. The highest of the several mesas formed by these ancient streams is about 1000 feet higher than Boulder, showing that at least that much uplift of the mountains or downcutting by streams has occurred in fairly recent geologic history. NCAR Mesa is one of the gravel-capped areas created by this erosion process, with Skunk Creek to the north and Bear Canyon Creek to the south. From the Boulder Valley Trail in north Boulder you can see the pyramid shape of Haystack Mountain. This is another example of an isolated mesa remnant. Thousands of years ago, Haystack Mountain was actually the southeastern tip of Table Mountain. A former channel of Lefthand Creek cut through this mesa, creating a valley that separated Haystack Mountain from Table Mountain. Haystack Mountain now stands on its own, an isolated hilltop that has resisted erosion.

The relative thickness and main characteristics of the aforementioned sedimentary units can be observed in Figure 17.

### Sedimentary Rocks of the Boulder Valley

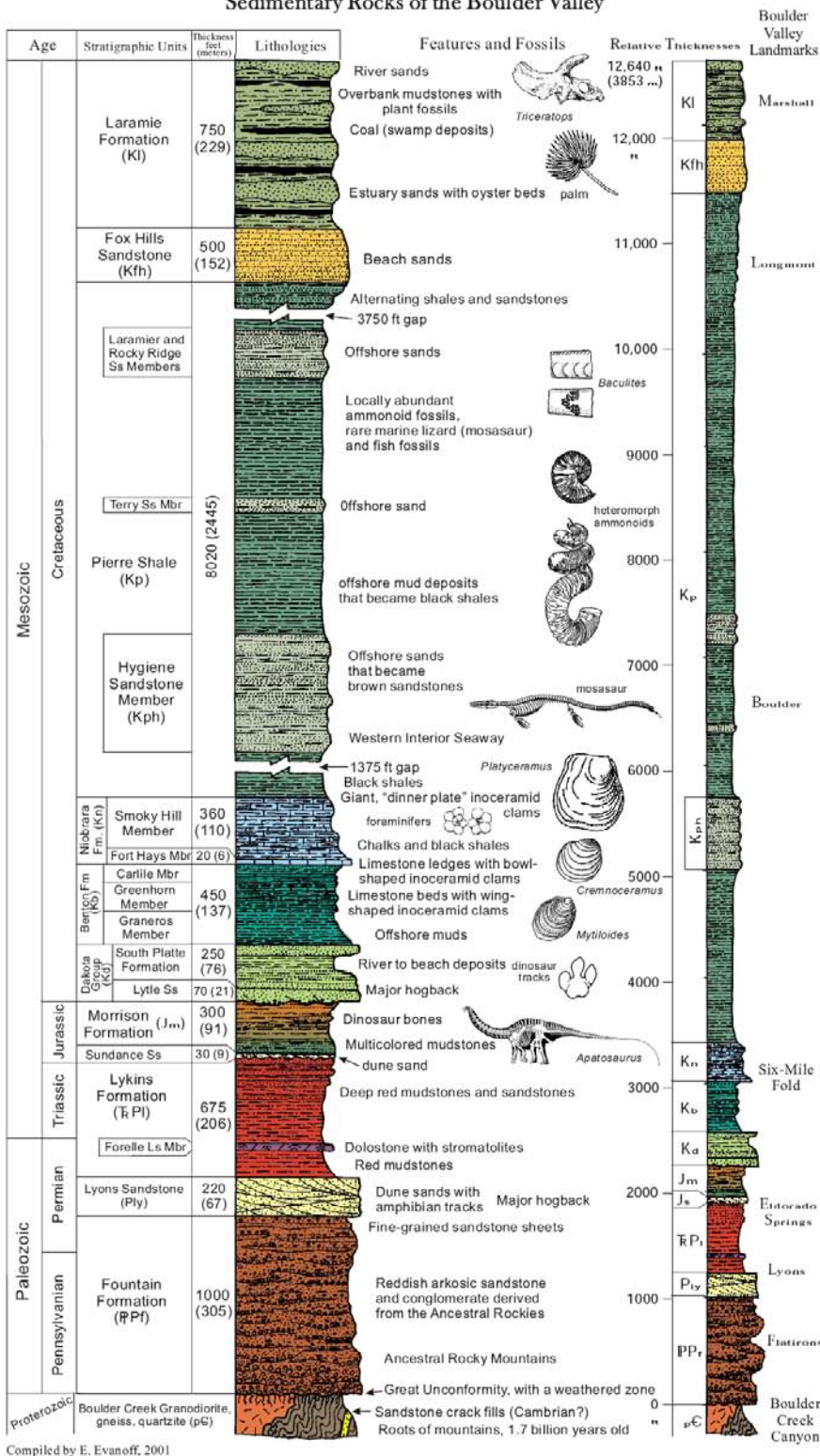


Figure 17. Stratigraphic column showing main characteristics of the sedimentary units of the Boulder area. From : [www.bouldercolorado.gov/files/openspace/pdf\\_education/Boulder\\_Sediments.pdf](http://www.bouldercolorado.gov/files/openspace/pdf_education/Boulder_Sediments.pdf)

## Yellowstone Hotspot

### Volcanism Associated with Yellowstone hotspot (Snake River Plain)

*Contributed by Natalia Zakharova*

The Snake River Plain is a prominent arc-shaped depression across southern Idaho that extends about 400 miles in an east-west direction and has the width of about 50-125 miles (Figure 18) [1]. Although the plain is continuous, its structure differs in the western and eastern parts. The western Snake River Plain (WSRP) is a large tectonic graben or rift valley while the eastern Snake River Plain (ESRP) is a large structural downwarp that formed due to the weight of the overlying volcanic rocks tracing the migration of the Yellowstone hotspot. The western plain began to form around 11-12 Ma with the eruption of rhyolite lavas and ignimbrites. It is now filled with several km of lacustrine (lake) sediments that are underlain by rhyolite and basalt, and in some places overlain by basalt. The WSRP is not parallel to North American Plate motion, and lies at a high angle to the eastern Snake River Plain, which traces the path of the North American plate over the Yellowstone hotspot. The eastern plain is a topographic depression that cuts across Basin and Range Mountain structures, more or less parallel to North American plate motion. It is underlain mostly by basalt erupted from numerous volcanic vents. Beneath the basalts are rhyolite lavas and ignimbrites that erupted as the lithosphere passed over the hotspot [2].



Figure 18. Topographic expression of the Snake River Plain.

The Yellowstone hotspot activity started 17 Ma under McDermitt caldera in northern Nevada [3]. Initial melting formed a flood basalt province (Columbia River Basalt Group, CRBG) followed by the initiation of time-transgressive volcanism trending NE from its initial position under McDermitt caldera to its final position under the Yellowstone Caldera (Figure 19). The CRBG is a continental flood basalt province that covers over 70,000 square miles of the Pacific Northwest (in Washington, Oregon and Idaho), with a total estimated volume of 53,700 cubic miles [4]. The flood basalts erupted from linear fissures between 17.5 and 6 Ma ago (late

Miocene-early Pliocene). The CRBG consists of a sequence of over 300 tholeiitic basalt flows, the majority of which erupted during a period of 2.5 million years (17-14.5 Ma ago). During this peak activity, many individual flows exceeded 1,000 km<sup>3</sup> in volume, and traveled hundreds of miles from their vent source. Each flow represents a single extrusive event that may cover as much as 5,000 mi<sup>2</sup>.

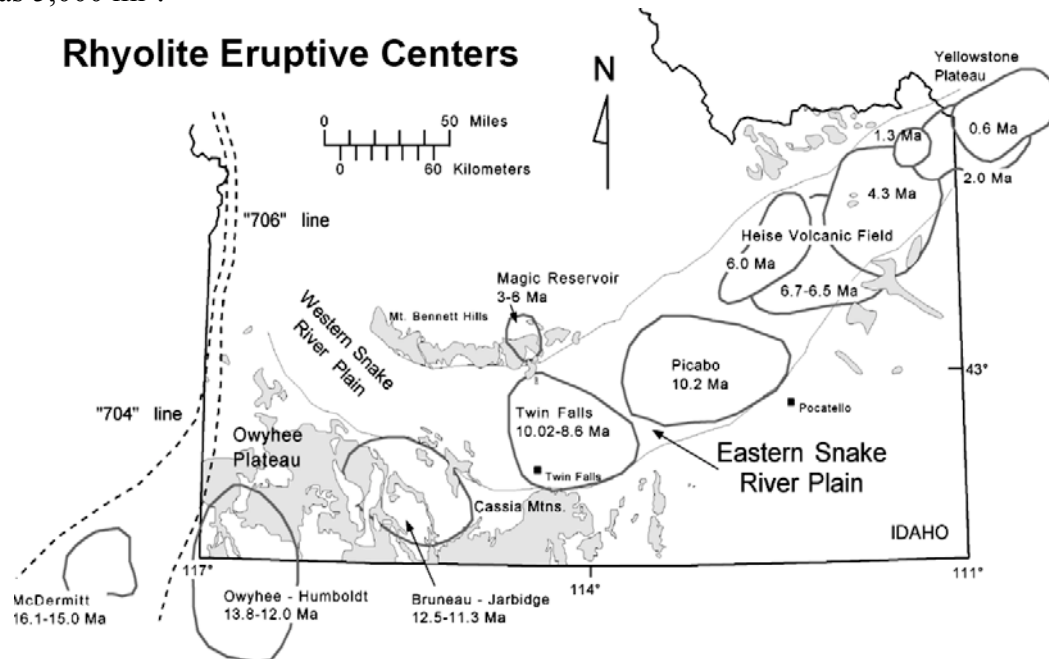


Figure 19. Time-transgressive volcanism of the eastern Snake River Plain.

The plume head–plume tail paradigm is generally accepted as the model that best explains the large volume of the initial flood basalts and the subsequent time-transgressive nature of the younger volcanics (Figure 20) [5]. CRBG are attributed to the large plume head, while the rhyolite caldera complexes of the eastern Snake River Plain mark the positions of the plume tail as the North American Plate moved westward over the plume. The rhyolitic calderas become younger to the northeast and include McDermitt, Owyhee- Humboldt, Bruneau-Jarbridge, Twin Falls, Picabo, Heise, and Yellowstone caldera complexes (Figure 19). The silicic volcanics associated with the Yellowstone hotspot are represented by ignimbrites and ash-tuff deposits. These deposits are overlain by about a mile of younger basaltic lava fields, polygenic eruptive centers, and rhyolite domes. Many of the basalts of the ESRP erupted along volcanic rift zones that are oriented parallel to the direction of regional Basin and Range extension.

#### References:

- [1] [http://en.wikipedia.org/wiki/Snake\\_River\\_Plain](http://en.wikipedia.org/wiki/Snake_River_Plain)
- [2] [http://geology.isu.edu/Digital\\_Geology\\_Idaho](http://geology.isu.edu/Digital_Geology_Idaho)
- [3] Shervais and Hanan, 2008, Lithospheric topography, tilted plumes, and the track of the Snake River–Yellowstone hot spot, *TECTONICS*, VOL. 27, TC5004.
- [4] Hooper, 1988, The Columbia River Basalt, in *Continental Flood Basalts* (pp. 1-33), ed. By Macdougall, Kluwer Academic Publishers.
- [5] Camp and Ross 2004, Mantle dynamics and genesis of mafic magmatism in the intermontane Pacific Northwest, *J. Geophys. Res.*, 109.

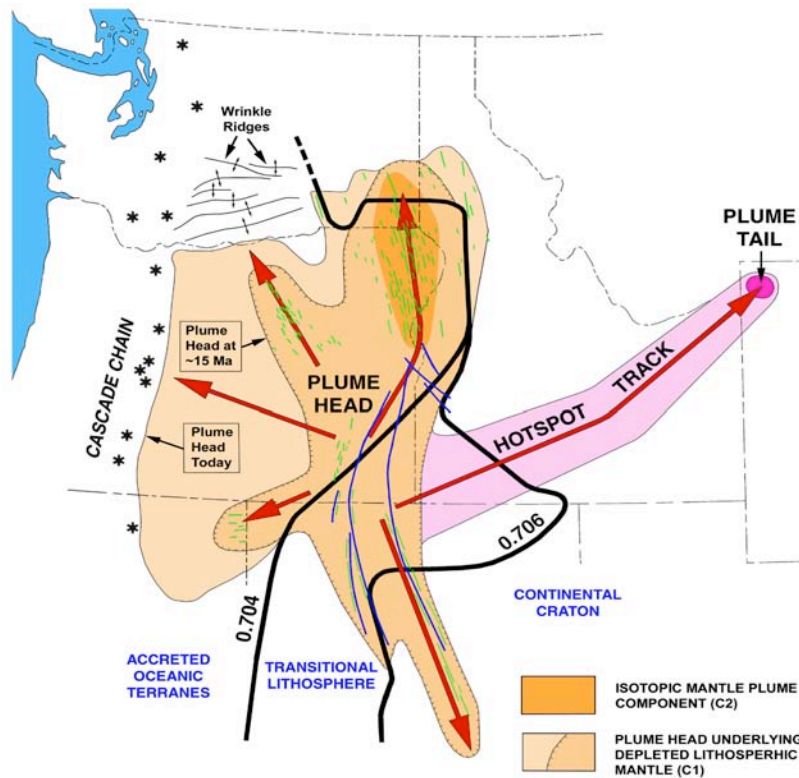


Figure 20. Two-stage spreading model of the Yellowstone mantle plume [5].

## Volcanism of Yellowstone National Park

*Contributed by Jason Jweda*

Yellowstone National Park, the first national park in the world, is one of the most popular and scenic parks in North America partly because it is one of the most geologically-volcanically-hydrothermally dynamic areas on the planet. Yellowstone NP spans almost 9,000 km<sup>2</sup> of northwestern Wyoming (the western and northern edges of the park overlap with Idaho and Montana) and is located at the eastern terminus of the Snake River Plain over the current position of the Yellowstone hotspot. Although Yellowstone derives most of its beauty and geological-geothermal phenomena from the current hotspot volcanic activity, the park actually contains the remnants of two volcanic systems: the Absaroka Volcanics and the Yellowstone Calderas (Huckleberry Ridge, Island Park – just outside the park, and Lava Creek).

The Absaroka Range is a large (9,000 mi<sup>2</sup>) volcanic field that is composed of ~5,000 ft of interlayered basaltic (and some andesitic) volcanoclastic rocks and lahar (volcanic mudflows) deposits (Figure 21) that were deposited during the Eocene (~45 Ma) [1]. The Absarokas stretch from the Bighorn Basin to the Yellowstone Caldera and form the skyline on the eastern and northeastern sides of the park, which is especially apparent when looking east across Yellowstone Lake. Three main vents for the Absaroka volcanics have been identified, but only the Washburn Range is easily accessible within the park (Figure 21). Mt. Washburn rises to just over ~10,000 ft. and consists of north-dipping dark breccia layers that were deposited over a 10 Myr time period [2]. Interestingly, the volcanic layers only appear to slope to the north and no

evidence of these rocks can be found to the southwest. Early geologists once believed that the Absarokas were associated with the same volcanic activity that produced the Yellowstone Calderas. However, in 1961 Francias Boyd recognized that the high elevation Absaroka Volcanic field (composed of basaltic volcanoclastic rocks) was in fact truncated by the low-lying rhyolitic welded-tuffs of the Yellowstone Caldera [2]. It was further demonstrated that the Absaroka volcanics were not only ~45 Myr older than the Yellowstone rhyolites but they were geochemically distinct as well. Based on the calc-alkaline nature and trace element patterns of Absaroka volcanics, and geological evidence for thick-skinned shortening in the western U.S. during the Eocene, the origin of the Absarokas has been attributed to mantle and lower crustal melting associated flat-slab subduction of the Farallon Plate [3, 4, 5].

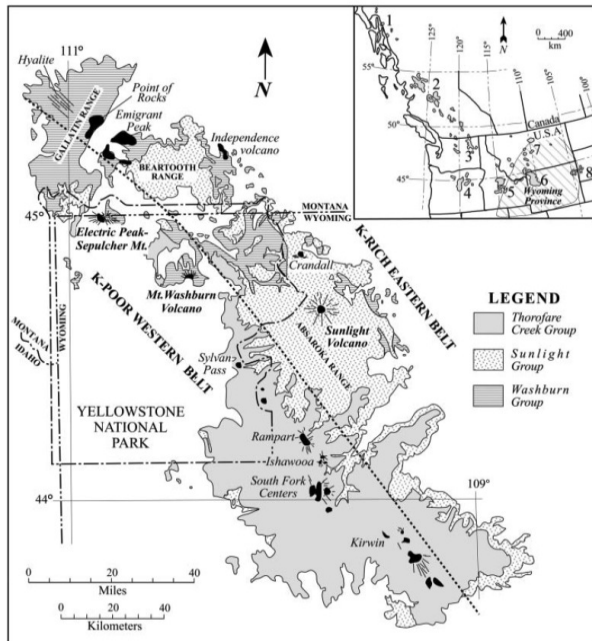


Figure 21. Absaroke Volcanic Province. (a) Map of the province, from [5]; (b) picture of layered basaltic-andesitic volcanoclastic rocks and lahar deposits in the Absaroka Range near Dubois, WY; (c) picture of Absaroka lahar deposit with hammer for scale. Photos © Jason Jweda

The Yellowstone Volcano is the largest volcanic system on the North American continent and has been called a “supervolcano” because of the extremely large explosive eruptions that have been (and could be) generated at the volcano. Volcanism at Yellowstone is the current expression of sublithospheric mantle and crustal melting associated with a convective thermal mantle plume. Although the Yellowstone hotspot migration has produced caldera-forming eruptions across North America since ~17 Ma (see Volcanism associated with Yellowstone hotspot section of this field guide), there have been three exceptionally large eruptions under Yellowstone NP within the last 2.1 Myr that have been identified based on the locations of caldera rims and associated welded-tuffs. Figure 22 shows the locations of these most recent caldera-forming eruptions as well as two resurgent domes in Yellowstone NP. These eruptions have ejected exceptionally voluminous rhyolitic pyroclastic tuffs and coeval ash fall deposits. The first and most explosive of these eruptions occurred at 2.1 Ma and formed the Huckleberry Ridge Caldera, one of the largest known explosive volcanic eruptions on Earth (Figure 23). Estimates suggest that ~600 mi<sup>3</sup> of volcanoclastic material was ejected during

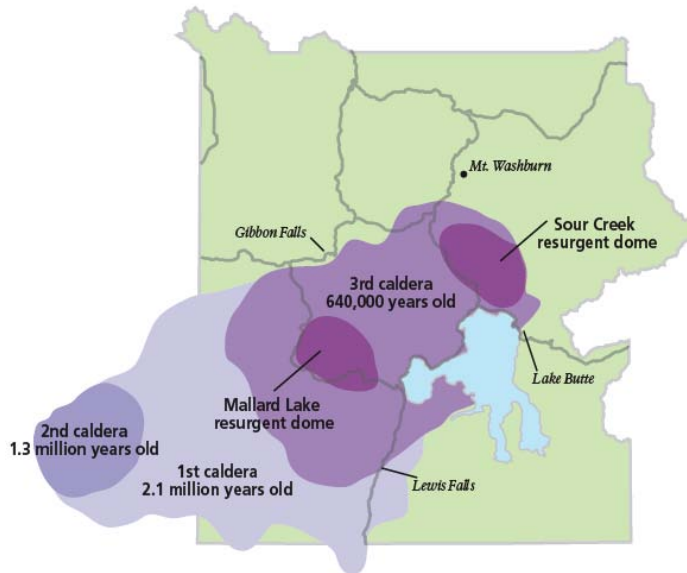


Figure 22. Location of Yellowstone calderas and resurgent domes generated within the last 2.1 Myr. 1<sup>st</sup> Caldera at 2.1 Ma produced the Huckleberry Ridge Tuff; 2<sup>nd</sup> Caldera at 1.3 Ma (Island Park Caldera) produced the Mesa Falls Tuff; and the 3<sup>rd</sup> Caldera at 0.64 Ma (current Yellowstone Caldera) produced the Lava Creek Tuff. From [7].

the eruption, ~2,400 times as much as that of the 1980 Mt. St. Helens eruption. The ensuing pyroclastic flows from this volcanic event produced the Huckleberry Ridge Tuff, a thick welded-tuff covering a staggering 15,000 km<sup>2</sup>, and spread ash as far away as Iowa. The second and least explosive caldera-forming eruption occurred at 1.3 Ma and produced the Island Park Caldera, which is the smallest of the three calderas. The most recent caldera-forming eruption at Yellowstone occurred at 0.64 Ma, which destroyed part of the Washburn Range and produced the Yellowstone Caldera and associated Lava Creek welded tuff. This eruption produced an ellipsoidal caldera that is approximately 50 miles in length and 30 miles in width. The internal stratigraphy and lack of evidence for significant erosion within the welded-tuffs indicate rapid accumulation (hours to a few days) of volcanoclastic material.

The majority of exposed igneous rocks in Yellowstone Caldera are post-caldera-forming rhyolite lavas that have erupted within the caldera periodically between ~600 ka and ~275 ka, and constitute the Plateau Rhyolite group (geologic map shown in Figure 24) [8]. Beginning ~170 ka, two resurgent rhyolitic domes have been uplifted within Yellowstone Caldera: (1) Mallard Lake dome, which is associated with a ‘relatively’ smaller caldera forming eruption that produced a 10 km diameter caldera in the West Thumb of Yellowstone Lake; and (2) Sour Creek dome located northeast of Yellowstone Lake. It is estimated that magma resides at a depth of 3-8 miles below Sour Creek dome and at a depth of 8-12 miles below Mallard Lake dome. The most recent intra-caldera volcanic activity, ending ~70 ka, produced large rhyolitic lavas that buried the caldera floor. Extra-caldera eruptions have both basaltic and rhyolitic lava flows between ~500 ka and ~80 ka, but significantly smaller in volume compared to the intra-caldera eruptions [8].

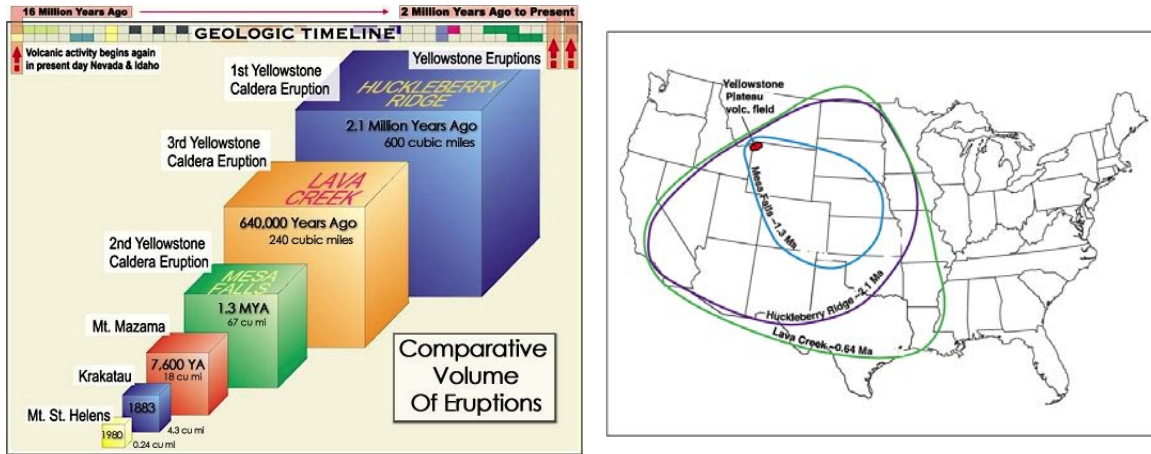


Figure 23. Volumes and spatial distribution of Yellowstone volcanics. (a) Comparative volumes of material ejected from different explosive eruptions. From [7]. (b) Inferred distributions of ash fall deposits from the three caldera-forming eruptions at Yellowstone. From [6].

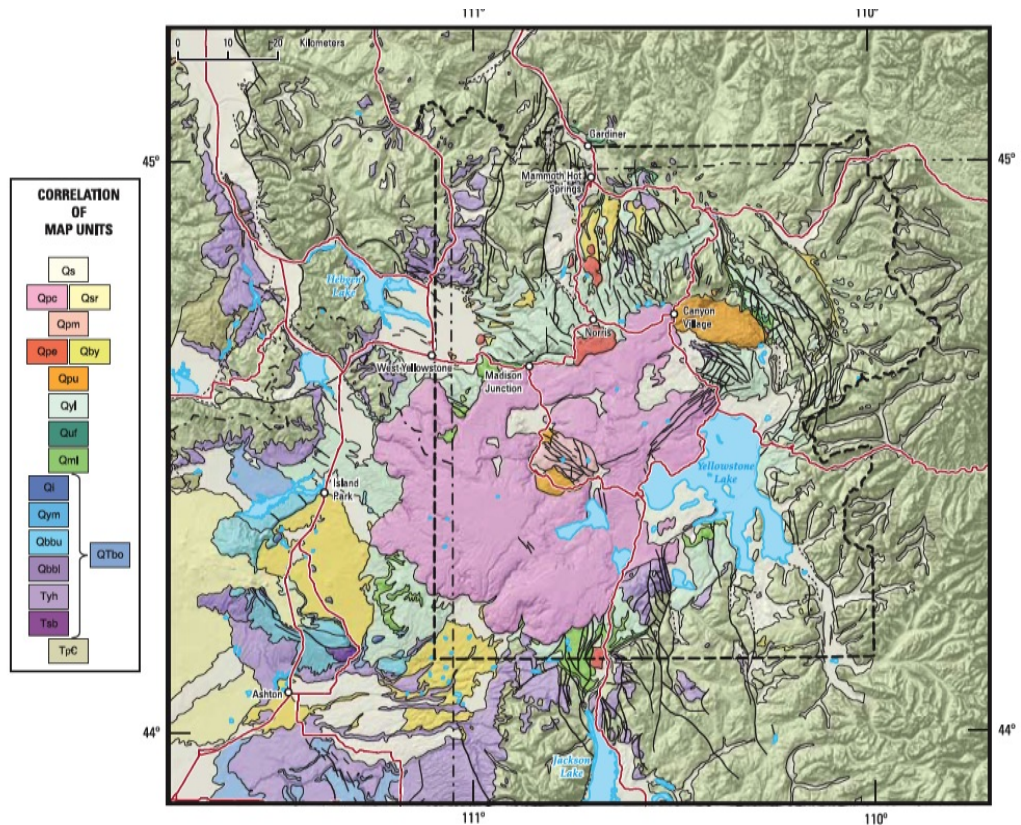


Figure 24. Geologic map of the Yellowstone National Park and surrounding areas. Symbols are: Qs is surficial deposits; Qpc is Central Plateau Rhyolite; Qsr is Snake River Basalts; Qpm is Mallard Lake Rhyolites; Qpe is extra-caldera rhyolites; Qby is extra-caldera basalts; Qpu is Upper Plateau Rhyolite; Qyl is Lava Creek Tuff; Quf is Undine Falls Basalt; Qml is Mt. Jackson and Lewis Canyon Rhyolites; Qi is Island Park Rhyolite; Qym is Mesa Falls Tuff; Qbbu is Upper Big Ridge Rhyolite; Qbbi is Lower Big Ridge Rhyolite, Tyh is Huckleberry Ridge Tuff; Tsb is Snake River Butte Rhyolit; and QTbo is older basalts. From [8].

**References:**

- [1] Wyoming State Geological Survey: Absaroka Range, <http://www.wsgs.uwyo.edu/StratWeb/AbsarokaRange/Default.aspx>
- [2] Good, J. M. and Pierce, K. L. (1996). Recent and Ongoing Geology of Grand Teton and Yellowstone National Parks.
- [3] Peterman, Z. E., Doe, B. R., and Prostka, H. J. (1970). Lead and strontium isotopes in rocks of the Absaroka volcanic field, Wyoming. *Cont. Min. Pet.*, 27, p. 121-130.
- [4] Lipman, P. W., Prostka, H. J., and Christiansen, R. L. (1972). Cenozoic volcanism and plate-tectonic evolution of the western United States. *Phil Tran Royal Soc London. A* 271, p. 217-248.
- [5] Feely, T.C., Cosca, M. A., and Lindsay, C. R. (2002). Petrogenesis and implications of calc-alkaline cryptic hybrid magmas from Washburn Volcano, Absaroka Volcanic Province, USA. *J. Pet.* 43, no. 4, p. 663-703.
- [6] Izett, G.A., and Wilcox, R.E. (1982) Map showing localities and inferred distribution of the Huckleberry Ridge, Mesa Falls, and Lava Creek ash beds (Pearlette family ash beds) of Pliocene and Pleistocene age in the western United States and southern Canada: U.S. Geological Survey Miscellaneous Investigations Map I-1325, scale 1:4 000 000.
- [7] Smith, R. B. and Siegel, L. J. (2000). *Windows into the earth: the geologic story of Yellowstone and Grand Teton national parks.* Oxford University Press, p. 242.
- [8] Christiansen, R. L., Lowenstern, J. B., Smith, R. B., Heasler, H., Morgan, L. A., Nathenson, M., Mastin, L. G., Muffler, L. J. P., and Robinson, J. E. (2007). Preliminary Assessment of Volcanic and Hydrothermal Hazards in Yellowstone National Park and Vicinity. U.S. Geological Survey Open-file Report 2007-1071, p. 94.

## **Thermal and Mechanical Effects of the Yellowstone Hotspot**

*Contributed by Yang Zha*

The North American plate has been moving southwestward over the Yellowstone hotspot for the past 17 Ma, at an approximate rate of 2 cm/yr [1]. The interaction of the moving continental lithosphere and a hotspot has produced extensive volcanic activity and extension. Over the past 17 million years the hotspot has caused a series of violent eruptions and basaltic flows. Some of the eruptions have produced more than 1000 cubic kilometers of ejecta, and are categorized as super-eruptions.

The eastern Snake River plain (SRP) is the result of this series of eruptions and active extension caused by the migration of the hotspot [2]. In the eastern SRP, there is a pattern of seismicity and late Quaternary faulting along the hotspot track. The region of high seismicity is bounded by two concentric parabolas whose apices are located over the Yellowstone Plateau (

Figure 25) [3]. However, many active normal faults terminate at the edge of the eastern SRP. There is very little seismicity inside the innermost parabola or outside the outermost parabola. GPS measurements suggest that strain rates in the eastern SRP are an order of magnitude smaller than the circum-SRP region [4]. Studies have also shown that faults are inactive within the eastern SRP, ruling out the possibility that aseismic creep accommodates extension in this region [3, 5].

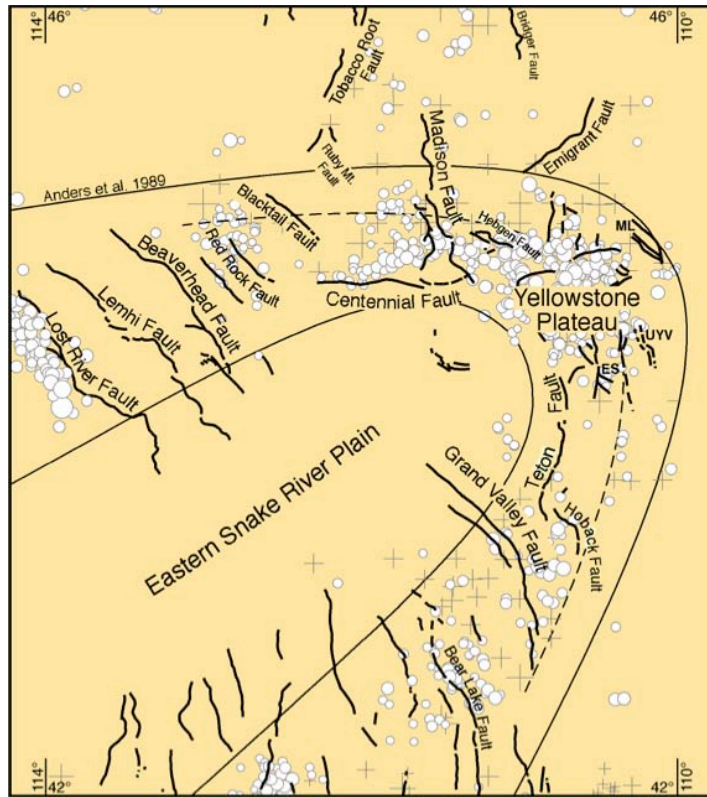


Figure 25. Map of the late Cenozoic normal fault and historic earthquakes in the region surrounding the Eastern Snake River Plain. (From Anders, 1994). Regions between the two parabolas indicate regions of high seismicity.

The intrusion of magma into the lithosphere from the underlying mantle plume has significant effects on the pattern of seismicity and faulting in the SRP. Seismic and gravity studies have indicated velocity anomalies in the lower crust and immediately beneath the Moho [6, 7]. These anomalies correspond to the intruded basaltic magma, and can explain the elevation contrast between the eastern SRP and the active seismic zones. One possible scenario involving the movement of the hotspot and magma intrusion can explain the lack of seismicity in the eastern SRP [2]. There are three phases in this scenario. In phase one, when the hotspot started interacting with the SRP, basaltic magma intruded into the crust and ponded at a density or permeability barrier near the base of the crust. The near solidus basaltic magma ( $\geq 1100^{\circ}\text{C}$ ) began to heat and then melt the surrounding granitic crust. In phase two, at  $\sim 2$  Myr after the onset of the interaction, the temperature in the crust was high enough that the total yield strength of the crust was reduced. This phase is the period in which most extension and faulting activities occurred. In phase three, the hotspot moved away from the SRP and the basaltic magma began to cool down. About 4 Myr after the onset of the interaction, the once molten magma became solid basaltic rock. Because the yield strength of basalt is greater than that of granite, the total yield strength of the lithosphere was greater than before the intrusion (Figure 26). Therefore the faulting activities ceased under the same horizontal stresses. The time period during which active faulting occurred is about 2 Myr to 4 Myr after the onset of the hotspot-lithosphere interaction. Considering the relative motion of the hotspot and the North

American plate, this active faulting region is represented by the area between the two parabolas in Figure 1.

To sum up, the Yellowstone volcanic field and the eastern Snake River Plain are results of the interaction of a hotspot and a region that was already undergoing active extension prior to the introduction of the hotspot [2]. Basaltic magma intruded into the lithosphere and subsequently the lower crust, changing the thermal and mechanical properties of the lithosphere. The magmatic intrusions along with the movement of the North American plate are responsible for the seismicity and faulting in the circum-SRP region, as well as the lack of seismicity in the eastern SRP.

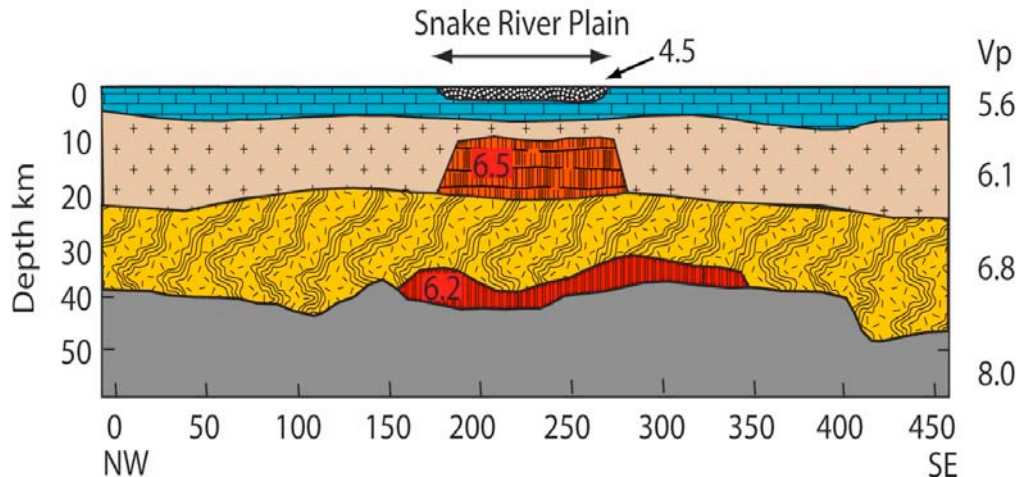


Figure 26. Schematic cross section of the crust with a sill complex beneath the eastern Snake River Plain. (From Shervais *et al.*, 2006.) Red indicates mafic intrusion.

#### References:

- [1] Anders, M.H., Constraints on North American Plate velocity from the Yellowstone hotspot deformation field, *Nature*, 369, 53-55, 1994.
- [2] Anders, M.H., and Sleep, N.H., 1992, Magmatism and extension: The thermal and mechanical effects of the Yellowstone hotspot: *J.Geophys. Res.*, v. 97, p. 15,379–15,393, doi: 10.1029/92JB01376.
- [3] Anders, M. H., J. W. Geissman, L. A. Piety, and J. T. Sullivan, Parabolic distribution of circum-eastern Snake River Plain seismicity and latest Quaternary faulting: migratory pattern and association with the Yellowstone hotspot, *J.Geophys. Res.*, v.94, p.1589-1621, 1989.
- [4] Suzette J. Payne *et al.*, Strain rates and contemporary deformation in the Snake River Plain and surrounding Basin and Range from GPS and seismicity. *Geology* 2008;v.36; p.647-650 doi: 10.1130/G25039A.1
- [5] Parsons, T., Thompson, G.A., and Smith, R.P., 1998, More than one way to stretch: A tectonic model for extension along the track of the Yellowstone hotspot and adjacent Basin and Range Province: *Tectonics*, v. 17, p. 221–234, doi: 10.1029/98TC00463.
- [6] Braile, L. W. et al., The Yellowstone-Snake River Plain seismic profiling experiment: crustal structure of the eastern Snake River Plain, *J. Geophys. Res.*, 87(B4), 2597-2609, 1982.
- [7] Sparlin, M. A., L. W. Braile, and R. B. Smith, Crustal structure of the eastern Snake River Plain determined from ray trace modeling of seismic refraction data, *J.Geophys. Res.*, 87, 2619-2633, 1982.
- [8] Shervais *et al.*, Layered mafic sill complex beneath the eastern Snake River Plain: Evidence from cyclic geochemical variations in basalt. *Geology* 2006, v.34, p. 365-368;doi: 10.1130/G22226.1

## Seismicity and Tomography of the Yellowstone Region

*Contributed by Raj Moulik*

The Yellowstone region is one of the major seismically active areas in the western U.S. and occupies the central part of the intermountain seismic belt (ISB) that separates the active tectonism to the west from the more stable part of the North American plate to the east (Smith and Arabasz, 1991). The earthquakes in this region provide an excellent source for regional earthquake tomography studies and are characterized by swarms of shallow events (e.g. Waite & Smith, 2002), that have a distinct spatial clustering and temporal correlation with the underlying geodynamic and hydrothermal processes. Imaging studies of the Yellowstone region have been done by various approaches to understand the mantle flow in the region and in order to ascertain whether a deep-mantle plume source is warranted.

The earthquake epicenters as well as the Late Quarternary normal faulting in the area show a parabolic pattern (Figure 25) about the axis of the aseismic eastern Snake River Plain (SRP) (Anders et al., 1989). Even though the eastern SRP itself is seismically quiescent and lacks faulting, it has notable Late Quaternary basaltic dikes of similar orientation to regional faults. Although some of the faults have been mapped and dated in the area, many seismogenic structures are buried under post-caldera rhyolite flows (Christiansen, 2001). Anders et al. (1989) attributed the outward migration of the increased fault activity along the northeastward trending hotspot track to the reduced integrated lithospheric strength caused by the thermal effects of the Yellowstone hotspot. The outwardly propagating quiescent region inside the inner parabola was attributed to the increased strength of the crustal lithosphere by the addition of mafic materials. Other authors have noted that the lack of earthquakes may also be related to high temperatures that inhibit earthquakes, or to complex stresses related to the Yellowstone hotspot apart from the increased crustal strength resisting earthquakes (e.g. Smith and Arabasz, 1991).

The seismicity in the Yellowstone Caldera is characterized by shallow hypocenters with identified spatial & temporal clusters (Farrell et al., 2009) and occasional moderate-sized earthquakes like the  $M_s$  6.1 in 1975 near Norris Junction (Pitt et al., 1979). The most seismically active area is associated with the 1959,  $M_s$  7.5, Hebgen Lake main shock that occurred about 30 km from the northwestern side of the caldera. This large earthquake may have resulted from unusual lithospheric uplift and viscoelastic relaxation associated with the Yellowstone hotspot (Smith and Arabasz, 1991). The most intense seismicity usually occurs between the Hebgen Lake fault and the northern rim of the Yellowstone caldera. The released seismic moment is concentrated between the Hebgen Lake fault and the caldera, implying the dominance of aseismic mechanisms for the caldera (Smith et al., 2009). Some of the intra-caldera earthquakes are associated with hydrothermal areas such as the Mud Volcano and the Geyser Basin. The geophysical evidence suggests that Yellowstone earthquakes in general are influenced by the presence of magmas, partial melts, and hydrothermal activity at crustal depths from near surface to depths of ~5 km (Smith and Arabasz, 1991), and are probably related to variations in heat flux and rock composition.

The shallow crustal structure in the area was studied by inverting a P & S-wave velocity structure and improved hypocenter locations from local earthquake and controlled source tomography to show strong evidence for crustal magma chambers (Miller and Smith, 1997). While the higher wave velocities outside the caldera coincided with thermally undisturbed basement and sedimentary rocks, the decrease across the caldera is thought to be coincident with a negative gravity anomaly and is interpreted as a hot, sub-solidus, granitic batholith. The localized reductions at 8 km and 4 km depths beneath Yellowstone's domes are

interpreted as deeper partial melts and vestigial magma systems thermally driving the shallow hydrothermal fracture zones.

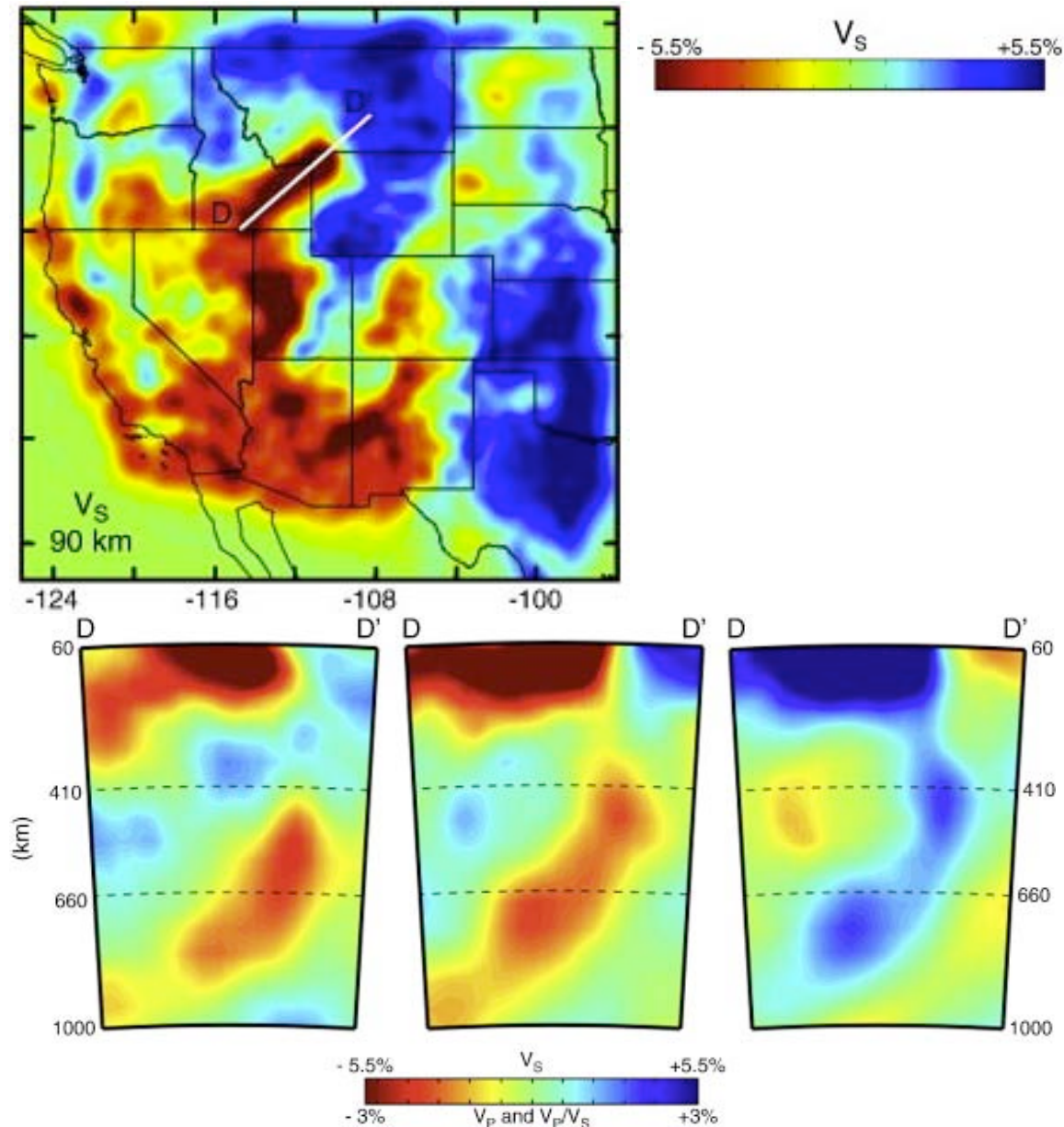


Figure 27. Map view of shear velocity anomalies and tomographic cross-sections through the eastern SRP and Yellowstone from Schmandt & Humphreys, 2010. The location of the cross-section D-D' is labeled on the map. All panels show the same section. Below are the Isolated  $V_p$  model (left), isolated  $V_s$  model (center), and  $V_p/V_s$  model from the joint inversion (right).

Many studies have pointed to a mantle plume source for the Yellowstone hotspot (e.g., Morgan, 1971; Smith and Sbar, 1974; Anders and Sleep, 1992) though the depth extent of the source remains an unresolved question. Some studies have suggested there is no definitive evidence for or against a mantle plume (e.g. Humphreys et al., 2000), while others have argued against a plume source (e.g. Christiansen et al., 2002). The most compelling evidence against a

plume source has been the lack of a clear seismic image of the plume in regional P-wave tomography studies (Christiansen et al., 2002, Waite et al., 2006). While these regional studies show a low-velocity anomaly to at least 200 km depth, the limitations in the data may preclude resolution of deeper anomalies.

Global P wave tomography models (e.g. Bijwaard et al., 1998; Montelli et al., 2004) are a part of the ongoing debate about the interpretation of the low-velocity anomaly beneath Yellowstone as a conventional plume, as the observed anomaly does not continue into the lower mantle. Moreover, newer travel-time tomography studies (e.g. Smith et al., 2009; Schmandt & Humphreys, 2010) also do not find a strong low-velocity conduit that extends continuously into the lower mantle. However, Schmandt & Humphreys (2010) observe very weakly connected shallow and deep anomalies extending to the depths of ~900 km (Figure 27).

Global S-velocity models (Kustowski et al., 2008; Ritsema et al., 2010; Panning & Romanowicz, 2006) consistently show a slower S-velocity region around the Basin & Range and shear-wave anisotropy (when resolved) of around 4-6% in the shallow mantle. Global shear attenuation models such as by Dalton et al. (2008) show higher attenuation consistent with the low velocity region found in the velocity models and interpret this as a suggestion that the same factors may control both seismic attenuation and velocity at this depth range. As the resolution of the tomography images increases, and the earthquake sources and their distribution are further studied, additional insights into Yellowstone may be obtained.

#### References:

- Anders, M.H., Geissman, J.W., Piety, L.A., Sullivan, J.T., 1989. Parabolic distribution of circumeastern Snake River Plain seismicity and Late Quaternary faulting: migratory pattern and association with the Yellowstone hotspot. *J. Geophys. Res.* 94, 1589–1621.
- Anders, M.H., Sleep, N.H., 1992. Magmatism and extension: The thermal and mechanical effects of the Yellowstone hotspot. *J. Geophys. Res.* 97, 15,379–15,393.
- Bijwaard, H., W. Spakman, and E. R. Engdahl (1998), Closing the gap between regional and global travel time tomography, *J. Geophys. Res.*, 103, 30,055–30,078.
- Christiansen, R.L., 2001. The Quaternary and Pliocene Yellowstone Plateau volcanic field of Wyoming, Idaho, and Montana. *U. S. Geol. Surv. Prof. Pap.* 729-G. U. S. Geol. Surv., Denver, CO. 120 pp.
- Christiansen, R. L., G. R. Foulger, and J. R. Evans (2002), Upper-mantle origin of the Yellowstone hotspot, *Geol. Soc. Am. Bull.*, 114, 1245–1256.
- Dalton, C.A., G. Ekström, and A.M. Dziewonski (2008), The global attenuation structure of the upper mantle, *J. Geophys. Res.*, 113, B09303, doi:10.1029/2007JB005429.
- Farrell, S., Husen, R.B., Smith, 2009. Earthquake swarm and b-value characterization of the Yellowstone volcano-tectonic system. *J. Volcanol. Geotherm. Res.* 188, 260–276.
- Humphreys, E. D., K. G. Dueker, D. L. Schutt, and R. B. Smith (2000), Beneath Yellowstone; evaluating plume and nonplume models using teleseismic images of the upper mantle, *GSA Today*, 10, 1–7.
- Miller, D. S. and R. B. Smith, 1999, P and S velocity structure of the Yellowstone volcanic field from local earthquake and controlled source tomography, *J. Geophys. Res.* v. 104, 15,105-15,121.
- Montelli, R., G. Nolet, F. A. Dahlen, G. Masters, E. R. Engdahl, and S.-H. Hung (2004), Finite-frequency tomography reveals a variety of plumes in the mantle, *Science*, 303, 338–343, doi:10.1126/science.1092485.
- Morgan, W. J. (1971), Convection plumes in the lower mantle, *Nature*, 230, 42–43.
- Nettles, M., and A. M. Dziewonski, Radially anisotropic shear-velocity structure of the upper mantle globally and beneath North America, *J. Geophys. Res.* 113, B02303, doi:10.1029/2006JB004819, 2008.
- Panning, M.P., and B.A. Romanowicz, "A three dimensional radially anisotropic model of shear velocity in the whole mantle," *Geophys. J. Int.* 167, 361-379, 2006
- Pitt, A.M., Weaver, C.S., Spence, W., 1979. The Yellowstone Park earthquake of June 30, 1975. *Bull. Seismol. Soc. Am.* 69, 187–205 *Geol. Surv.*, Denver, CO, 39 pp.
- Smith, R.B., Arabasz, W.J., 1991. Seismicity of the Intermountain Seismic Belt. In: Slemmons, D.B., Engdahl, E.R.,

- Zoback, M.L., Blackwell, D.D. (Eds.), Neotectonics of North America. Geological Society of America, Boulder, CO, pp. 185–228
- Smith, R.B., Jordan, M., Steinberger, R., Puskas, C.M., Farrell, J., Waite, G.P., Husen, S., Chang, W.-L., O'Connell, R., 2009. Geodynamics of the Yellowstone hotspot and mantle plume: seismic and GPS imaging, kinematics, and mantle flow. *J. Vol. Geotherm. Res.* 188, 26–56
- Smith, R. B., and M. L. Sbar (1974), Contemporary tectonics and seismicity of the western United States with emphasis on the Intermountain Seismic Belt, *Geol. Soc. Am. Bull.*, 85, 1205–1218.
- Schmandt, B. & Humphreys, E. D. Complex subduction and small-scale convection revealed by body-wave tomography of the western United States upper mantle. *Earth Planet. Sci. Lett.* 297, 435–445 (2010).
- Kustowski, B., G. Ekstrom, and A. M. Dziewon'ski (2008), Anisotropic shear-wave velocity structure of the Earth's mantle: A global model, *J. Geophys. Res.*, 113, B06306, doi:10.1029/2007JB005169.
- J. Ritsema, H. J. van Heijst, A. Deuss, and J. H. Woodhouse, S40RTS: a degree-40 shear velocity model for the mantle from new Rayleigh wave dispersion, teleseismic traveltimes, and normal-mode splitting function measurements, *Geophys. J. Int.*, **184**, 1223–1236, doi: 10.1111/j.1365-246X.2010.04884.x, 2011
- Waite, G. P., and R. B. Smith (2002), Seismic evidence for fluid migration accompanying subsidence of the Yellowstone caldera, *J. Geophys. Res.*, 107(B9), 2177, doi:10.1029/2001JB000586.
- Waite, G. P., D. L. Schutt, and R. B. Smith (2006), Vp and Vs structure of the Yellowstone hot spot from teleseismic tomography: Evidence for an upper mantle plume, *J. Geophys. Res.*, 111, B04303, doi:10.1029/2005JB003867.

## InSAR measurements of Yellowstone Caldera

*Contributed by Ge Jin*

As one of the most volcanically active areas in North America, it is no surprise that the Yellowstone area has a high level of seismicity, hydrothermal activity, as well as vertical surface deformation. The Satellite interferometric synthetic aperture radar (InSAR) method provides us precise and continuous measurement of vertical surface displacement over the whole Yellowstone caldera area. Comparing the phase difference between two InSAR photo pairs shot at the same place can provide information on the relative vertical deformation at that location during the period between the taking of the two photos. These measurements can be related to the movement of molten basalt into and out of the Yellowstone volcanic system [5].

By gathering the results from several papers, the surface vertical displacement of Yellowstone caldera from 1992 to 2009, we summarized in (Figure 28) [2, 3, 4, 5]. Significant displacement can be observed over the time. Lifting and subsidence happening at the same place back and forth in short periods can be modeled numerically, providing information of where the magma source is and how much volume has been brought into or taken out of the system.

In the period from 1992 to 2009, four different episodes of caldera deformation can be identified: 1992-1995 subsidence of 2.7 cm/yr; 1996-2000 subsidence of 0.5 cm/year with local uplift of 1.7 cm/year at Norris; 2000-2004 subsidence of 0.7 cm/year with local uplift of 0.6 cm/year at Norris; and 2004-2009 uplift of 3-8 cm/year with local subsidence of 1-4 cm/year at Norris [1].

The caldera-wide subsidence can be explained by either magma crystallization or magma chamber depressurization beneath the caldera, or both. And the associated uplift at Norris could have been caused by the pressurization of the Norris hydrothermal system. The uplift of the caldera after 2004 is likely related to aseismic magma injection from a deeper source, while the local subsidence of Norris might associated with magma crystallization and/or fluid loss from the deep hydrothermal system. Both GPS and InSAR results show that the

inflation of the Sour Creek resurgent dome is followed by the inflation of the Mallard Lake resurgent dome. This detail might hint that the deep magma source is directly connected to or is much closer to the Sour Creek dome rather than Mallard Lake [1].

With the constraint of surface deformation, the magma and hydrothermal structure as well as the activity underneath the caldera is estimated. Figure 29 illustrates a concept model to explain the surface deformation of the Yellowstone area.

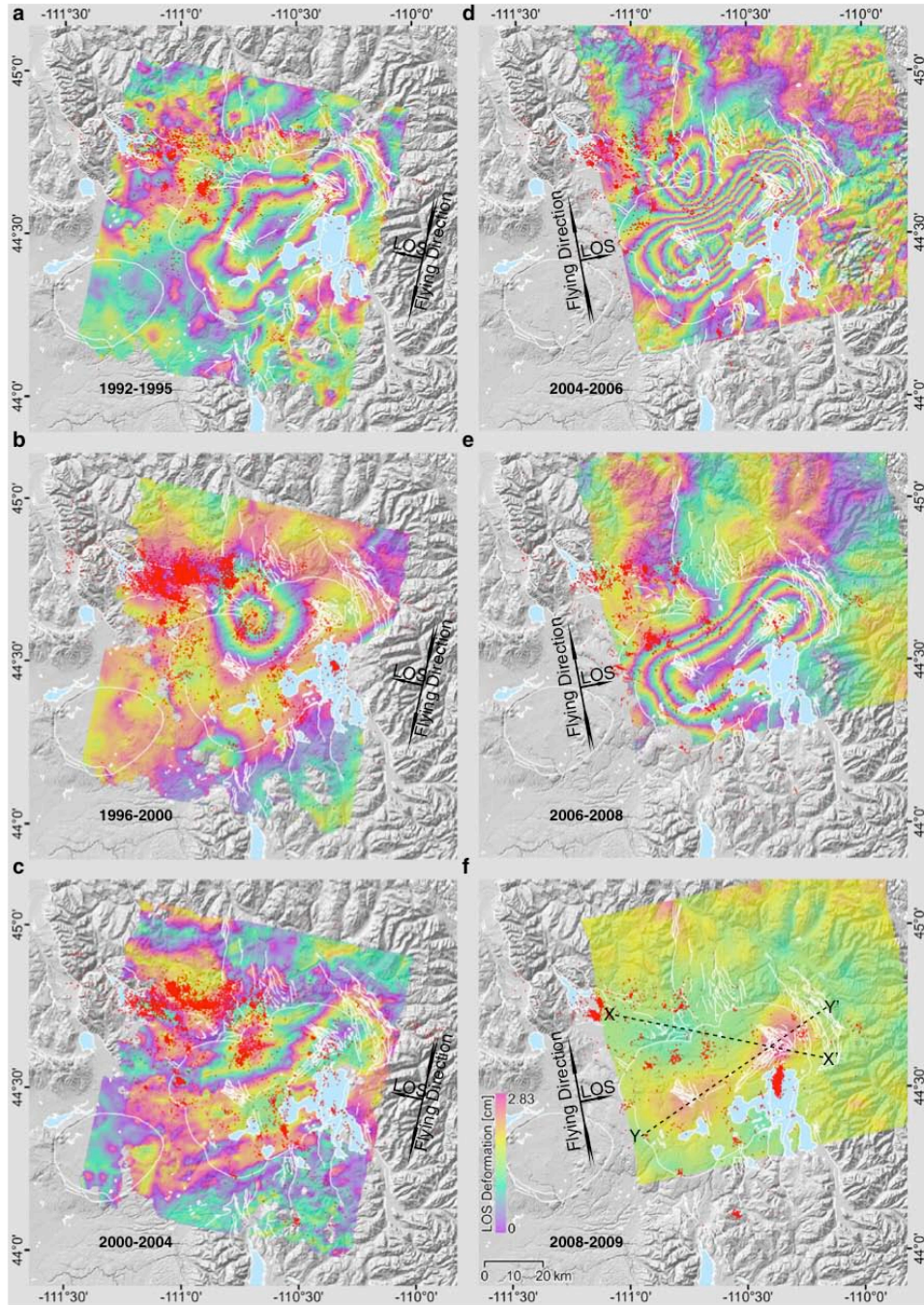


Figure 28. InSAR measurements of the Yellowstone region from 1992 to 2009.

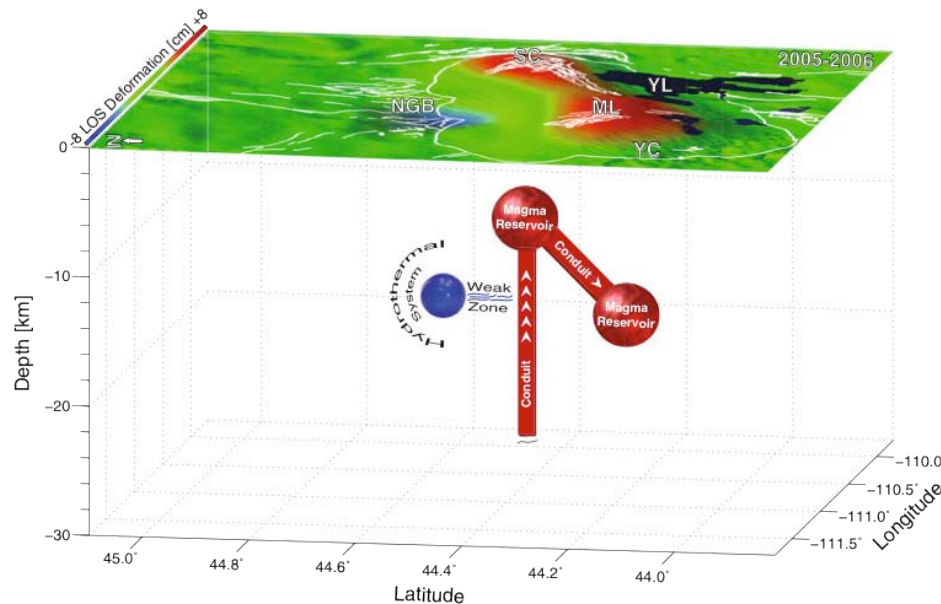


Figure 29. Concept model for Yellowstone Deformation.

## References

- [1] M.H. Aly and E.S. Cochran. Spatio-temporal evolution of yellowstone deformation between 1992 and 2009 from insar and gps observations. *Bulletin of Volcanology*, pages 1–13, 2011.
- [2] W.L. Chang, R.B. Smith, J. Farrell, and C.M. Puskas. An extraordinary episode of yellowstone caldera uplift, 2004–2010, from gps and insar observations. *Geophysical Research Letters*, 37:L23302, 2010.
- [3] W.L. Chang, R.B. Smith, C. Wicks, J.M. Farrell, and C.M. Puskas. Accelerated uplift and magmatic intrusion of the yellowstone caldera, 2004 to 2006. *Science*, 318(5852):952, 2007.
- [4] C. Wicks, W. Thatcher, and D. Dzurisin. Migration of fluids beneath yellowstone caldera inferred from satellite radar interferometry. *Science*, 282(5388):458, 1998.
- [5] C.W. Wicks, W. Thatcher, D. Dzurisin, and J. Svarc. Uplift, thermal unrest and magma intrusion at yellowstone caldera. *Nature*, 440(7080):72–75, 2006.

## Hydrology of Yellowstone National Park

*Contributed by Amelia Paukert*

*Unless otherwise cited, information in this section is taken from Fournier et al. [1989]*

Yellowstone National park attracts about 3 million visitors annually, in large part due to its extensive hydrothermal activity. While best known for Old Faithful Geyser, the most regular large geyser in the world, Yellowstone has a plethora of other geothermal attractions: with over 10,000 other hydrothermal features and 300 geysers, Yellowstone has ½ of the world’s hydrothermal features and 2/3 of the world’s active geysers.

Yellowstone’s hydrothermal areas are primarily located within the areas of the Huckleberry Ridge (2.1 Ma) Caldera and Yellowstone (0.64 Ma) caldera. On the northeast side of the park, in an area rimmed by only the 0.64 Ma caldera, the geothermal activity is primarily vapor dominated. Near the center of the park, where the 2.1 and 0.64 Ma calderas overlap, the hydrothermal activity is hot-water dominated. It is thought there is a large, deep hydrothermal reservoir at high temperature (~350°C) that supplies hot water to smaller, shallower reservoirs,

which then supply water to the visible hydrothermal features. These local reservoirs are typically situated at 100-550 m depth, have a temperature ranging from 180-270°C, and have different chemical characteristics depending on the geology of their surrounding formations.

The Yellowstone hydrothermal system is fed by recharge from meteoric water. Surface water from rain and snowmelt infiltrates into the subsurface and eventually percolates down to depth, where the hotspot provides a large geothermal heat source. The isotopic composition of cold, shallow groundwater clusters around the local meteoric water line, while geothermal waters are typically enriched in  $^{18}\text{O}$  and  $^2\text{H}$  from boiling and exchange with aquifer materials [2]. The volume of water flow through the aquifer system is 3-4  $\text{m}^3/\text{s}$ , but the residence time is not well constrained and may be less than 2,000 years or more than 10,000 years.

The surface manifestations of hot water dominated systems are geothermal spring waters, mudpots, acid boiling pools, and geysers. Geothermal spring waters form when heated water rises from depth to the surface. In Yellowstone, these are typically from local reservoirs in rhyolitic lava flows. When the waters outlet at the surface, they are 80-95 °C, have neutral to basic pH (7 - 9.5), and high Cl (250-700 ppm). Dissolution of rhyolite has enriched these waters in  $\text{SiO}_2$ - they typically have 200-650 ppm  $\text{SiO}_2$ , which is 10-40 times that usually seen in groundwater. Mammoth thermal waters have different chemical characteristics because the flowpath to the surface is through limestone, dolomite, and gypsum-bearing shales instead of through rhyolite. The carbonate and gypsum rocks cause the water to be higher in  $\text{HCO}_3$ , and  $\text{SO}_4$ , but lower in  $\text{SiO}_2$ . In addition, the water in this hydrothermal reservoir is of lower temperature, up to a maximum of 120°C, which allows Mg and Ca to remain in solution rather than precipitating out as silicate minerals. When these waters reach the surface and cool, they precipitate Ca and Mg carbonates in the form of surficial travertine deposits.

Mud pots and acid boiling pools have acidic pH's, usually 2-3. Unlike geothermal spring waters, which come directly from depth, the water in these pools is shallow groundwater that has been heated by steam from the geothermal water. Deeper hydrothermal reservoirs are in a reducing state so sulfur is present in the form of  $\text{H}_2\text{S}$ . When steam rises off the water, it carries with it  $\text{H}_2\text{S}$  gas. When the gas hits shallow groundwater, it oxidizes to  $\text{H}_2\text{SO}_4$ , making the water highly acidic. In areas with plentiful water, this process forms acid boiling pools. In areas with less water, the process forms mud pots: the acid dissolves the surrounding rock into fine particles of clay and silica, and since there is little water, this creates a concentrated solution that is visible as seething mudpots. Waters from both of these features are depleted in Cl because shallow groundwater is not Cl enriched, and although hydrothermal fluids were enriched with Cl, it was left behind when the steam evaporated off.

Geysers form where the upward flow of geothermal water is restricted such that the water is unable to freely rise to the surface. This often occurs by a spring clogging its own pipes, precipitating silica sinter along the water's subsurface flowpath and constricting the channels. Since the water cannot rise as fast as it would like, the system becomes pressurized and the water becomes superheated. This superheated water is overlain by cooler water near the surface. As the superheated water expands, it pushes some of the cooler water out onto the surface. This relieves some of the overburden, releasing pressure and allowing the superheated water to flash to steam. When the steam rises, it also pushes out the overlying cooler water and creates a geyser eruption.

Yellowstone is ideal for geyser formation because it meets the four conditions critical for geyser formation: 1) heat source, 2) frequent seismicity, 3) source of water recharge, and 4) capped fluid reservoir [3]. The first two conditions are met because of the hotspot, the third by

rain and snowmelt, and the fourth by alternating layers of permeable rhyolite flows and impermeable ash-flow tuffs - the rhyolite flows act as water reservoirs, while the ash-flow tuffs act as reservoir caps. Yellowstone boasts the largest active geyser in the world – Steamboat Geyser has been known to reach heights of 300-400 ft during eruptions.

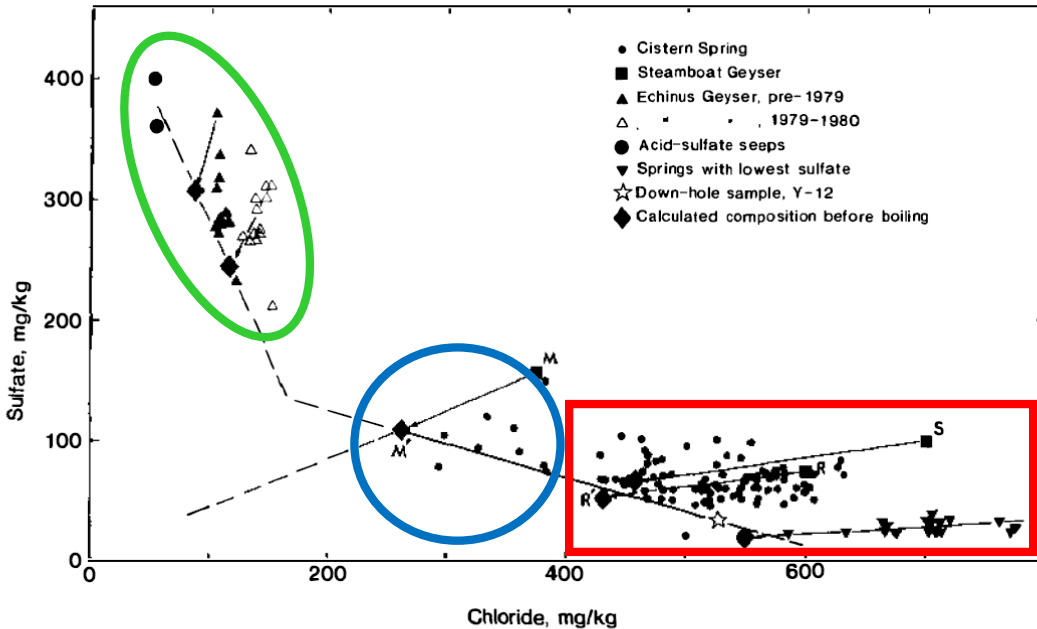


Figure 30. Composition of thermal waters from the Norris Geyser Basin: green circle encloses acid-sulfate pools, red rectangle encloses geothermal waters, blue circle encloses mixtures between geothermal waters and shallow groundwater [Fournier et al., 1989].

The vapor dominated hydrothermal areas are characterized by surface expressions of fumaroles, acid-sulfate boiling pools, and ammonium-sulfate springs. Fumaroles are vents releasing steam that has risen from the hydrothermal reservoirs up to the surface. The acid-sulfate boiling pools are like the ones in the hot-water dominated system, but typically with less water. Ammonium-sulfate springs occur where the vapor has distilled the Paleozoic or Mesozoic sediments underlying the volcanics on its way from the geothermal reservoir to the surface. This distillation forms methane, ethane, and ammonium. These gases travel up with the steam, interacting with shallow groundwater, and resulting in springs that have basic pH, low Cl, high Si, and very high  $\text{NH}_4$ , and  $\text{SO}_4$ .

Vapor dominated systems below the water table are underpressured with respect to the hydrostatic pressure, so there must be constraints preventing groundwater from flowing into the vapor saturated area. This suggests that the permeability of both the cap and sides of the vapor-dominated area must be relatively low.

#### References:

- [1] Fournier, R.O. (1989). Geochemistry and Dynamics of the Yellowstone National Park Hydrothermal System. *Annual Review of Earth and Planetary Sciences*. 17: 13-53.
- [2] Kharaka, Y.K., Thordsen, J.J., White, L.D., (2002). Isotopic and Chemical Compositions of

Meteoric and Thermal Waters and Snow from the Greater Yellowstone National Park Region. *U.S. Geological Survey Open File Report 02-194.*  
[3] Geysers and how they work. *National Park Service.*

## Microbiology of the Yellowstone Hot-springs

*Contributed by Ellen Crapster-Pregont*

Extremophiles are organisms that thrive in extreme chemical and physical conditions. Often these conditions are found in difficult to access localities, such as black smokers at the bottom of the ocean. The hot springs in Yellowstone National Park maintain relatively constant temperature and composition conditions and are relatively easy to access (Stockner, 1967). This makes the Yellowstone Hot Springs and Geysers optimal locations for field studies aimed to study the diversity and conditions in which extreme organisms live. Such studies of extremophile occurrence and diversity began in the 1960's and continue today.

Many microorganisms in the Yellowstone hot springs are able to live through their entire life cycle at temperatures greater than 50°C. Each species tends to live within a specific temperature range. Besides temperature, the chemical character of the water, whether acidic, alkaline, or sulfurous, determines which species are present. Species found in the Yellowstone hot springs and geysers come from the bacteria, archaea, and eukarya domains of the phylogenetic tree of life (LASP, 2005; NPS). Due to the extreme conditions in which these organisms live, there is a reduction in their complexity and in the number of species present for a given set of conditions (Stockner, 1967). Observations confirm this conclusion with a majority of the thermophiles, and other extremophiles belonging to the bacteria and archaea domains (LASP, 2005).

There are two main types of growth habits exhibited by the organisms in the hot springs: streamers and mats (Castenholz, 1969; LASP, 2005). Streamers are string-like amalgamations of organisms formed due to the flowing water associated with springs and geysers. Conversely, mats form in relatively stagnant water and are characterized by overlying layers of organisms that extend horizontally for some distance in the hot spring or geyser. The position each organism occupies in the mat depends on the specific temperature and sunlight requirements of that organism. A wide range of conditions may be present in a thick microbial mat, resulting in organisms migrating through the mat until they reach regions of optimal conditions (LASP, 2005).

The spectacular colors associated with the Yellowstone hot springs and geysers are directly related to the type of microorganisms present (Figure 31-31, Table 1) (LASP, 2005; NPS). Changes in color, within a hot spring system and between different hot springs, reflect variations in conditions and temperatures (LASP, 2005; Stockner, 1967). Chemosynthetic organisms (those that convert specific elements into energy) and anoxygenic photosynthetic organisms (those that break down compounds like hydrogen sulfide) are found closest to the spring source or in the bottom layers of mats where elements such as sulfur and iron are most abundant. Oxygenic photosynthetic organisms (those that convert sunlight into energy) are found at the tops of mats and further from the spring source where toxic elements are less concentrated (LASP, 2005; Stockner, 1967).



Figure 31. Grand Prismatic Spring in Yellowstone National Park. This image exemplifies the variation of and dependence on hot spring conditions of microorganisms. Each distinct color band represents a different species. The concentric pattern correlates with radial changes in temperature (and chemical) conditions within the hot spring. Photo from National Geographic webpage.

| LOCATION                           | CONDITIONS | COMMUNITY TYPE | TEMPERATURE (°C) | COLOR                     |
|------------------------------------|------------|----------------|------------------|---------------------------|
| WEST THUMB, GEYSER BASIN           | ALKALINE   | STREAMER       | 73-92            |                           |
|                                    |            | MAT            | 75               |                           |
| MUD VOLCANOES, NORRIS GEYSER BASIN | ACIDIC     | STREAMER       | 60               | YELLOW, RED-BROWN         |
|                                    |            | MAT            | 60               | YELLOW, RED-BROWN         |
| MAMMOTH HOT SPRINGS                | CARBONATE  | STREAMER       | 66               | CREAM                     |
|                                    |            | MAT            | 66, 58, 25-54    | GREEN, PURPLE, RED-BROWN* |

**Table 1:** Table summarizing the variety of thermophilic environments within Yellowstone National Park. Included information exemplifies how organisms vary (different colors represent different species) between the conditions in Yellowstone Hot Springs. All values from LASP, 2005. \*In carbonate conditions at Mammoth Hot Springs the characteristic orange color does not result until hydrogen sulfide has been removed from the system.



Figure 32. Cistern Spring in the Black Basin of Norris Geyser Basin in Yellowstone National Park. Brilliant color variation from the center of the spring exemplifies the transition between conditions as well as species of microorganisms. The surrounding vegetation is bleached from exposure to the acidic fumes.



Figure 33. Mats of red-brown cyanobacteria growing on travertine/carbonate terraces of Mammoth Hot Springs, Yellowstone National Park. These organisms are able to survive here because a majority of the sulfur and iron has been removed via chemosynthesis closer to the spring source.

Microorganism diversity varies both downstream and cross-sectionally in streams originating from hot springs and geysers (Figure 34). The distribution of organisms is directly related to the temperature and conditions present at a particular point in a given hot spring system. Fouke et al. (2003) concluded that species isolation is due to geological setting, which is reflected in the water chemistry (Figure 35). In general, organisms with highest temperature tolerances are found nearest source and in the central stream channel the species then change systematically as surrounding geologic, chemical, and temperature conditions change. It is also notable that the abundance of an individual species decreases with temperature and inversely with diversity (Fouke et al., 2003; Stockner, 1967). As each species occupies a specific niche in the hot spring environment, annual changes in organism abundance and location may occur due to temperature and sunlight variations (Castenholz, 1969). This migration phenomenon is typically absent in organisms using chemosynthesis rather than photosynthesis. In either case, downstream transport is minimal, less than 25%, indicating that observed changes in color, or species present, in a given hot spring system are due to changes in chemistry and temperature (Castenholz, 1969; Fouke et al., 2003; LASP, 2005).

Why do we care? Modern day simple microorganisms capable of thriving in such extreme conditions are proxies for organisms that may have been present in early Earth's harsh environments. It is such organisms that are most likely responsible for creating a world, by oxygenating the atmosphere, where more complex and diverse organisms could inhabit. These early extremophiles could thus be considered our ultimate ancestors. By studying modern analogs we can better understand the capabilities and limitations of these organisms, thus elucidating Earth's biological past and whether life could exist in extraterrestrial extreme environments (LASP, 2005; NPS).

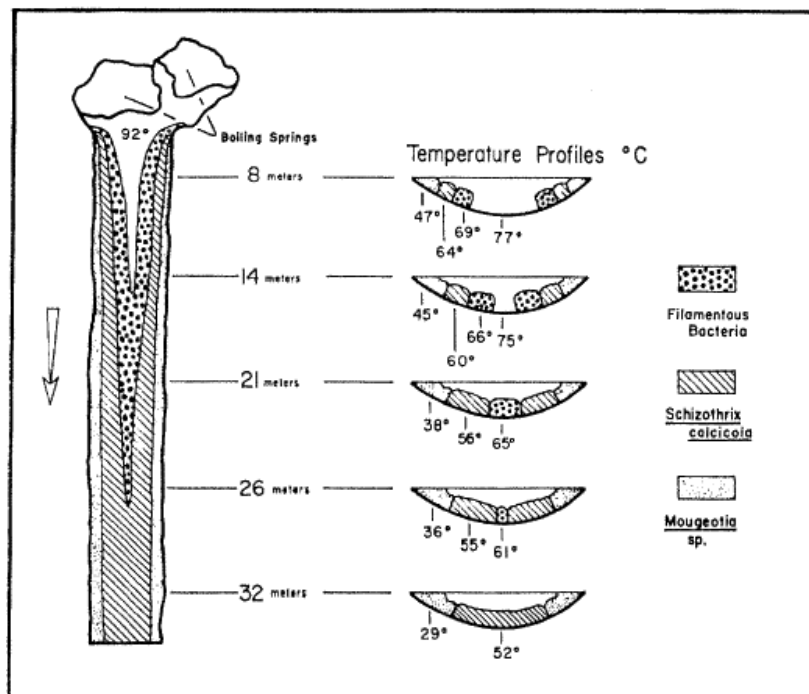


Figure 34. Schematic diagram of downstream variation in microorganisms in Upper Geyser Basin, Yellowstone National Park. This variation is due mainly to temperature variation within the stream channel. [From Stockner, 1967].

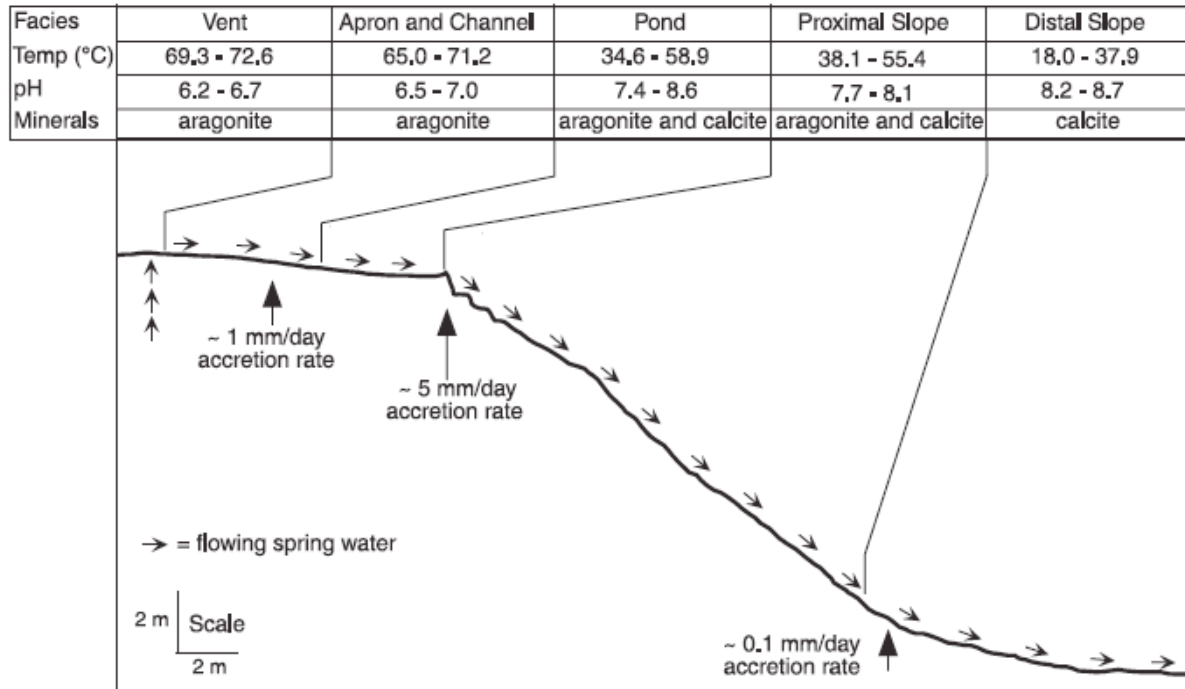


Figure 35. Schematic diagram of facies and conditions variation with distance from the spring source of Angel Terrace, Mammoth Hot Spring, Yellowstone National Park. Rates are travertine depositional rates. [From Fouke et al., 2003].

As a visitor to Yellowstone National Park you do not need specialized equipment to observe the microbial community, just your eyes. On this fieldtrip there were several stops, such as Mud Volcanoes, Norris Geyser Basin, and Mammoth Hot Springs that exhibited a wide variety of thermophilic microorganisms. When visiting these two locations, take care with cameras as steam from acidic pools can etch lenses. Beyond careful camera usage and sulfuric fumes, enjoy the colorful element that the extremophiles add to the geologic phenomena of the Yellowstone National Park hot springs and ponder what these extreme organisms adapted to in a harsh early Earth environment.

#### References:

- Castenholz, R.W. 1969. Thermophilic Blue-Green Algae and the Thermal Environment. *Bacteriological Reviews*. 33, 476-504.
- Fouke B.W., Bonheyo, G.T., Sanzenbacher, B., and Frias-Lopez, J., 2003. Partitioning of bacterial communities between travertine depositional facies at Mammoth Hot Spring, Yellowstone National Park, U.S.A. *Canadian Journal of Earth Sciences*. 40, 1531-1548.
- Laboratory for Atmospheric and Space Physics (LASP): University of Colorado at Boulder. Yellowstone Journalist Workshop. 2005. Thermophiles.  
[http://lasp.colorado.edu/education/journalists/yellow\\_stone/Articles/CH4.PDF](http://lasp.colorado.edu/education/journalists/yellow_stone/Articles/CH4.PDF)
- National Parks Service (NPS). 'Hydrothermal Systems and How They Work.'  
<http://www.nps.gov/yell/naturescience/geothermal.htm>
- Stockner, J.G., 1967. Observations of Thermophilic Algal Communities in Mount Rainier and Yellowstone National Parks. *Limnology and Oceanography*. 12, 13-17.

## Other Geologic Features of Interest

### Stillwater Complex

*Contributed by Jill VanTongeren*

The Stillwater Complex is among the world's largest-known layered mafic intrusions (large stratified fossil magma chamber) (Figure 36). Multiple successive pulses of mafic magma were intruded into the upper crust of the Wyoming Craton at approximately 2.7 Ga (DePaolo and Wasserburg, 1979; Nunes, 1981; Premo et al., 1990). The source of the magma is thought to be the result of extensive crustal assimilation by a rising komatiitic melt (Longhi et al., 1983). Thrusting along the main Horseman Thrust (Fig. 34) as a result of Laramide deformation exposed the Complex, and subsequent erosion has removed much of the uppermost portions.

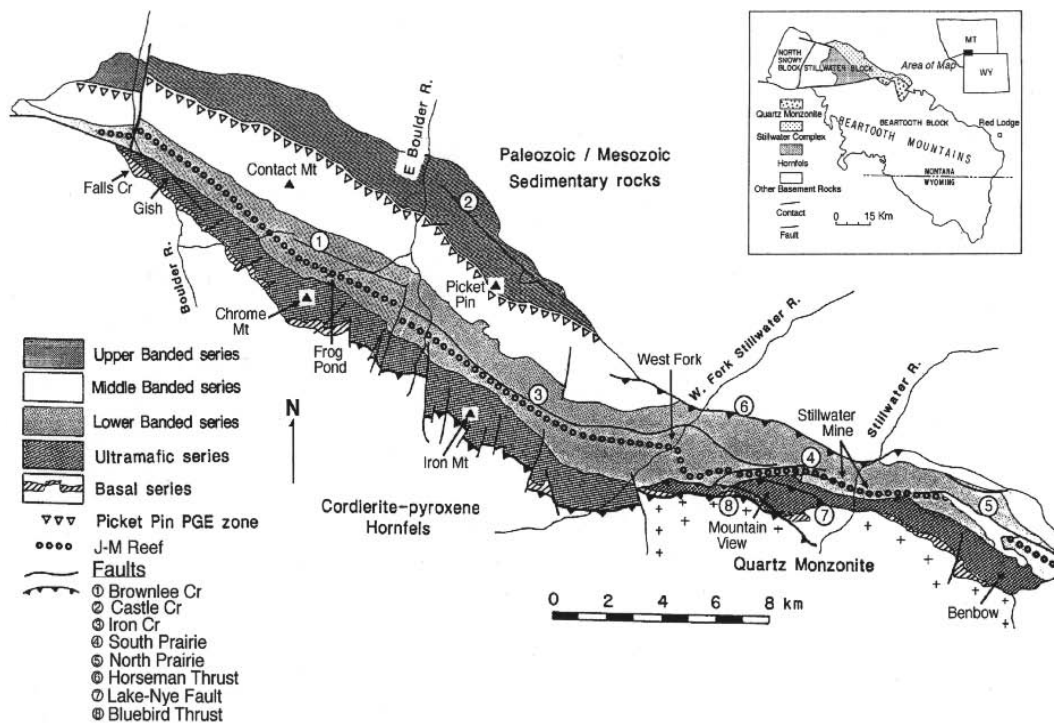


Figure 36. Geologic map of the Stillwater Complex.

The Stillwater Complex is divided into three principle zones: The Basal Zone, Ultramafic Zone, and the Banded Series. The ~160 m thick Basal Zone is largely comprised of marginal rocks formed during the initial intrusion of magma into the crust. The Ultramafic Zone is dominated by olivine and orthopyroxene cumulate rocks with numerous chromitite seams (seams A-G). There are several competing hypotheses for how these layers were formed (see below). Chromitite seams A-G were mined at the Mouat Mine (now part of the Stillwater Mining company) during the 2<sup>nd</sup> World War. The Banded Zone marks the appearance of cumulus plagioclase, where anorthosite (monomineralic plagioclase) layers are common. Approximately 500 m above the start of the Banded Zone is the J-M Reef (see section below).

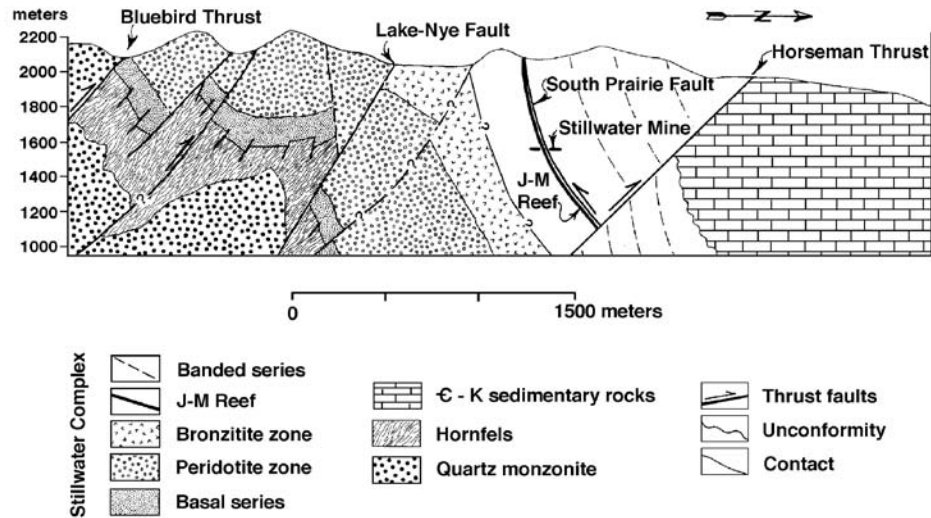


Figure 37. Cross-section of the Beartooth Range and Stillwater Complex including tectonic features.

Layered intrusions are one of the principle means of understanding the nature of igneous differentiation on earth. When the mantle initially melts, the composition of the magma is basaltic. Yet the upper and middle continental crust is largely granitic. There are two ways to generate a granitic composition from a basaltic composition: partial melting or fractional crystallization. Layered intrusions are the primary observational evidence available to study how fractional crystallization works and how magma (and ultimately rock) compositions evolve on Earth. This is because as these large basaltic magma chambers cool, they start to crystallize. These crystals form at the base of the chamber, either by crystal settling, or by crystallization on the chamber floor, and are then removed from “communication” with the rest of the magma. Certain minerals, such as olivine and orthopyroxene, form at higher temperatures and are the first to be removed. In the Stillwater, the removal of olivine and orthopyroxene is recorded by the Ultramafic Zone rocks. Other minerals, such as plagioclase, clinopyroxene, and magnetite, form later (this is seen in the Banded Zone). Thus, the succession of rock types records the progressive cooling and crystallization of a previously homogeneous magma composition. After removing these minerals, with their different chemical compositions, the last bit of magma to crystallize will have a much different chemistry – it will look very much like a granite. We don’t see this stage in the Stillwater because the uppermost portion has been eroded away. However, there are other intrusions like the Bushveld Complex, South Africa or the Skaergaard Intrusion, East Greenland, that show the full progression.

Layered intrusions are also one of the world’s leading sources for Platinum Group Elements (PGEs), such as Platinum and Palladium. In fact, the Stillwater Complex has the highest grade PGE ore body on the planet, and is highly prized for its palladium contents. The PGEs are primarily found in disseminated sulfides located throughout the J-M reef (Figure 38). The J-M reef is a pegmatitic olivine-orthopyroxene layer that was likely formed by a massive influx of new magma that was near sulfide saturation.



Figure 38. J-M reef in Stillwater Complex. Brown-bronze mineral is Pt/Pd-rich pyrrhotite, yellow- chalcopyrite, dull green-gray - serpentinite host rock (formerly dunite).

The Stillwater Complex is famous among magma chamber dynamicists for its inch-scale layering (Figure 39). The origin of igneous layering is still highly debated. Various mechanisms have been proposed ranging from mechanical sorting (due to crystal settling, density, flow segregation, or tectonic deformation) to geochemical “refining” (due to magma mixing, double-diffusive convection, crystal nucleation rates, flow and interaction with interstitial fluids, metasomatism). For a more detailed review of layering mechanisms see Naslund and McBirney (1996).

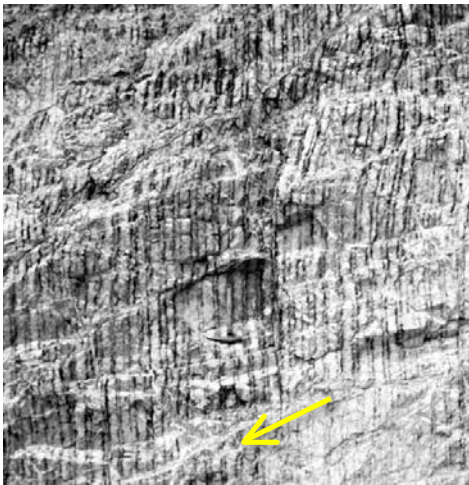


Figure 39. Inch-scale layering in Stillwater Complex. Yellow arrow indicates location of hammer for scale.

For a more detailed description of the Stillwater Complex and its petrologic significance see “The Stillwater Complex: A review of the geology” document from I.S. McCallum.

**References:**

- [1] DePaolo and Wasserberg (1979) *Geochim. Cosmochim. Acta* **43**
- [2] Nunes (1981) *Geochim. Cosmochim. Acta* **45**
- [3] Premo et al. (1990) *Geology* **18**
- [4] Naslund and McBirney (1996) in *Layered Intrusions* edited by R.G. Cawthorn

[5] McCallum Review of Stillwater Complex can be found at:  
<http://serc.carleton.edu/files/NAGTWorkshops/petrology03/McCallum.Stillwater.doc>

## Heart Mountain Landslide

*Contributed by Rafael Almeida*

The Heart Mountain Detachment (HMD) is the world's largest landslide ( $> 3400 \text{ km}^2$  – about the size of Long Island!!!). The HMD surface is flat and nearly level, having a slope of less than 2 degrees. The underlying rocks are undisturbed. The rocks that have been detached are extensively deformed and broken up.

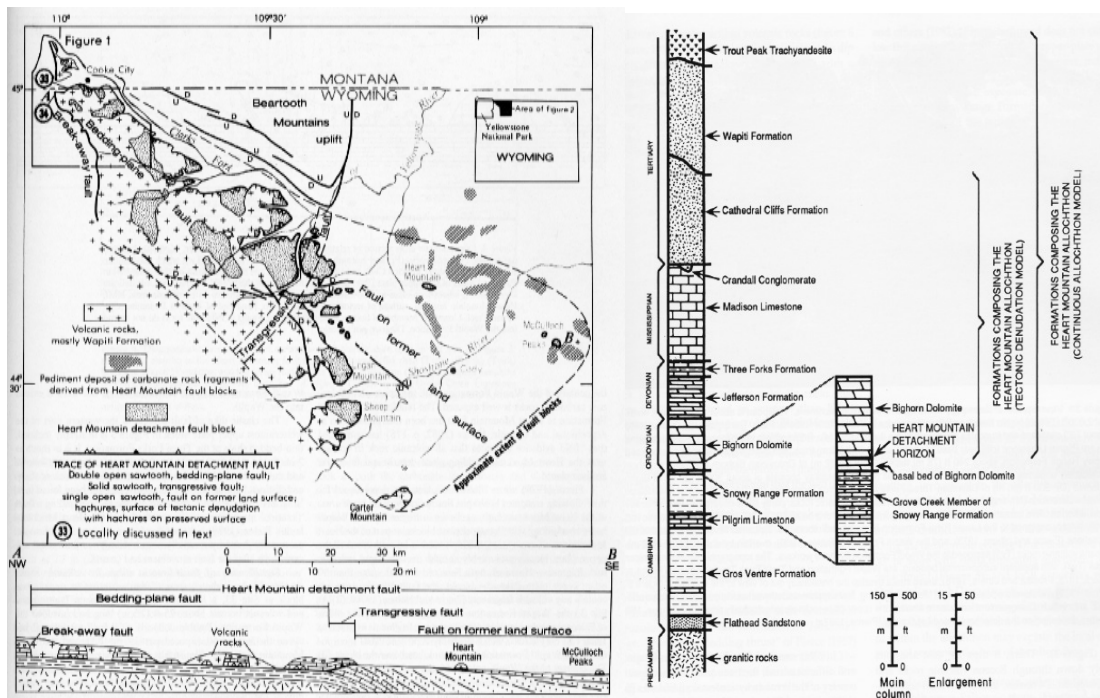


Figure 40. A) Location of the Heart Mountain Detachment with a cross-section indicating three parts of the fault. B) Stratigraphic column showing the location of the detachment horizon. From Hague, 1993.

The fault has 3 parts, the Bedding Plane Fault, the Transgressive Fault and the Land Surface Fault (Figure 40). The first is the surface along which the allocthon detached. It is located towards the base of the Big Horn Dolomite (~ 2 m above it). The second part is where the HMD cut up-section and breached the surface. The third part is the surface along which the allocthonous sheet overrode the Eocene landscape. The bulk of the rock sheet ends at the north side of Dead Indian Hill (where the Transgressive Fault begins), but more pieces are found as far as 50 kilometers beyond – including Heart Mountain (Hague, 1993). The Transgressive Fault forms where the sedimentary layers increase in dip towards the SE. This made it easier for the HMD to cup up section than to continue along the Bedding Plane Fault. At Dead Indian Pass, the rocks underlying the HMD are extensively brecciated due to the passage of the allocthonous rocks over them. The HMD was initially identified in its Land Surface Fault portion and initially

interpreted as a thrust in 1916 (Dake, 1916) as it placed Ordovician rocks over Eocene basin fill. Erosion later removed much of the slide for this part of the HMD but a few klippen remain, including Heart Mountain, to testify how far it once spread. The landslide origin of this rock mass was first recognized by Bucher (1933).

Rocks above the Heart Mountain detachment were once a much thicker (2-4 km) and less extensive body. Carbonate rocks of Paleozoic age (as old as Ordovician or 400 million years) were overlain by younger ones, topped with a thick pile of volcanic rocks (Absaroka Volcanics) dating from the Eocene, about 50 million years old. These rocks were structurally thinned during the emplacement of the slide and later covered by younger volcanic rocks.

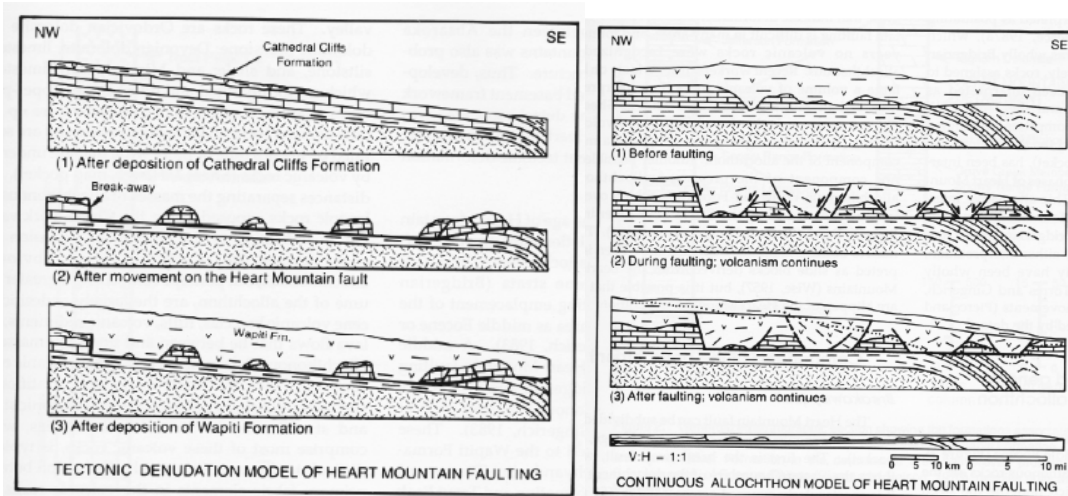


Figure 41. Diagrams of HMD formation. A) HMD formation with catastrophic emplacement and only Paleozoic rocks in the hanging wall (Pierce, 1960, 1980). B) HMD formation with slow emplacement and with Paleozoic and Tertiary rocks in the hanging wall (Hague, 1985). From Hague, 1993.

The rate of emplacement of the slide has been debated, but most researchers seem to favor a catastrophic emplacement over a slow one (Pierce, 1960; Beutner and Craven, 1996, Anders et al., 2000, 2010; Beutner and Gerbi, 2005; Craddock et al., 2009; Craddock et al., 2000; Goren et al., 2010). Pierce (1960) suggested the detached sheet of rock was composed only of sedimentary rocks and that the existing volcanic rocks were emplaced later, filling up the remnant topography (Figure 41). Subsequent studies though seem to agree that there was a preexisting section of Eocene volcanics overlying the sedimentary section prior to the formation of the HMD and that these rocks were also extended as part of the allochthonous sheet.

The main hypothesis for the formation of the HMD is that an earthquake initiated its movement (Bucher, 1947). Once this happened, superfluid conditions at the base caused by either volcanic gas or hot water combined with almost equal vertical and horizontal stresses (due to regional diking) allowed a reduction in friction, which allowed the HMD to continue sliding. The slide is thought to have achieved velocities of 10's to 100's of m/s (20-200 mph!). The slide is thought to have moved over 50 km (Figure 42).

The idea is that hot fluids (gas or water) were trapped by a thick layer of dolomite that was impervious to them. At some point, ~48 Ma, probably during an eruption, the rock gave way and began to slip along a plane 2 meters above the base of the dolomite. Friction on the detachment quickly raised a tremendous amount of heat causing the rock within the fault to melt.

The dolomite could not take this amount of heat, which led to the vaporization of the rock, liberating CO<sub>2</sub>. Within seconds the detachment was turned into a frictionless plane as the cushion of gas reached the supercritical stage, a high-pressure hot form of matter that is neither gas nor liquid (Beutner & Gerbi, 2005). This would have led to a fluidization of the basal layer and the calcining of the carbonates (Anders et al., 2010) that resulted in the concrete-like appearance of the HMD.

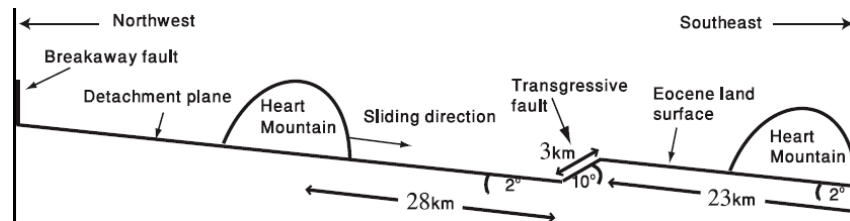


Figure 42. Magnitude and path of Heart Mountain transport (from Goren et al., 2010).

#### References:

- Anders, M. H.; Aharonov, E.; and Walsh, J. J. 2000. Stratified granular media beneath large slide blocks: implications for mode of emplacement. *Geology*, 28, 971–974.
- Anders, M., Bruce W. Fouke, Aubrey L. Zerkle, Enrico Tavarnelli, Walter Alvarez and George E. Harlow. 2010. The Role of Calcining and Basal Fluidization in the Long Runout of Carbonate Slides: An Example from the Heart Mountain Slide Block, Wyoming and Montana, U.S.A. *The Journal of Geology*, 118 (6), 577-599.
- Beutner, E. C., and Craven, A. E. 1996. Volcanic fluidization and the Heart Mountain detachment, Wyoming. *Geology*, 24, 595–598.
- Beutner, E. C., and Gerbi, G. P. 2005. Catastrophic emplacement of the Heart Mountain block slide, Wyoming and Montana, U.S.A. *Geol. Soc. Am. Bull.*, 117, 724–735.
- Bucher, W. H. 1933. Volcanic explosions and overthrusts. 14th annual meeting, Am. Geophys. Union, 238–242.
- Bucher, W.H. 1947. Heart Mountain problem. In Blackstone, D. L., Jr., and Sternberg, C. W., eds. *Field Conference Guidebook, field conference in the Bighorn Basin*. Wyo. Geol. Assoc., 189–197.
- Craddock, J. P.; Malone, D. H.; Magloughlin, J.; Cook, A. L.; Rieser, M. E.; and Doyle, J. R. 2009. Dynamics of emplacement of the Heart Mountain allochthon at White Mountain: constraints from calcite twinning strains, anisotropy of magnetic susceptibility and thermodynamic calculations. *Geol. Soc. Am. Bull.*, 121, 919–938.
- Craddock, J. P.; Nielson, K. J.; and Malone, D. H. 2000. Calcite twinning strain constraints on the emplacement rate and kinematic pattern of the upper plate of the Heart Mountain detachment. *J. Struct. Geol.*, 22, 983–991.
- Dake, C.L. 1916. The Haert Mountain overthrust and associated structures in Park County, Wyoming. *Journal of Geology*, 26, 463-68.
- Goren, L., E. Aharonov and M. Anders. 2010. The long runout of the Heart Mountain landslide: Heating, pressurization, and carbonate decomposition, *Journal Geoph. Research*, 115, B10210, doi:10.1029/2009JB007113.
- Hague, T. 1985. Gravity-spreading origin of the Heart Mountain allochthon, northwestern Wyoming. *Geol. Soc. Am. Bull.*, 96, 1440–1456.

- Hague, T. 1993. The Heart Mountain detachment, northwestern Wyoming: 100 years of controversy. In Snoke, A. W.; Steidtmann, J. R.; and Roberts, S. M., eds. *Geology of Wyoming: memoir*. Laramie, WY, Geological Survey of Wyoming, 530–571.
- Pierce, W.G. 1960. The “break-away” point on the Heart Mountain detachment fault in northwestern Wyoming. *U.S. Geol. Surv. Prof. Pap.* 400B:236–237.
- Pierce, W.G. 1980. The Heart Mountain break-away fault, northwestern Wyoming. *Geol. Soc. Am. Bull.* 91, 272–281.

## Glacial Deposits

*Contributed by Michael Wolovick*

The Pinedale and Bull Lake glaciations are names given in the western US to the ultimate and the penultimate glacial maxima, respectively. They are also called the Wisconsin and the Illinoian. Regardless of the name, they represent the local manifestation of the last two cold swings of the eccentricity-driven 100 kyr glacial cycle (MIS 2-4 and 6) that governed global climate in the last half of the Pleistocene. Both of these glaciations consisted of valley glaciers and local ice caps on elevated topography; full continental scale ice sheets did not develop in the field area. Modern analogues would be places such as Alaska, Iceland, or Svalbard, not Greenland or Antarctica.

The Bull Lake glaciation reached its maximum at 160 ka (Horse Butte) and its deposits can be distinguished from Pinedale deposits by a greater level of weathering and erosion. Bull Lake moraines are gently sloping and broadly breached by streams. Because they are broadly breached, they tend not to interfere with local hydrology as much as Pinedale moraines do. Boulders within Bull Lake till, when present, are highly weathered and grussified (Figure 43). However, there is a lower abundance of boulders in Bull Lake till than is found in Pinedale till. In addition, the Bull Lake glaciation was more extensive than the Pinedale glaciation. Where deposits from both glaciations are present, the Bull Lake terminal moraines are more distal than the Pinedale terminal moraines. Like most glaciations, the Bull Lake glaciation was not a single event; often multiple nested terminal moraines can be observed. At the type locality (Bull Lake) there are three till strata separated by a paleosol and a disconformity.



Figure 43. Bull Lake morainal till. Note highly grussified granite rock in the middle of the image (there are two rocks; the upper one directly behind the hammer is less weathered than the one below it).

The Pinedale glaciation peaked at the Last Glacial Maximum (LGM, ~20 ka). Its deposits are less eroded than Bull Lake deposits. Moraines are steeply sloping, narrowly breached by streams, and hydrology in their vicinity is often disorganized. Pinedale moraines also contain extensive quantities of unweathered or only mildly weathered boulders. As a result, they can be distinguished at a distance as low boulder-strewn hills (Figure 44). Near Yellowstone National Park, there was a local ice cap on Beartooth plateau that fed a 30-40 km long glacier in Lamar valley during the Pinedale glaciation. Cirques throughout the region supported numerous minor glaciers.



Figure 44. Pinedale moraine. Left: view from the top of a Pinedale moraine. Note boulder-strewn hillside in the foreground and moraine-dammed Fremont Lake in the background. The glacier flowed out of the valley in the deep background. Right: view of a Pinedale moraine from the road. Note the hillside is strewn with boulders without a local source.

#### References:

- Foster, D., S.H. Brocklehurst, and R.L. Gawthorpe, "Glacial-topographic interactions in the Teton Range, Wyoming," *JOURNAL OF GEOPHYSICAL RESEARCH-EARTH SURFACE*, vol. 115, Feb. 2010.
- Richmond, G., "STRATIGRAPHY AND CHRONOLOGY OF GLACIATIONS IN YELLOWSTONE-NATIONAL-PARK," *QUATERNARY SCIENCE REVIEWS*, vol. 5, 1986, pp. 83.

## Detailed Itinerary and Description of Visited Sites

### Day 1 (June 25, 2011) – Boulder, CO

*Contributed by Amelia Paukert and Rafael Almeida*

- 8:00 Loaded up in vans and headed to EWR
- 8:45 Arrived EWR
- 11:00 Flew to Denver, CO
- 13:30 Landed in Denver, got baggage, took shuttle to Hertz to get vehicles
- 14:30 Arrived at Hertz
- 15:15 Left Hertz, headed for NCAR in Boulder
- 16:15 Arrived at National Center for Atmospheric Research (NCAR), hiked around and looked at the stratigraphic section
- 17:45 Left NCAR
- 18:00 Arrived at contact corner between Precambrian granite and conglomerate from 250 Ma
- 18:15 Left for Greeley, CO
- 19:45 Arrived in Greeley, unloaded sleeping gear at Mark's Aunt Fluorine's house
- 20:15 Went to Coyote's Southwestern Grill for dinner
- 21:45 Stopped at Wal-Mart for personal supplies, then went to King Soopers for group groceries
- 23:15 Went back to Aunt Fluorine's and went to bed

### Site Descriptions:

The first stop was at Flagstaff Mountain just west of the National Center for Atmospheric Research (NCAR) facility in Boulder. Here we saw the Boulder fault, a 'Laramide age' thrust fault, Paleozoic-Mesozoic stratigraphic section, and spectacular flatirons – steeply sloping wedge-shaped features created by differential erosion of inclined rock layers. The exact age of the thrust faulting is difficult to assess because the youngest offset unit is the late Cretaceous Pierre Shale and the oldest undisturbed unit is the early Quaternary Rocky Flats Alluvium. This thrust dips 34 ° to the west and thrusts late Paleozoic rock over late Mesozoic along the eastern flank of the Front Range. Maximum displacement is determined to be 1.5 km at Flagstaff Mountain based on stratigraphic omission. The fault length is difficult to assess because the fault surface is untraceable in the Cretaceous shale north and south of the site. Depth at this location at the time of faulting is estimated to be less than 3.5 km based on the thickness of the stratigraphic section in the Denver Basin to the east of the Front Range.

At this location we also observed a sedimentary section comprised of rocks with ages spanning the Pennsylvanian to the Tertiary (Table 2). The flatirons (Figure 45) are formed of Pennsylvanian Fountain Formation (mostly arkose, coarse, feldspar-rich sandstone that is typically pink in color because of the abundant pink feldspar grains). The Fountain formation was uplifted and tilted to its present position during the Laramide uplift of the Rocky Mountains (68-40 Ma). A structural cross-section can be seen in Figure 46. The next stratigraphic unit in the cross-section is Permian Lyons formation, comprised mainly from aeolian sandstone. The stone used for many of the buildings on the University of Colorado campus was excavated from the Lyons Sandstone. The pink color of the Lyons Sandstone is caused by traces of iron oxide between the small grains of sand. The Cretaceous Dakota Sandstone, forming a hogback, has been extensively mined for fire clay and contains a third of the state's oil and gas deposits in the Denver Basin. You can see this formation at Echo Rocks, and by the water tank just west of NCAR. You can also hike over Dakota Ridge on the NCAR Trail (west of NCAR), the Red Rocks trails north of Canyon Blvd., and the Dakota Ridge Trail in north Boulder. The city of Boulder and NCAR are built on the Pierre Shale, a soft Cretaceous formation best seen in fresh roadcuts and ditches.

The second stop was at 'contact corner' to observe the contact between the Boulder Granodiorite and the Fountain Formation. The uplift of Ancestral Rocky Mountains exposed the Precambrian granodiorite and pegmatites and allowed for severe chemical weathering. This weathering formed a soil profile on the surface of the granodiorite, a process that is known as grussification, which can be observed along the Flagstaff Mountain road.

| INTERVALS OF TIME |               | MILLIONS OF YEARS AGO | FORMATION  | THICKNESS (FEET) | DESCRIPTION   | WEATHERING CHARACTERISTICS                     |
|-------------------|---------------|-----------------------|--|------------------|---|--|
| ERA               | PERIOD        |                       |  |                  |   |  |
| CENOZOIC          | QUATERNARY    | 2                     | NOT NAMED  | 0-25             | GRAVEL, SAND, SILT                                  | LOOSE  |
|                   | TERTIARY      |                       |  |                  |   |  |
| MESOZOIC          | CRETACEOUS    | 70                    | LARAMIE, FOX HILLS, PIERRE, MORA, BENTON, DAKOTA | 10,400           | GRAY TO TAN SHALES, SANDSTONES, LIMESTONES, FOSSILS | SANDSTONES STAND ON RIDGES, SHALE FORMS SLOPES |
|                   | JURASSIC      | 135                   | MORRISON   | 300              | SHALE TO SANDSTONE                                  | FORMS SLOPES                                   |
|                   | TRIASSIC      | 180                   | ENTRADA  | 30               | CROSS-BEDDED SANDSTONE                              | RESISTANT                                      |
|                   |               | 225                   | LYKINS   | 675              | RED SHALE, SILTSTONE SANDSTONE                      | SOFT, VALLEYS AND SLOPES                       |
|                   |               | 270                   | LYONS  | 220              | PINK SANDSTONE                                      | HARD RIDGES                                    |
| PALEOZOIC         | PENNSYLVANIAN | 270                   | FOUNTAIN   | 800              | RED SANDSTONES AND CONGLOMERATE                     | LOCALLY HARD RIDGES                            |
|                   | MISSISSIPPIAN | 305                   |  |                  |   |  |
|                   | DEVONIAN      | 350                   |  |                  |   |  |
|                   | SILURIAN      | 400                   |  |                  |   |  |
|                   | ORDOVICIAN    | 420                   |  |                  |   |  |
|                   | CAMBRIAN      | 500                   |  |                  |   |  |
|                   |               | 600                   |  |                  |   |  |
| PRECAMBRIAN       |               | 1700                  | IDAHO SPRINGS FM, BOULDER CREEK GR.              | UNKNOWN          | METAMORPHIC & IGNEOUS ROCKS                         | CRYSTALLINE, HARD                              |

APPROXIMATE AGE OF THE EARTH = 4.6 BILLION YEARS

Geologic and Stratigraphic Column for the Boulder Area (Based on Runnells, 1976)

**Table 2.** Chronostratigraphic column of the sedimentary rocks of the Boulder area. From: <http://bcn.boulder.co.us/basin/natural/geology/historic.html>



Figure 45. View of one of the Boulder Flations from the NCAR trail.

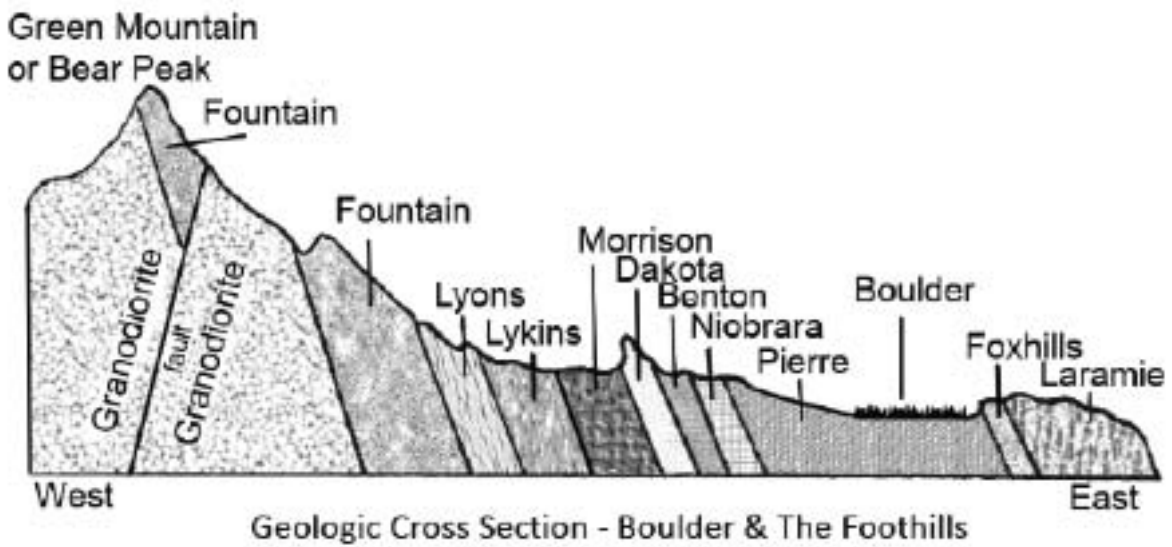


Figure 46. Geologic cross-section through the Front Range and Boulder Valley.  
[http://www.bouldercolorado.gov/index.php?option=com\\_content&view=article&id=2847&Itemid=1068](http://www.bouldercolorado.gov/index.php?option=com_content&view=article&id=2847&Itemid=1068)

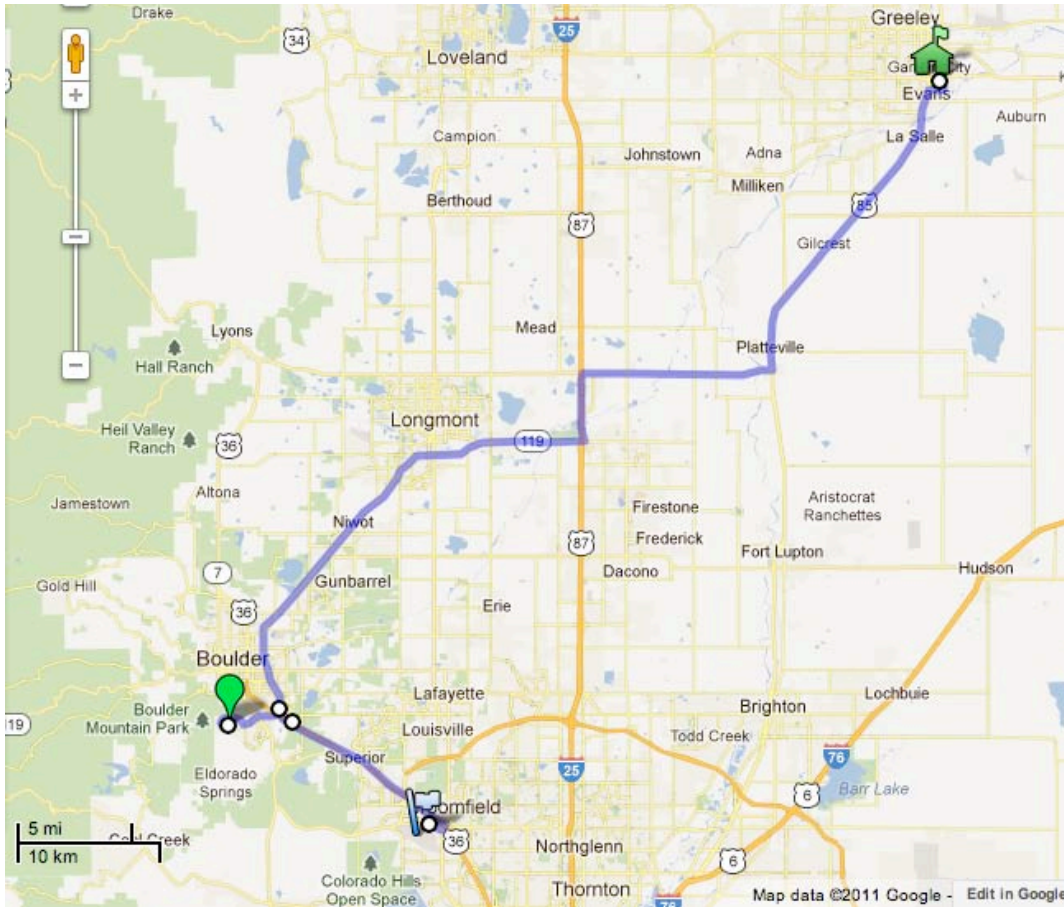


Figure 47. Map of the route for Day 1.

## Day 2 (June 26, 2011) – Wyoming Stratigraphy

*Contributed by Natalia Zakharova and Jason Jweda*

- 7:00 Woke up, breakfast
- 9:00 Left Greeley, CO (Aunt Fluorine's)
- 10:00 Rest stop at Cheyenne, WY
- 11:00 Stopped to observe Lincoln monument (west side of I-80 between Cheyenne and Laramie) – 13.5 feet tall bronze head of Abraham Lincoln atop of 30-foot high granite pedestal.  
Observed Elk Mountain, south of I-80.
- 12:00 Rest stop  
Drove along the axis of long anticline along I-80.
- 13:00 Stopped for lunch

Drove past Sinclair oil refinery, one of the largest high conversion refineries in the Rocky Mountain region, producing over two million gallons of products a day, including jet fuel for military, industrial and commercial applications.

- 14:00 Gas stop
- Drove through the continental divide
- 14:30 Stopped at Split rock rest area (in heavy rain with hail): observe basement granites and an early settlers' route in the Sweetwater River valley
- 15:30 Pulled out to look at the rim between Cretaceous and Tertiary rocks
- 16:00 Drove through Lander
- 16:10 Stopped to look at stratigraphic section from Achaean to Jurassic
- 16:35 Stopped to look at Pinedale and Bull Lake glacial deposits
- 16:45 Stopped at Sinks Canyon State Park to look at Sinks of the Popo Agie River
- 18:00 Stopped to look at exposed sections of the Chugwater and Nugget formations in Red Canyon
- 20:00 Arrived to Pinedale camp
- 22:00 Dinner

### Site Descriptions:

**Elk Mountain** – a mountain peak in the Snowy Range of the Medicine Bow Mountains that was formed during the Laramide Orogeny by thrust faulting along the Laramie thrust fault. The now exposed up-thrusted plate consists of Proterozoic granites capped by a resistant Proterozoic quartzite.



Figure 48. A view of Elk Mountain.

**Split Rock** – a landmark within the Granite Mountains, located along the valley of the Sweetwater River, that was used for navigation purposes by western-bound settlers. The distinctive “gun sight” notch of Split Rock (which we did not see due to the rain and hail) rises 1000 ft. in elevation and could be seen for 2 days by early settlers. The notch also pointed directly toward South Pass, ~75 miles to the west. Initially, the Sweetwater River valley

provided a route used by fur trappers, mountain men, and fur traders as they went to their annual summertime Rocky Mountain rendezvous, located usually somewhere along the Green River, Wyoming. These trappers and traders soon established a path for their pack trains along the Sweetwater and eventually cleared a rough wagon trail to the Green River. By 1843 the Sweetwater River valley was a regular wagon trail providing the water, grass and fuel needed on the Oregon, California and Mormon Trails across Wyoming.

**The Granite Mountains**, of which Split Rock is part of, were formed by the Laramide Orogeny and were once a much higher mountain range, similar to other mountain ranges in the state. The exposed range is formed of weathered Archean granite outcropping in characteristically rounded boulders that stand above light-colored, flat-lying Tertiary sedimentary rocks.



Figure 49. A view of the Granite Mountains.

### **Precambrian-Mesozoic stratigraphy**

Precambrian igneous and metamorphic rocks form the cores of the Wind River Range, Washakie Range, and Owl Creek Mountains. These rocks, which are widely exposed in the Wind River Range and in Wind River Canyon through the Owl Creek Mountains, are typically granite, granite gneiss, or schist, although locally mafic dikes are present. Paleozoic rocks are composed mostly of sandstone, shale, limestone, and dolomite, with some chert, formed by transgressions and regressions of an epicontinental sea. In the Late Paleozoic Period, phosphoric beds and gypsiferous shale also were deposited. Many of these rocks are cliff forming and are exposed in steep walled canyons of the Wind River Range and in Wind River Canyon. Permian Phosphoria (shallow-water limestone with rich organic content) is a source formation for oil-bearing Mesozoic sandstones. The Chugwater Formation and oil-bearing Nugget Sandstone represent Mesozoic rocks in this area. The Triassic Chugwater Formation primarily consists of red siltstone and sandstone, and is mapped across Wyoming, Montana, and Colorado. The Jurassic aged Nugget Sandstone is a texturally heterogeneous reservoir: predominantly eolian processes deposited cross-bedded, low-angle to horizontally bedded and rippled, very- fine- to coarse-grained sand in dunes, interdune areas, and associated environments. The Navajo Sandstone is the Nugget equivalent Mesozoic sandstone on the Colorado Plateau.



Figure 50. Mesozoic formations and recent alluvial formations in Red Canyon, Wyoming, on the eastern flank of the Wind River Mountains just south Lander. Prominent layers include: Chugwater Formation (thick red layers) and Nugget Sandstone (tan layers above).

**Pinedale and Bull Lake Glacial deposits:** There is evidence for two glaciations in the Wyoming area, the older and more extensive Bull Lake event (~150 kyr), and the more recent but less extensive Pinedale event (~110 kyr), which displaced many of the Bull Lake deposits. The two deposits are easily differentiated: the Bull Lake deposits are grussified, highly degraded and crumble when touched, appear reddish in the outcrops due to high Fe content, and have a thick soil layer at the top, whereas the Pinedale deposits look less weathered and have thin soil layers.

**Sinks Canyon State Park** is located 7 miles southwest of Lander, where the Middle Fork of the Popo Agie River comes out of the Wind River Mountains, and abruptly vanishes into a large cavern down canyon. The river later emerges in a large, calm pool on the other side of the canyon and then continues its course into the valley below. The lower portion of the canyon is made up primarily by Madison Limestone, a massive, off-white limestone formation that is very soft and soluble. The Sinks could have been formed along a pre-existing cavern or crack in the limestone, and/or carved by the river. The exact route of the underground passage is unknown, and dye tests have shown that the water takes over 2 hours to make the 1/4 mile journey between the Sinks and the Rise. Additionally, more water flows from the Rise than enters the cavern at the Sinks. The central mystery of “where does the water go for over two hours?” has yet to be solved. There could be a large underground aquifer or lake that slows the progress of the water, or there could be a myriad of channels and passages that the water has to circulate through before it reaches the Rise.



## Day 3 (June 27, 2011) – Wyoming-Idaho Thrust Belt

*Contributed by Anna Foster and Guleed Ali*

|             |  |
|-------------|--|
| 06:15       | Wake-up call   |
| 08:00       | Leave Pinedale Camp  |
| 08:20-08:55 | Stop 1: Fremont Lake   |
| 09:20       | Short stop at Ridley's Grocery for water, ice, etc.  |
| 10:05       | Stop 2: Roadside pull-off- view of the Gros Ventre Mountains   |
| 10:30-10:45 | Stop 3: Kozy Campground to see the Hoback Formation  |
| 10:55-11:10 | Stop 4: Roadside pull-off- duplex structures   |
| 11:15-13:00 | University of Michigan's Camp Davis- set up camp, lunch, and some downtime. Joined by Aaron, a former student of Mark Anders   |
| 13:35-13:45 | Gas stop   |
| 14:30-14:45 | Stop 5: Gros Ventre landslide  |
| 16:15-16:40 | Stop 6: Signal Mountain Overlook in Teton National Park  |
| 17:00-17:30 | Stop 7: Rockchuck Peak fault scarp   |
| 17:45-18:40 | Teton Park museum  |
| 18:50-19:35 | Stop 8: Jenny Lake, formed during the Pinedale glaciation, banked by a terminal moraine. This is now a popular and picturesque location for hiking.<br><br>Dinner at Snake River Brewery in Jackson Hole, returned to Camp Davis as each group finished, games available in Camp Davis rec room. |

### Site Descriptions:

#### Fremont Lake

Pinedale and the area surrounding Fremont Lake is the type locale for the Pinedale glacial deposits. The lake itself was carved by glaciers, and is the second-largest lake in Wyoming at 600 feet deep, 9 miles long, and 1 mile wide. Lateral moraines flank the north and west sides of the lake (Figure 53), with a terminal moraine to the south, and outwash ridges across the road to the east (Figure 54). Outwash ridges can be recognized by their terraced structures, although these have steep slopes from erosion.

The short walk to the top of the terminal moraine at the south shore of the lake offers a good vantage point. Bull lake deposits extend beyond the Pinedale to the south, with flat outwash plains in the distance. Oil and gas wells are abundant in the area. The Salt Range, a product of Laramide thrusting, can be seen to the southwest, with the Gros Ventre Range to the northwest and the Wind River Thrusts to the north and east.



Figure 53. Fremont Lake facing northeast, with Pinedale glacial till in the foreground. Lateral moraines visible on the north and west edges of the lake.

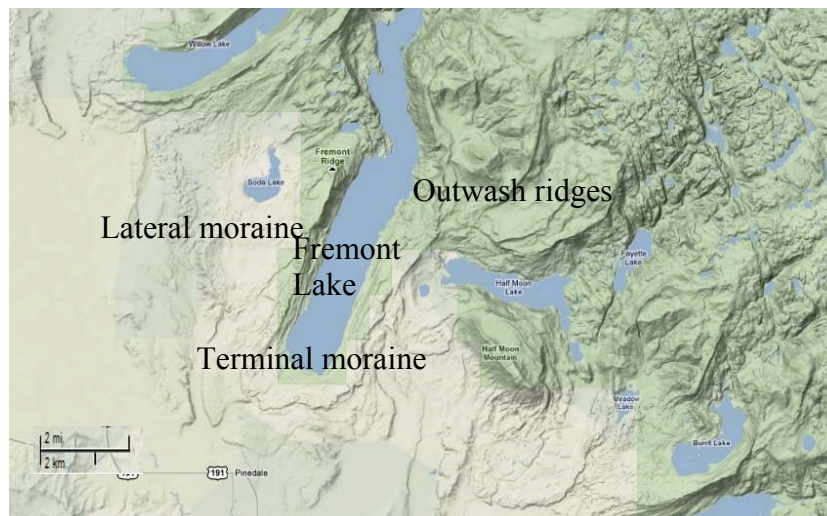


Figure 54. Map view of the area surrounding Fremont Lake. (Image from maps.google.com).

### **Gros Ventre Mountains**

The Gros Ventre range is an example of “pancake stratigraphy”, with mostly layered Paleozoic sediments that were tilted in the early Cenozoic. This range was uplifted by thrusting in the Laramide Orogeny. The folding related to these thrusts has formed what is called the ‘Flying Buttress’, a syncline between two strands of the range-bounding Cache Creek thrust (Nelson and Church, 1943). This syncline is clearly visible from the roadside stop (Figure 55).



Figure 55. Views of the Gros Ventre Range: Left, “Pancake” stratigraphy of the southeast slope of the Gros Ventre Range as seen from Fremont Lake, and Right, a syncline in the Gros Ventre Range on the southwest slope.

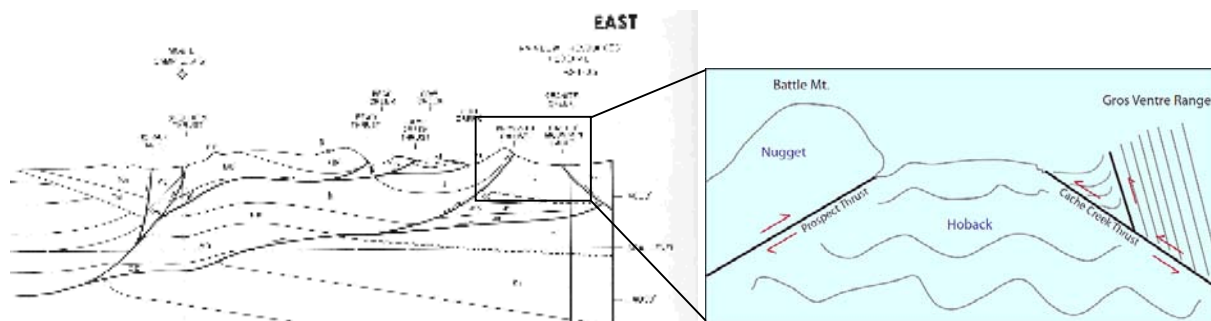


Figure 56. Schematic diagram of the Sevier thrusting, Hoback formation, and Laramide thrusting (Ore and Kopania, 1987).

**The Hoback Formation** is a highly deformed Paleocene-age foreland unit wedged between the youngest Sevier thrust to the west and the Laramide thrusting of the Gros Ventre viewed at the previous stop to the east. The leading edge of the Sevier Orogeny is the Prospect Thrust, the hanging wall of which is the Jurassic-aged Nugget formation, the footwall of which is the Hoback formation, and which had top-to-the-east motion. The hanging wall has been eroded by glaciation, leaving the klippe now known as Battle Mountain. On the eastern side of the Hoback formation is the Laramide-age Cache Creek Thrust, which forms the basal thrust of the syncline seen in the Gros Ventre. The cross section and relevant fault system can be seen in Figure 56.

**Duplex Structures** are features that commonly occur in a fault ramp (when a fault cuts up-section). This creates slivers of rock bounded by faults called horses. This geometry results in several fault strands that eventually sole back in to the main fault (Figure 57). At this location, duplex structures are seen in the Madison Limestone.

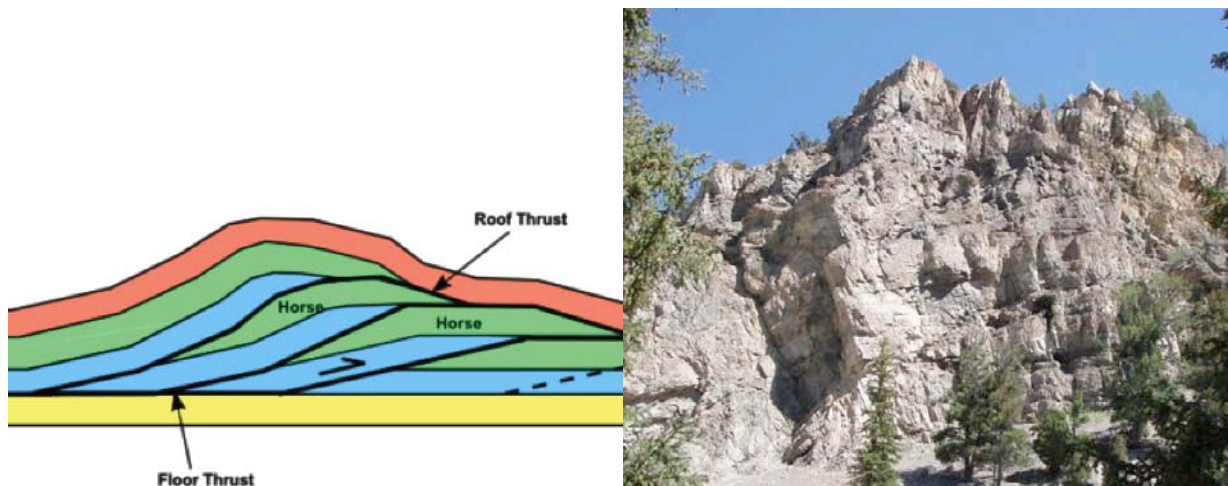


Figure 57. Duplex structures: left, schematic of duplex structures ([http://www.qwiki.com/q/?\\_escaped\\_fragment=/Horse\\_%28geology%29](http://www.qwiki.com/q/?_escaped_fragment=/Horse_%28geology%29)); right, a view of duplex structures observed at the roadside pull-off in the Hoback Canyon.

**The Gros Ventre Landslide** occurred on June 23<sup>rd</sup>, 1925 on the north slope of Sheep Mountain. The “pancake” layers of this range are tilted at steep angles. This structure, compounded with heavy rains and snowmelt, allowed slip along a bedding plane in the Tensleep Formation. The landslide moved all of the overlying Tensleep formation as well as some of the Chugwater Fm. Rock and debris behaved as a granular flow, traveling down the valley and up the opposite slope. This debris dammed the Gros Ventre River at the base of the valley. This natural dam, which was deemed structurally sound, burst two years later on May 1927, causing catastrophic flooding in the nearby towns of Kelly and Wilson. ([www.wyomingtalesandtrails.com/tetons3.html](http://www.wyomingtalesandtrails.com/tetons3.html)). The landslide scarp is still clearly visible (Figure 58).



Figure 58. Scarp from the 1925 Gros Ventre landslide.

**Signal Mountain** is a small peak made of volcanic ash and glacial moraine. The summit allows a view of the Teton Range and Snake River (Figure 59). It is relevant to the discussion of the age of the Teton Range, which can be determined using the age and tilt of ash layers, and underscores the seismic hazards in the Teton area. Ash layers are always deposited horizontally; any tilting must have occurred after deposition. The Teton Range is formed by normal faulting, so as the range rises, the basin in which the ash is deposited goes down. The closer to the fault it is, the more the basin drops, resulting in layers tilting towards the range (Figure 60). Ash layers dated at 6 and 10 Ma are parallel, indicating no motion on the fault during that time span. Another ash layer on the far side of the Tetons is dated at 4 Ma and is also parallel to the 6 and 10 Ma ash layers. However, a 2 Ma ash layer has a smaller dip, indicating that motion took place between 2-4 Ma (Anders, 1994). This means that the Tetons are uplifting at a very rapid rate, estimated to be 2 mm/yr, with all motion occurring approximately within the last 3 Ma.



Figure 59. Views from Signal Mountain overlook: left, view of Snake River (facing southeast), right, view of the Teton Range (facing southwest).

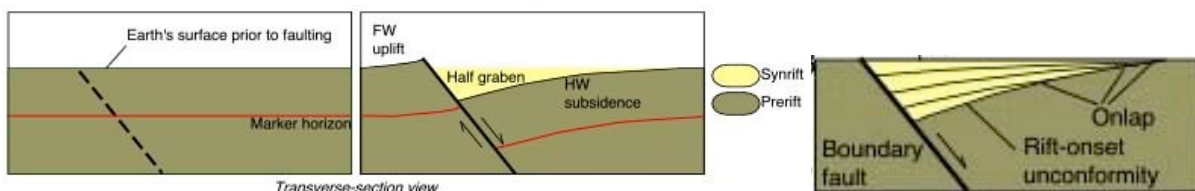


Figure 60. Schematic diagram of fanning layers due to normal faulting, as occurred in the basin adjacent to the Teton Range. This is used in combination with ash-layer dating to determine the timing of uplift (<http://www.ldeo.columbia.edu/~polsen/nbcp/breakupintro.html>).

### Rockchuck Peak Fault Scarp

The rapid rate of uplift of the Teton Range increases the likelihood of large earthquakes. The dangers of this are illustrated by the visible fault scarp on Rockchuck Peak (Figure 61). This fault scarp is approximately 60 feet high, and motion likely occurred around 15,000 years ago. Microearthquake locations extend down to 15 km depth, indicating that the fault has potential for up to a magnitude 7.5 earthquake.

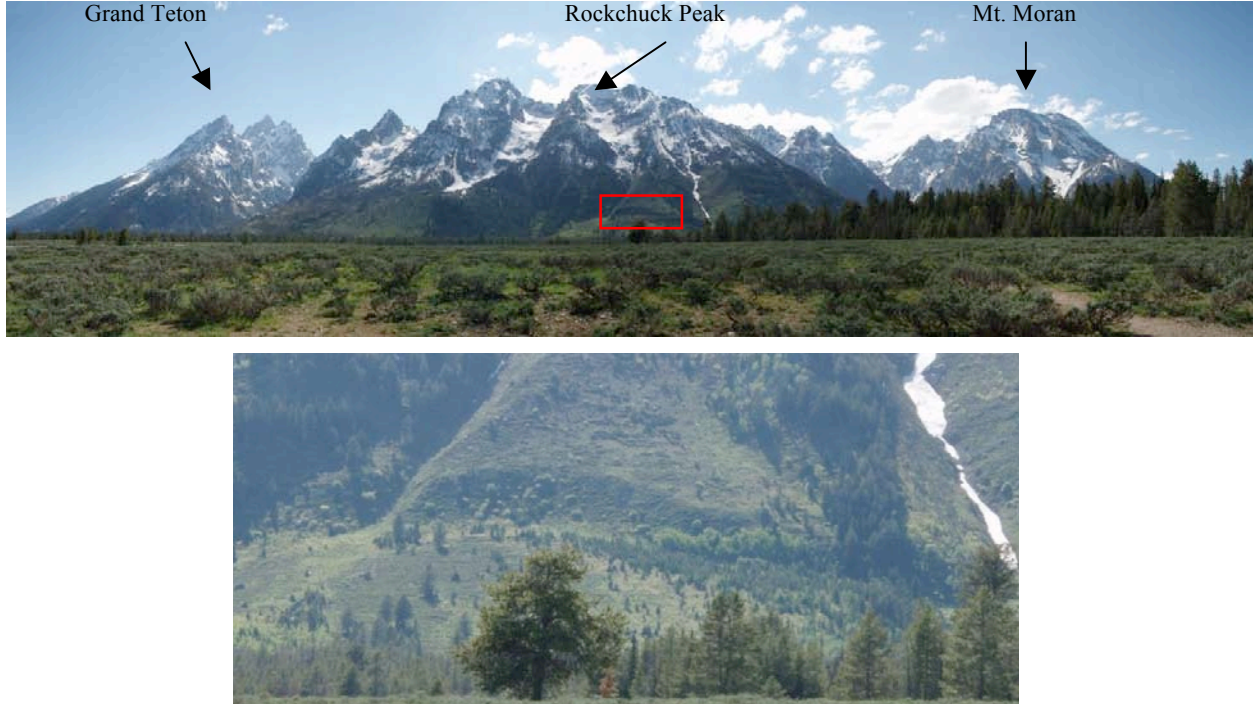


Figure 61. Teton range, with visible fault scarp near the base of Rockchuck Peak.

#### References

- Anders, M.H., Constraints on North American plate velocity using the Yellowstone hotspot deformation field. *Nature*, v 369, p 53-55.
- Dorr Jr., J.A., Spearing, D.R., Steidtmann, J.R., Wiltschko, D.V., and Craddock, J.P., Hoback River Canyon, central western Wyoming. *GSA Centennial Field Guide—Rocky Mountain Section*, 1987.
- Nelson, V.E. and Church, V., Critical structures of the Gros Ventre and Northern Hoback Ranges, Wyoming. *Journal of Geology*, Vol 51, No 3, 1943.
- Ore, H.T., and Kopania, A.A, Idaho-Wyoming thrust belt: Teton Pass, Hoback Canyon, Snake River Canyon. *GSA Centennial Field Guide- Rocky Mountain Section*, 1987.

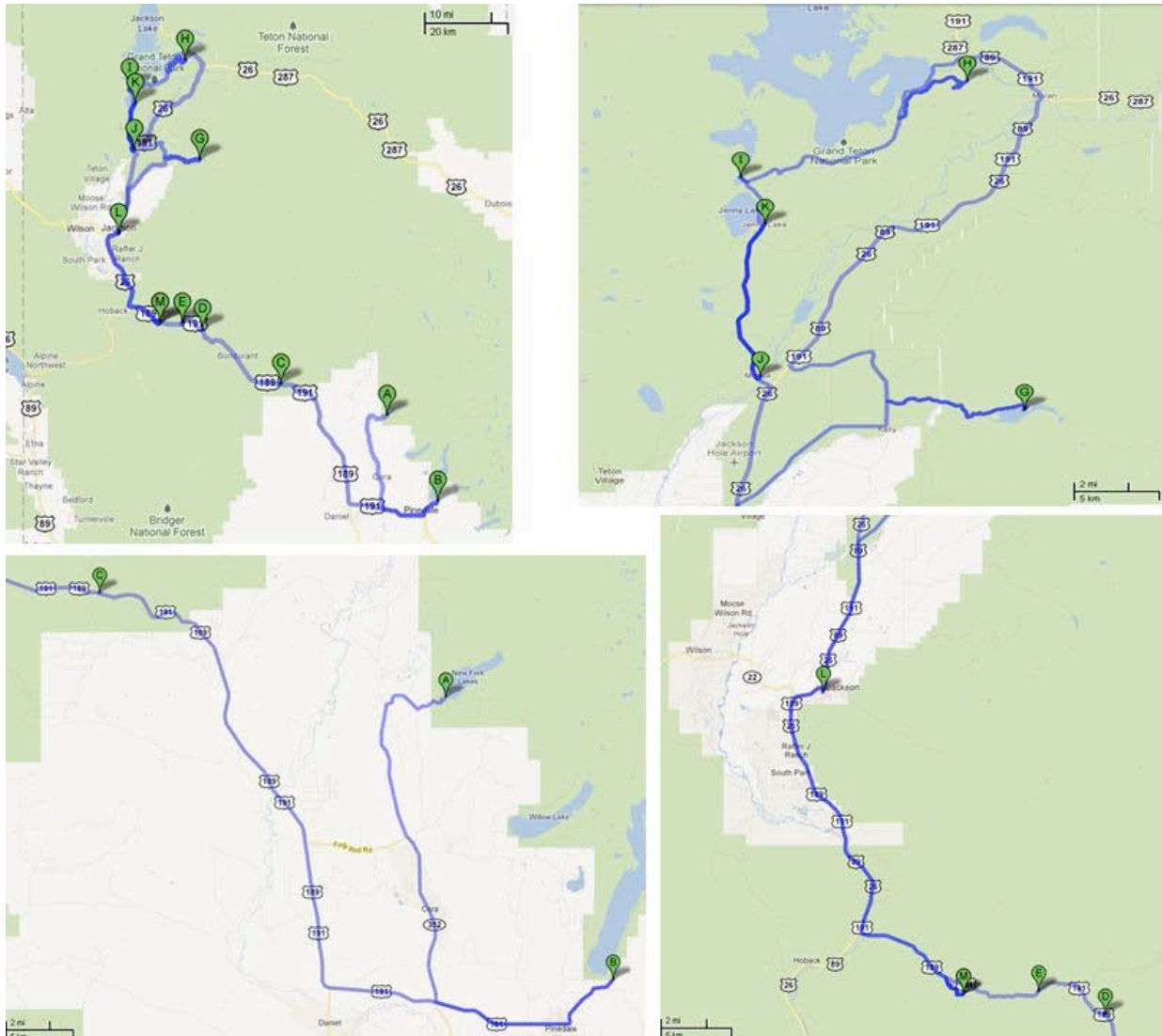


Figure 62. Map of all stops for Day 3. Top left shows full route, with close ups on right and bottom. (Images from maps.google.com). Stops are: A- New Forks Lake Campsite; B- Fremont Lake; C- Gros Ventre Pull-off; D- Kozy Campground/Hoback Formation; E- Duplex structures pull-off; F- Camp Davis; G- Gros Ventre Landslide; H- Signal Mountain; I- Rockchuck Peak fault scarp; J- Teton Park museum; K- Jenny Lake; L- Snake River Brewery; M- Camp Davis.

## Day 4 (June 28, 2011) – Teton National Park

*Contributed by John Templeton and Jason Jweda*

- 9:00 Leave Camp Davis for Teton Village
- 9:30 Board Teton tram, ride to the top.
- 9:45 - 13:00 Hike around snowy Teton highlands (Stop #1)
- 13:00 Return to Teton Village on tram
- 13:15 -14:30 Picnic lunch around Teton Village
- 15:00 Grocery stop in Jackson
- 16:00 Drive south following Hwy 26/89 along Snake River, through Snake River canyon, stopping near Hoback to view the Darby thrust (Stop #2 and #3)
- 18:00 Stop at east end of E 4<sup>th</sup> Ave, Afton, ID to see active fault scarp (Stop #4)
- 19:00 Camp at the Palisades Reservoir NFS campground in Alpine, WY

### Site Descriptions:

**Teton Village** offers tram rides to Rendezvous Mountain Peak (Figure 63). From the peak, the views to the north and west show Precambrian crystalline basement rocks overlain by Paleozoic sediments (Table 3). The basement rocks were uplifted during the Laramide Orogeny (as part of the Gros Ventre-Teton uplift) on structures related to the Buck Mountain and the Cache Creek thrust faults. This uplift verges to the southwest and reactivation along the same faults during recent (late Cenozoic to present) normal faulting has uplifted the basement as much as ~7 km above the basement rocks not involved in Laramide thrusting; the Teton-Gros Ventre uplift meets the Sevier deformation front just south of the Teton range.



Figure 63. Teton Village Tram with Rendervous Mountain Peak in the background.

**Table 3. Paleozoic Stratigraphy.**

| <b>Formation Name</b> | <b>Age</b>                                    | <b>Description</b>  | <b>Thick-<br/>ness<br/>(m)</b> |
|-----------------------|---|---|--------------------------------|
| Madison Limestone     | Mississippian, Mm                             | fossiliferous, thinly bedded blue-gray limestone with sparse, very thin shale layers  | 350                            |
| Darby Formation       | Devonian, Dd                                  | thinly bedded gray and buff dolomite, with interbeds of gray, yellow and black shale. Some fossils.   | 110                            |
| Bighorn Dolomite      | Ordovician, Ob                                | thin beds of blue gray or brown dolomite, weathering white, capped by ~10m or white dolomite at the top (Leigh Member). Few fossils.  | 145                            |
| Gallatin Limestone    | Cambrian Cg                                   | Mottled blue-gray limestone   | 58                             |
| Gros Ventre Formation | Cambrian Cgd, Cgf                             | <i>Park Shale Mbr</i> : upper member; grey-green shale with beds of limestone conglomerate  | 67                             |
|                       |   | <i>Death Canyon Mbr</i> : two thick blue-grey limestone beds separated by 5m of (locally fossiliferous) shale, representing deepening of ocean and clearing of water, followed by short-lived shoreline retreat and deposition of shale bed followed by return to deep water limestone. | 87                             |
|                       |   | <i>Wolsey Shale Mbr</i> : greenish gray shale with purple and green sandstone at base. Mudcracks from brief subaerial exposure in tidal flats. Some brachiopods and trilobite fossils.  | 30                             |
| Flathead Sandstone    | Cambrian, Cf                                  | Brown, maroon and white sandstone, locally containing pebbles of quartz and feldspar. Mid-Cambrian (~510 ma) transgressive sandstone unit, representing first phase of passive margin deposition on the continental basement rocks  |                                |
| Precambrian basement  | Archean and Late Proterozoic (0.765 – 2.6 Ga) | crystalline rocks: granite, gneiss, and pegmatite   |                                |



Figure 64. The Teton Range, as viewed from the top of the tram near Rendezvous Peak (looking north).

### **Sevier-aged thrusts in the Snake River Canyon**

Exposures in the canyon show the Absaroka and Darby thrust faults that outcrop in the Snake River Canyon along Hwy 89. These thrust faults place older Paleozoic rocks on top of younger Mesozoic age rocks. At the first stop just to the west of Hoback, we could see that the upper plate of the Darby fault, composed of the Permian Phosphoria Formation, was thrust over the Jurassic Twin Creek limestone. The contact surface was difficult to identify because the rocks on the hill slope were bunched up. The Darby Thrust is the younger of the two thrust faults, and the upper plate of the Darby is actually the lower plate of the Absaroka thrust. At the second stop (boat ramp) further west, we could identify the Absaroka Thrust fault which thrust Mississippian Madison limestone (upper plate) over Cretaceous strata.

### **Active fault scarp**

At the east end of 4<sup>th</sup> Ave in Afton, the road dead-ends at a steep 10 m scarp, and a driveway climbs up the scarp to the south to a small house sitting on the top of the scarp (Figure 65). This scarp is related to the last movement on the range-bounding fault along the east side of Star Valley. There were well-developed diamond facets on the range front along the east side of the valley, indicative of active faulting. Diamond facets develop on a range front when the active faulting outpaces the ability of surface processes to erode the range front and wear it down.



Figure 65. Active fault scarp in Afton.

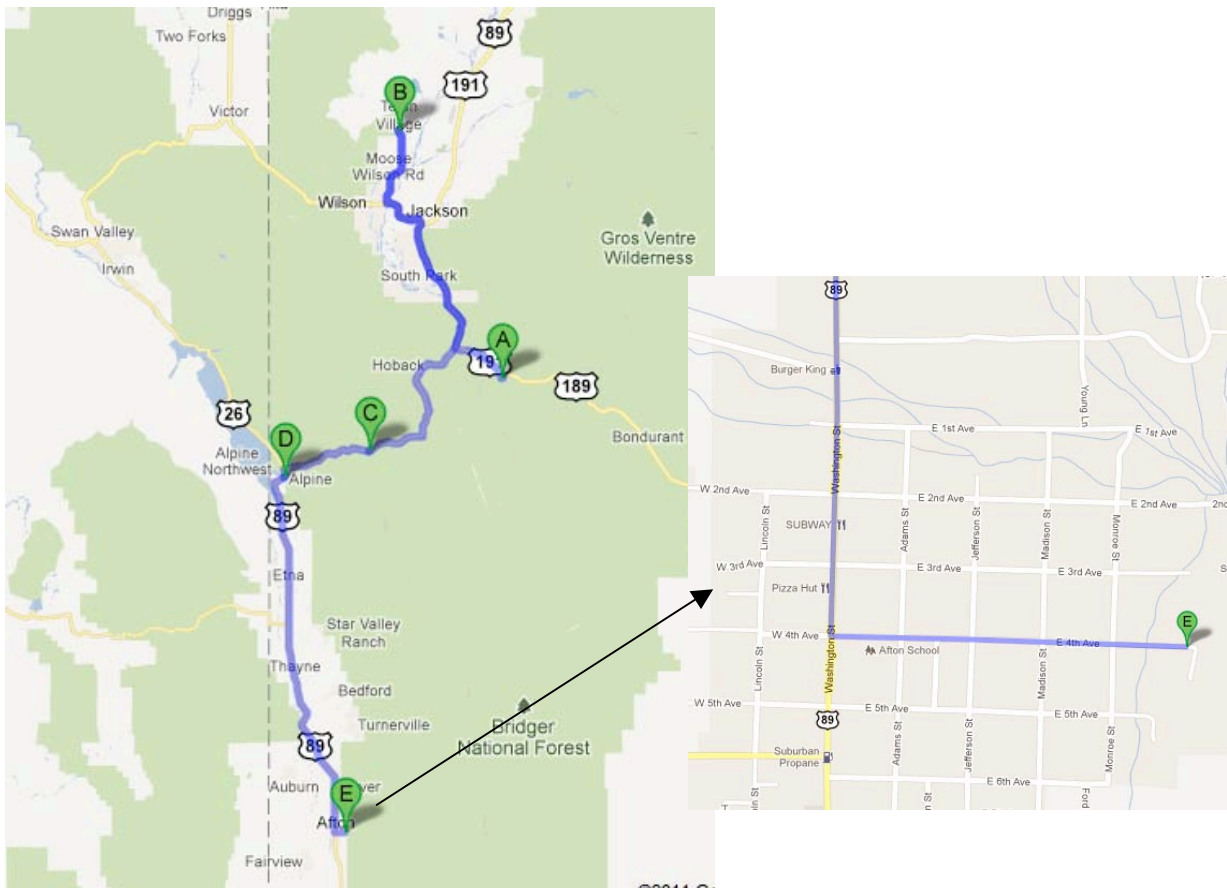


Figure 66. Map of the route for Day 4. A: Camp Davis. B: Teton Village tram, stop #1. C: Snake River Canyon, stops #2 and #3. D: Palisades Reservoir NFS campground in Alpine, WY. E: Active fault scarp, stop #4 with detailed street plan of Afton, ID.

## Day 5 (June 29, 2011) – Yellowstone Hotspot Volcanics

*Contributed by Ellen Crapster-Pregont and Ge Jin*

- 6:30 Wakeup, breakfast, break camp
- 7:45 Leave Alpine Campground
- 7:59-8:12 Stop 1: Star Valley – loading due to successive volcanic flow deposits
- 8:30-8:40 Stop 2: Primary ash fall of 4.45Ma Yellowstone eruption
- 8:50-9:20 Stop 3: Andesite stock and sill
- 9:32-10:05 Stop 4: Slide block of Gros Ventre limestone
- 10:18-10:34 Stop 5: Block flow basalt
- 10:34-11:05 Stop 6: Palagonite and loess
- 11:30 Stop 7: Clark Hill rest stop; Scale of caldera associated with 4.5Ma eruption
- 12:07 Stop 8: Ash flow tuff
- 16:55-17:00 Stop 9: Madison Range, terraces
- 17:05-17:10 Stop 10: Landslide associated with 1959 earthquake
- 17:19-17:46 Stop 11: Fault scarps associated with 1959 earthquake
- 19:00 Dinner at Old Faithful Lodge, Yellowstone National Park
- 19:40 Stop 12: viewing of Old Faithful Geyser eruption
- 20:00 Drive to Grant Village Campground \* (~45 minute drive)

\*showers available (\$2.00 in quarters for 6 minutes of warm water) from 7:00am to 9:30pm

### Site Descriptions:

#### Stop 1: Star Valley, Wyoming (Palisades Reservoir along Rt. 26, mile stone 398)

Located southwest of the Tetons, Star Valley is an extensional feature formed due to normal faulting associated with the Yellowstone Hotspot. Subsequent loading of basaltic material from volcanic eruptions caused additional basin depression. At this roadside location you are able to see slide blocks and debris / ash flows. Pumice and obsidian can be seen in hand-samples and there is some coherency in the material. These flows were initiated by faulting events and traveled 5-6 km from the basin front within ~1 Ma.

#### Stop 2: Primary ash fall (Big Elk creek, turn right at mile stone 292 on route 26)

Primary ash fall deposit from the 4.54Ma Yellowstone eruption that outcrops 75-100 km from its source (Figure 67). The ash is incompletely lithified and friable. Small, black obsidian balls are visible in hand-samples. The deposit experienced some reworking by wind and exhibits some layering. Magnetic field polarity was preserved in magnetic mineral phases, specifically magnetite, indicating that the temperature of the fallout material was less than 573°C. The thickness of this ash layer is about 7m, and it dips 26° to the north.



Figure 67. Ash deposits from the 4.54 Ma Yellowstone eruption.

**Stop 3: Andesite stock and sill (Calamity Dam Recreation Area)**

The andesitic stock and sill are visible in an outcrop across from and in a roadcut nearby. It is the only known outcrop of andesitic material associated with the Yellowstone volcanics suite, which everywhere else consists of basalts and rhyolites. The intrusions were emplaced 6 Ma ago and the outcrop exhibits hyperbyssal flow (shallow intrusion) indicating near surface cooling. Radiation from the Yellowstone hotspot head or tail could have initiated crustal melting resulting in parent magma for this andesite. This region was once included in the Yellowstone parabola of death (rate of motion 2.2-2.3 cm/yr, which is similar to the velocity of the North American Plate) but is no longer active. Instead, deformation is related to acceleration in basin and range extension based on the change in slope of the deposits as illustrated in Figure 68.

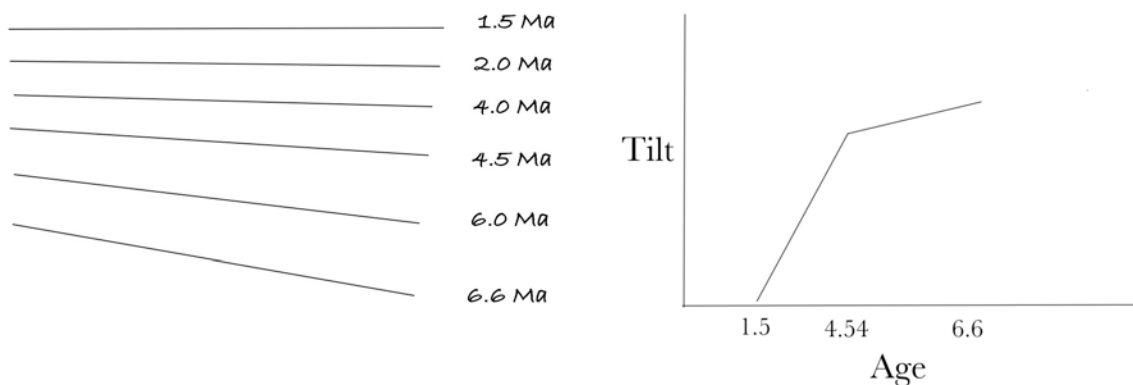


Figure 68. Slope of the deposits and tilt rate illustration.

**Stop 4: Slide block of Gros Ventre limestone** (About 282 mi of Rt 26, Cross-section of Old Irwin Rd and Palisades CR Rd)

After carefully climbing the steep talus-covered slope, we maneuvered so that small groups of students (~5) could sit or crouch beneath the overhanging block of Gros Ventre limestone (Figure 69). We carefully examined the rock face looking for the base of the slide block. There was a distinct gravel zone in which the movement of the overlying material was accommodated. The bottom portion is normally graded (large material under smaller material) while the top portion is reverse graded, with a thin layer of wood at the interface. This indicates the likely presence of fluidized material at the base lowering the coefficient of friction thus, facilitating low angle sliding. A low coefficient of friction will also increase the size or mass of the resulting landslide. This slide block was transported to its current location between 2 and 5 Ma before additional tilting.



Figure 69. Gros Ventre limestone slide block (right) with a detailed view of the basal layer (right).

**Stop 5: Block flow basalt** (Beside Rt 26 around milestone 272)

A basaltic lava flow that remained fluid in the interior of the flow, but became quite viscous near the edges toward the center and top portions which fractured and broke apart as cooling proceeded. The underlying lava remained hotter and less viscous, thus preventing rapid crystallization and preserving elongate vesicles and an intact flow.

**Stop 6: Palagonite and loess** (Intersection of Stagecoach Rd and Rt 26)

Another boot-wearing roadcut climb to an outcrop of palagonite with overlying

loess deposits. The palagonite formed  $\sim 1.5$  Ma by an eruption of basaltic lava from a spatter cone into an area surrounded by water (pyroclasts have an altered glassy texture). Layers (and a stream channel) within the palagonite deposit contain lava fragments and other lithics from near the basaltic source that are now altered and exhibit cross-bedding. Subaqueous conditions are corroborated by the presence of pillow basalts on the opposite side of the road (Figure 70), indicating that the Snake River Plain was a lake at the time of the palagonite eruption. The lake was formed by the lava flow blocking the Snake River. The loess deposits, which are extremely fine-grained wind-blown material glacial powder, are associated with both the Pinedale and Bull Lake glacial deposits. Both of these loess deposits are fertile, and the Bull Lake can be differentiated (from the Pinedale) because it has coarser material and caliche crusts. These two different glacial deposits were formed at  $\sim 15$  ka and  $\sim 125$  ka, respectively. The two deposits are separated by a thin soil horizon.



Figure 70. Examples of Yellowstone volcanics: Palagonite deposits (top), pillow basalt with orange palagonite crust (left), and loess deposits (right).

**Stop 7: Yellowstone 4.5Ma caldera scale** (Beside Rt 26, Clark Hill rest stop)

This highway rest stop affords an overlook of the 4.5Ma Yellowstone caldera and Snake River basalt flows.

**Stop 8: Ash flow tuff** (Ririe Dam and Reservoir)

This stop consists of an extensive roadcut outcrop of the Huckleberry Ridge formation (both the A and B eruption units are observable) with ash flow tuffs containing obsidian clasts, sanidine, and lithic fragments. Ar dating of the sanidine gives a 2.059Ma age to the deposit. The tuff sits on top of a basal surge deposit that was laid down prior to the ash as material was pushed ahead of the flow. Part way down the gavel road a degassing tube within the tuff was preserved. There is an erosional surface and conglomerate deposit stratigraphically below the Huckleberry Ridge Tuff that cuts stream channels in the underlying Heise Tuff. The Heise Tuff, related to the 4.5 Ma eruption, is visible below the conglomerate layer. This deposit has a basal vitrophyre, a super-compacted ash that is essentially glass, and a reddish colored baked zone in underlying older eruptive deposits. Another loosely compacted conglomerate layer separates the Heise Tuff from the older Wolverine Tuff. The Wolverine Tuff (6Ma) contains pumice and obsidian balls and is significantly reworked. Numerous small scale normal faults can be identified within this unit.

**Stop 9: Madison Range, terraces** (Intersection of Rt 87 and Rt 287)

A quick roadside stop to view spectacular examples of ‘diamond’ facets (also known as triangular facets), which are erosional features along currently inactive faults that have been cut by rapid fluvial erosion as illustrated by the schematic (Figure 71).



Figure 71. Diamond facets of the Madison Range: a photograph of the diamond facets (left) and a schematic illustration (right).

**Stop 10: 1959 landslide** (About 5 min east of the last stop)

Catastrophic landslide triggered in 1959 by a 7.9 earthquake on a normal fault near Hebgen Lake, Montana. This landslide was notable because it buried a portion of the Rock Creek public campground (killing 28 people) located on the Madison River. The material slide down into the valley and up the other side and dammed the river, creating Earthquake Lake. Eventually, the Army Corps cut a channel through the deposit to drain part of the lake to prevent catastrophic flooding (as had happened with the Gros Ventre Slide).



Figure 72. Consequences of 1959 earthquake: Catastrophic landslide produced by the 1959 earthquake (left) and a 1959 fault scarp at Hebgen lake campsite (right).

**Stop 11: 1959 earthquake fault scarp (Hebgen Lake)**

The 1959 earthquake had a 15 km focal depth and produced two high angle ( $50^\circ$ ) ruptures. This site documents the sudden formation of the visible fault scarp, which has a 2 m vertical relief. There is a short trail along the scarp toward the creek that suddenly ends due to a rupture barrier. Within 200 m, the slip decreased from 7 m to 0 m.

**Stop 12: Old Faithful Geyser (Yellowstone National Park)**

Old Faithful is one of the most viewed features in Yellowstone National Park and one of the most regularly erupting geysers in the world (Figure 73). With a chance every  $\sim 1.5$  hours to observe this geologic phenomena, it is a spectacular end to a long day of driving and a good preview of the geologic wonders Yellowstone has to offer.



Figure 73. Eruption of the Old Faithful Geyser in Yellowstone National Park.

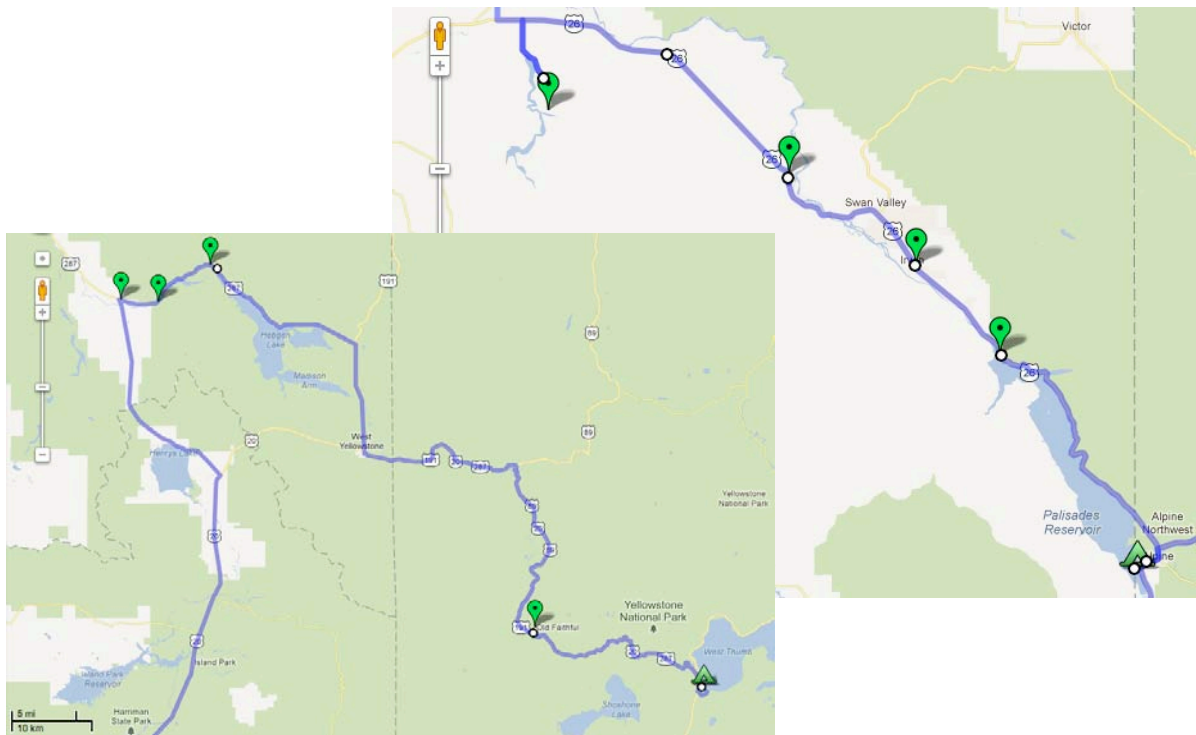


Figure 74. Maps of the route for Day 5: Alpine campground and major stops on Route 26 made in the morning (top), and 1959 earthquake features and Yellowstone Park covered in the afternoon (bottom).

## Day 6 (June 30, 2011) – Yellowstone National Park

*Contributed by Amelia Paukert*

- 6:45 Wake up call
- 6:50 Group drove over to showers (open at 7 am and there's a line already)
- 7:20 Went back to camp and packed up tents
- 8:20 Drove to Lake Lodge
- 9:00 Breakfast at lodge
- 10:15 Left for Mud Volcanoes and drove along Yellowstone River
- 10:30 Arrived at Mud Volcanoes and did walking loop
- 11:15 Finished walking loop and had lecture from Mark about the Sour Creek Dome magma chamber
- 11:45 Drove to Artist Point near Canyon Village
- 12:15 Arrived at Artist Point, walked out to the point and discussed the progression of colors in the hydrothermal alteration series
- 13:05 Drove to Norris Geyser Basin
- 13:25 Arrived at the Norris Geyser Basin, walked the Back Basin short loop
- 14:15 Drove to Norris Picnic Area (<5 min. away) and had lunch
- 15:15 Drove to Obsidian Cliff
- 15:30 Arrived at Obsidian Cliff but trail was closed
- 15:55 Left for Mammoth Hot Springs
- 16:15 Arrived Mammoth Hot Springs and walked down to Canary Spring, then down toward the Mound and Jupiter Terraces.
- 17:15 Left Mammoth Hot Springs
- 17:30 Stopped for gas at Mammoth Village
- 17:45 Left for Tower Falls
- 18:05 Arrived at Tower Falls and admired the columnar jointing (both on the east and west sides of the road)
- 18:15 Left for Hunter Peak Campground in Wyoming.
- 19:05 Stopped just outside of the north entrance to the park to look at the Heart Mountain Detachment – the largest terrestrial landslide.
- 19:15 Continued on toward campground
- 19:45 Arrived at Hunter Peak campground and quickly set up tents (mosquitoes were atrocious!)

- 20:00 Drove to Cooke City-Silver Gate
- 20:30 Arrived in Cooke City and had dinner at 9:30 pm. Played pool and foosball.
- 23:00 Drove back to campground
- 23:30 Arrived at campground and went to bed

### Site Descriptions:

**Mud Volcano** is located in the Sour Creek Dome area. There is an abundance of pungent smells from the sulphur emitted by the mud pots and mud volcanoes. The area consists of spectacular examples of mudpots and mud volcanoes oozing with boiling, burping slurries of acidic mud produced by acidic breakdown of volcanic ashes and rhyolites below (Figure 75).

Volcanic rocks in the area have olivine  $^3\text{He}/^4\text{He}_{\text{RA}}$  ratios as high as 16, which are high and indicate a deep, undegassed mantle source. The magma chamber below Yellowstone caldera is 30 km wide and 10 km long, but is mostly crystalline mush. A Yellowstone eruption may release  $\sim 1,000 \text{ km}^3$  of rhyolitic lava. About 4% of the volcanics in Yellowstone is basalt. High density basaltic material rises to neutral buoyancy in the crust and ponds at a depth of  $\sim 5 \text{ km}$  beneath the surface. The basalt ( $1300^\circ\text{C}$ ) is several hundred degrees warmer than the melting point of rhyolite ( $900^\circ\text{C}$ ), so it assimilates the overlying crust, resulting in Sr, Nd, and Pb ratios characteristic of the older continental crust. The overall thermal anomaly extends northwest. The Snake River Plain geothermal flow is on the order of  $100\text{-}200 \text{ mW/m}^2$  compared to  $\sim 40 \text{ mW/M}^2$  of normal continents.



Figure 75. Mud volcano in Yellowstone National Park.

**Artist Point** exhibits a deep canyon cut in multi-color formations made up of rhyolite flows (Figure 76). Different colors come from a temperature-dependent hydrothermal alteration. The spectacular canyon was formed in the last 15 ka due to the retreat of the Pinedale Glaciers. At this point, we discussed the effect of high silica content and volatiles on magma characteristics, and talked about three ways for an explosion – exsolution of volatiles due to cooling, magma injection or removal of overburden.



Figure 76. Artist Point, Yellowstone National Park.

### **Obsidian Cliff**

Obsidian was deposited in layers alternating with rhyolite. The lack of crystal structure in obsidian is explained as much by flow shear while cooling as rapid cooling rate. Numerous spherulites are observed in the outcrop. They represent devitrification structures with feldspars growing outward in concentric circles, and are common in rhyolite ash and flow deposits.

**Mammoth Hot Springs** - is a large terrace complex of hot springs on a hill of travertine (Figure 77) in Yellowstone National Park adjacent to Fort Yellowstone and the Mammoth Hot Springs Historic District. It was created over thousands of years as hot water from the springs cooled and deposited calcium carbonate (over two tons flow into Mammoth each day in solution). The water originates from a hydrothermal chamber up through the Madison Limestone. Although these springs lie outside the caldera boundary, their energy has been attributed to the same magmatic system that fuels other Yellowstone geothermal areas.



Figure 77. Travertine terraces at Canary Spring, Yellowstone National Park.

### **Tower Falls**

Spectacular columnar jointing in basalt is seen right in the road wall. The Pre-Huckleberry Ridge basalt flow dates from 2.2 Ma and exhibits thick entablature and narrow basal colonnade (Figure 78). Entablature structures formed by competing slower cooling from the bottom and from the top where meteoric and river water seeped into the flow. Two other columnar basalts (Post-Huckleberry Ridge) are seen across the river dating back to 1.3 Ma. Basalt layer are separated by glacial outwash from around 1.2 Ma.



Figure 78. Pre-Huckleberry Ridge columnar basalt.

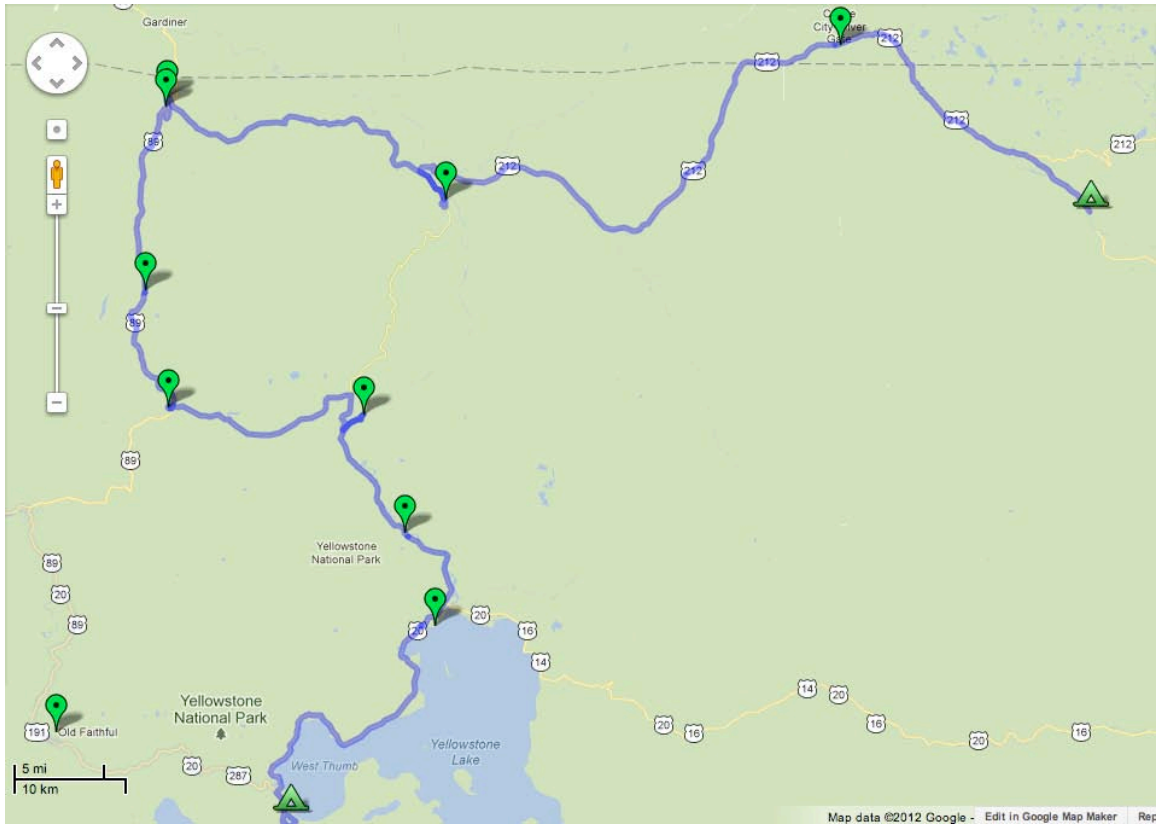


Figure 79. Map of the route for Day 6.

## Day 7 (July 1, 2011) – Stillwater mine and Heart Mountain Detachment

*Contributed by Yang Zha and Julius Busecke*

- 6:30 Wakeup, breakfast, break camp
- 7:45 Left Hunter Peak campground
- 08:25 Stopped at overlook on US 212 Highway to observe Heart Mountain detachment
- 08:55 Stopped at Beartooth Pass. The pass is at an altitude of 10,947 ft. The fine weather allowed us to see the massive dimensions of the Heart Mountain detachment.
- 11:10 Arrived at Stillwater Complex in Stillwater Mining Company, located in Nye, MT and met Geologist Mike Koski from the mining company who gave an introduction of the surrounding geology and mining operations, followed by a tour through of some of the facilities
- 12:55 Drove uphill through the abandoned mining area to see the Banded Series

- 13:08 Continued driving uphill into the Gabbro Zone to look at the layered intrusion more closely. Thin-layers are believed to have formed within one flow. It's not fully understood how the banding was formed. Some work suggests magma chamber scale pressure variations.
- 13:55 Continued driving uphill via narrow dirt road until end of road; arrived at a chromite tailings and spread out to pick hand samples
- 15:00 Stopped for lunch at an abandoned mining village, roamed around
- 17:00 Left the Stillwater mine complex
- 18:30 Snowball fight on top of Beartooth Pass
- 19:30 Returned to camp and had dinner

### Site Descriptions:

**Beartooth pass** has an altitude of 10,947 ft and offers spectacular views of the Beartooth Mountain Range, the Beartooth thrust and the Heart Mountain detachment. The fine weather allowed us to see the massive dimensions of the Heart Mountain detachment, which is the largest known terrestrial landslide in the world. The upper block covered over 3400 km<sup>2</sup>, and the landslide happened on a slope of only 2 degrees for over 50 km. The detachment happened about 50 Ma ago, as part of Laramide. Beartooth thrust is also of Laramide age, overturning Paleozoic sediments.



Figure 80. Beartooth Pass Panorama.



Figure 81. One of the 'bear's teeth' in the Beartooth Mountains.

The **Stillwater complex** is an Archean age (2.72 Ga) layered igneous intrusion. The large fossil magma chamber is exposed across ~30 miles of the north flank of the Beartooth Mountain range near Nye, Montana. It has extensive reserves of chromium ore and unique PGEs (platinum group elements) content with a very high palladium to platinum ratio. The main mining layers are the basal zone, ultra-mafic zone, and the banded series containing the J-M reef rich in PGEs. The J-M reef is the source of the world's highest grade Pd ore.



Figure 82. Banded Series outcrop (left) with a zoomed-in picture of the igneous stratification (right).



Figure 83. Stillwater mining facilities (left) and an abandoned mining village on the property (right).

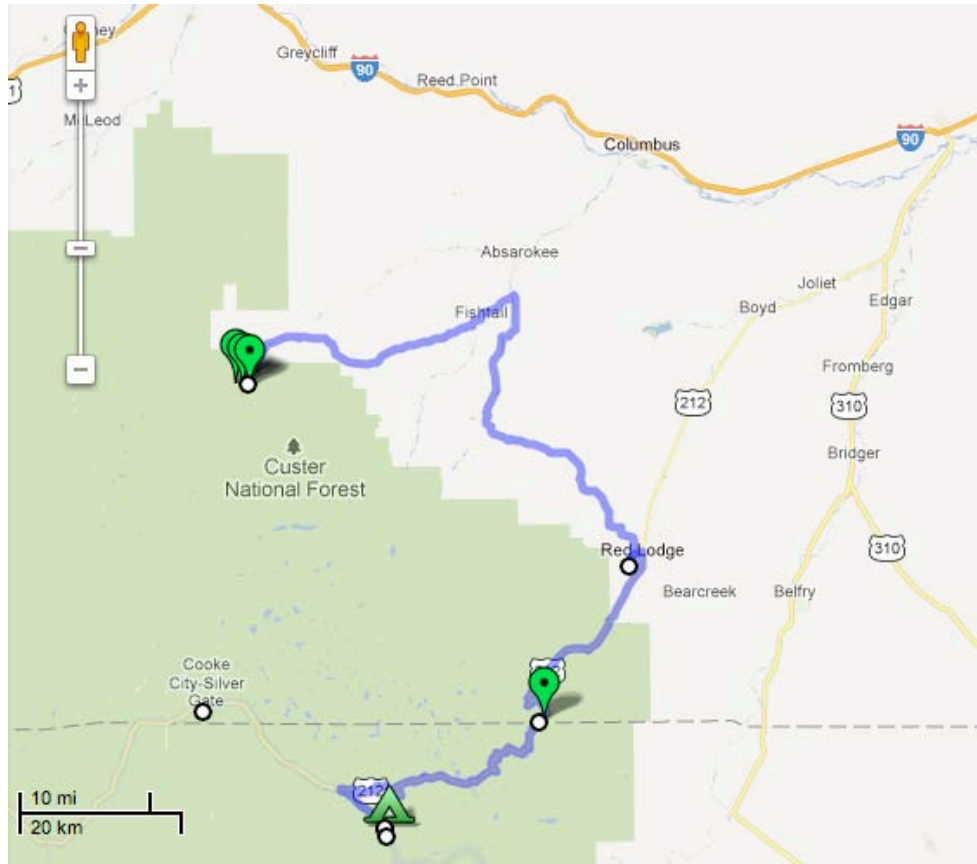


Figure 84. Map of the route for Day 7.

## Day 8 (July 2, 2011) – Heart Mountain Detachment

*Contributed by Michael Wolovick and Rafael Almeida*

- 8:10 Leave camp and drive to Cathedral Cliffs
- 8:25 Cathedral Cliffs overview
- 9:10 Stop at bottom of Sunlight Canyon (Sunlight Bridge scenic stop)
- 9:50 White Mountain overview
- 11:30 Dead Indian Pass overview
- 12:15 Stop on abandoned field road to observe at the Bighorn Mtns.
- 1:00 Lunch at Buffalo Bill State Park
- 2:10 Leave the picnic area and drive toward the Bighorn Mtns.
- 3:45 Rest stop along US-14 near the South Bighorn County Airport and observed doubly plunging anticlines (Sheep Mtn.)
- 5:15 Arrived at Bighorn Mountains Campground (past Shell Falls), set up camp, cooked dinner, and played card games

## Site Descriptions:

The **Heart Mountain Detachment (HMD)** is a colossal landslide (slide length ~100 km) around 50 Ma, and its mechanism is still debated. Geologic observations suggest that initially the slide broke on a single bedding plane within the Bighorn Dolomite, but subsequently cut up-section. The break was only a few meters above the bottom of the formation, which overlies a shale layer, but the break never took advantage of the shale layer. The slide surface had a low slope probably  $<2^\circ$  (max  $5^\circ$ ), and must have had a very low friction coefficient ( $<0.1$ ). There was no deformation in the lower plate when the slide was along the single bedding plane but the basal layer (upon which the sliding occurred) has graded bedding and flute casts, and it feeds clastic dykes in the upper plate. These observations support the hypothesis that the basal zone was pressurized by  $\text{CO}_2$  from the dolomite. The deformation occurred in the lower plate when the slide cut up-section (anisotropy in rheology matters!). The upper plate experienced longitudinal extension (“like an accordion”). Volcanic breccia pipes and other volcanic features associated with the upper plate seem to imply a volcanic trigger for the slide.

A) The town of **Silver Gate** can be reached after driving less than a mile from Yellowstone National Park’s Northeast Entrance. From here you can walk to Soda Butte Creek on the south side of town and, still looking south, see the Breakaway Fault of the Heart Mountain Detachment towards the south. North of fault “b” in Figure 85, the full pre-detachment stratigraphic column is observed.



Figure 85. A panoramic view of the Heart Mountain Detachment at Soda Butte near Silver Gate.

B) **Cathedral Cliffs:** From Silver Gate, we drove east on Route 212 for ~ 17 miles until we reached the junction with Chief Joseph Highway, at which point we turned right (south direction) and continued for 11 miles. There was a road on the right (just past a lake) that we turned right onto and then continued for ~ 1 mile. A panoramic view of the detachment is seen in Figure 86 below. The black vertical stripes are mafic dikes going through the upper plate of the HMD. They go through the Paleozoic section, and belong to the Crandall Valley volcanic center (associated with the Absaroka volcanics). These dikes predate the HMD and are cut by it. The cliff forming unit beneath the detachment level is the Pilgrim Limestone of Cambrian age (~ 35 m thick). Above this layer there is a talus forming argillite unit and the orange ledge which corresponds to the basal 2-3 m of the Bighorn Dolomite, above which the HMD is located.



Figure 86. Cathedral cliffs: panoramic view (left) and a close view of dykes in the upper plate (right). Most of what is visible here is Bighorn Dolomite in the upper plate. The strata in the lower left corner on the left picture are close to the detachment.

C) **White Mountain:** There is an outcrop of the detachment halfway up the hillside, close to where the detachment cuts up-section (Figure 87). Here we can observe a layer of “cement” that was produced by the super-heating of the carbonate rocks during the HMD emplacement. The Paleozoic carbonate rocks above the HMD detachment have been metamorphosed to marble in this outcrop. Microbreccia clastic dykes extend up to 100m into the upper plate while the basal microbreccia layer is only ~1 m thick (Figure 88). A clastic dike can be seen as a diffuse sub-vertical area of darker color in the hillside (Figure 87c). The basal layer is graded, has flute casts, round features that are analogous to ooids, which suggest fluidization of the layer. Quartzite in the lower plate does not contain microcracks, suggesting lack of the process zone found at slowly propagating fault tips. Where the detachment cuts up-section, it contains a “bowling ball breccia”: large rounded clasts in both the basal zone and the lower plate, with pieces of the lower plate incorporated into the “bowling ball breccia”.

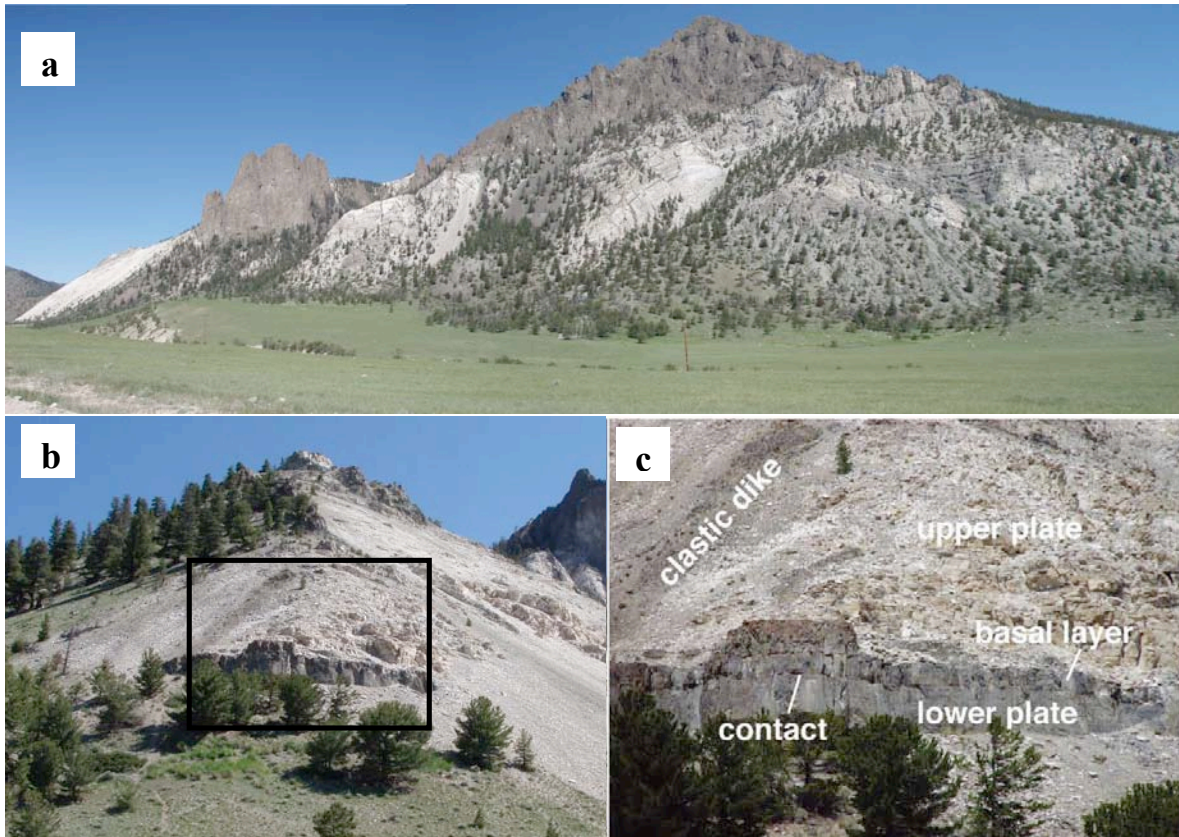


Figure 87. White Mountain: a - panoramic view; b and c – zoomed in view of the detachment area. The lower plate, upper plate, HMD contact, basal layer, and clastic dike are labeled in (c).



Figure 88. View of basal microbreccia layer with Julius Busecke for scale with the contact near his head (left). Detailed view of microbreccia (right). The block in the center of the image is a single fused piece of microbreccia.

D) **Sunlight Bridge** – Great Unconformity: There is a rest stop on the south side of the bridge. Here the Great Unconformity between Archean igneous/metamorphic basement rocks and Cambrian sediments can be observed. The Cambrian Flathead sandstone shows an abundance of sedimentary structures, such as ripples and cross bedding (Figure 89).



Figure 89. Archean granites (left) and Flathead sandstone (right).

D) **Dead Indian Pass**: There is a scenic road-stop at the top of the pass. From here a regional perspective of several parts of the HMD can be seen (Figure 90). The lower plate rocks (which are part of the Tensleep Fm.) here are completely brecciated due to the HMD emplacement (Figure 90). An example of this can be seen in a quartzite outcrop where the rocks have been brecciated forming bowling-ball size “clasts” in the outcrop. On the drive to Cody, WY after this stop, you will drive by Heart Mountain, where the Paleozoic section has been emplaced over Eocene sediments. Dead Indian Hill represents the ramp up of the HMD unto the Laramide monocline, which is inferred by the brecciated lower plate.



Figure 90. Dead Indian Pass: view from the summit (left) (White Mountain can be seen in the upper left side of the photograph, and brecciated Tensleep Sandstone (lower plate) with John Templeton for scale (right).

E) **Rattlesnake Mt:** Rattlesnake Mountain is the largest and most well exposed of the secondary basement-involved thrusts in the region. It is a NW trending feature of approximately 27 km in length. On the drive to Buffalo Bill reservoir you will pass through a tunnel bored through the basement rocks that form the core of this Laramide-style uplift. The road follows the steep forelimb of this fault-propagation anticline, formed by a Paleozoic and Mesozoic section that dips between  $45^\circ$  SW to overturned. The backlimb dips  $12^\circ$ - $15^\circ$  NE.



Figure 91. A fault -propagation anticline: map view of the location of the fault-propagation anticline with respect to Cody (left) and view of the forelimb towards the NW (right).

F) **Sheep Mt:** This is another example of an anticline associated with Laramide age deformation. This feature was produced by a secondary thrust off the Rio Thrust on the western flank of the Big Horn Mountain uplift. This mountain is dissected by a railroad cut which allows the internal geometry of the fold to be readily observed. The exposed section ranges in age from the Mississippian Madison Limestone to the Triassic Chugwater Formation. The forelimb is near vertical and is located on the NE flank of the mountain. The backlimb is relatively steep and dips towards the SW. There is an access roads marked by a dashed yellow line in Figure 92.



Figure 92. A view of the forelimb of Sheep Mountain anticline.

**G) Devils Kitchen:** This exposure of rocks is part of the Cloverly formation, a million year old sequence of sediments containing dinosaur tracks and fossil remains. For example, gastroliths and dinosaur footprints have been found in this formation. The soft colorful sandstone and shales of the Cloverly Formation form a badlands landscape of isolated spires and weathered hills (Figure 93). This rock formation also contains the fossilized remains of *Deinonychus*, a velociraptor.



Figure 93. View of the Cloverly formation at Devil's Kitchen.

**H) Bighorn Mts – Shell Canyon – Campground:** The Bighorn Mountains are a more or less continuous chain of mountains (formed during the Laramide) that sweep in a great arc (concave to the west) from southern Montana, around the Bighorn Basin, and then westward toward the Owl Creek Mountains. The highest and most rugged part of this arc lies west of the town of Buffalo, where the Bighorn Mountain front rises abruptly above the Powder River Basin on the east and culminates in the spectacular summit of Cloud Peak (elevation 13,166 feet). This mountain range contains Archean granitic and metamorphic rocks in its core, forming an extensive high, rolling, relatively flat sub-summit surface; steeply dipping or overturned Paleozoic and Mesozoic rocks are found on the eastern and western flanks (Figure 94). The western flank of the Bighorn Mountains is equally impressive: major highways cut through the mountain front in spectacular canyons such as Shell Canyon and Tensleep Canyon.

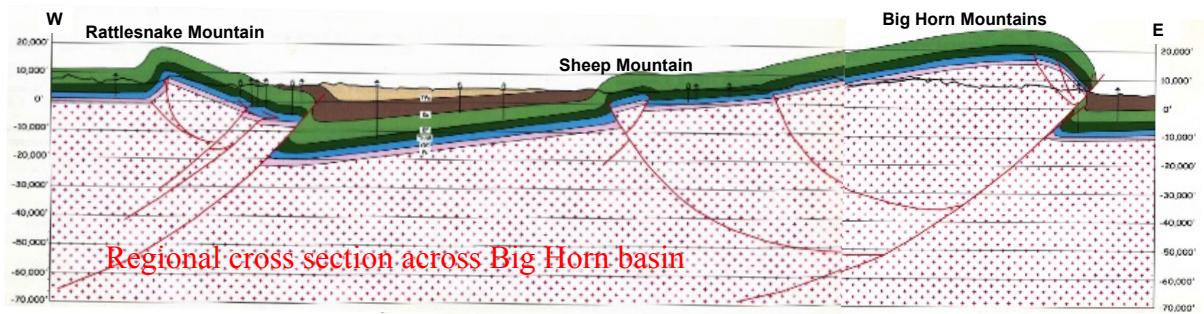


Figure 94. Big Horn Mountains: panoramic view (top) and geologic cross-section (bottom).



Figure 95. Map of the route for Day 8 (detailed views of the outline regions provided below).

1



2



3



Figure 96. Detailed views of the route.

## Day 9 (July 3, 2011) – Shell Falls and Red Gulch Dinosaur Tracks

*Contributed by Claire Bendersky and Natalia Zakharova*

- 7:00 Wake up
- 8:00 Breakfast
- 9:00 Leave campsite
- 9:05 Arrive at Shell Falls Interpretive Center in Shell Canyon and walk around
- 9:30 Roadside glimpse of Elephant rock and Copman's Tomb. Elephant rock is an eye-catching monocline that formed from thrust faulting in lower units (Gros Ventre) and propagated as a fold in the upper units (Madison).
- 9:45 Car and human refueling at Dirty Anne's Country Store.
- 10:15 Explore dinosaur tracks at the Red Gulch Dinosaur Tracksite hosted by the Bureau of Land Management. Check out the "ballroom" site where 125 dinosaur tracks have been documented with footprints that range from 9 cm to 20 cm!
- 13:00 Drive through Wind River Canyon.
- 14:00 Lunch just South of Wind River Canyon. Wind River Canon lies in the Owl Creek Range. It is bounded by an anti-curvilinear thrust fault. The 3D geometry is such that a normal fault is expressed at the surface to fill a gap created by thrust faulting.
- 20:00 Arrive at Aunt Flourine's house and have dinner.

### Site Descriptions:

**Shell Falls** are located in the Shell Canyon, a few miles east of Shell Wyoming and 14 miles east of Greybull. There is a small roadside interpretive center along highway 14 from which one can view the falls (Figure 97). The Shell Canyon is cut into the 2.9 billion year old granite, exposed in the Big Horn Mountains by Laramide uplift (started ~60 Ma) and subsequent erosion. This gray and pink granite is among the oldest rock on earth. Resting on the granites, Cambrian flathead sandstone (~550 Ma old) contains some of the earliest fossils of hard shelled creatures, giving the canyon and the falls their names. The falls are 120 ft in height, and water is falling at the rate of ~ 3,600 gallons per second, following the course of fractures in the resistant granite. Younger sedimentary rocks outcrop in the flanks of the Big Horns, and can be seen along the road in the area.



Figure 97. Shell Falls (left) and a fold within the Big Horn Mountains called Elephant Rock (right).

**Red Gulch Dinosaur Tracksite** is the largest track site in Wyoming and one of only a few worldwide from the Middle Jurassic (160-180 Ma). It is located on a byway along western slopes of the Big Horns, a few miles from Shell and Greybull, WY. The site contains over 1,000 fossil footprints imprinted in Jurassic Sundance formation (Figure 98), a green-gray shaley limestone layer formed on the ancient shoreline of the Sundance Sea, and they are attributed to a large and diverse group of dinosaurs. All the tracks identified so far were formed by two-legged (bipedal) dinosaurs. Some of the tracks appear to have been made by meat-eating dinosaurs (theropods). They weighed between 15-400 pounds. Because Middle Jurassic dinosaurs are so rare, it is very difficult to match the tracks to any particular dinosaur. Typically, a well-preserved theropod dinosaur track is three-toed and nearly symmetrical, exhibits tapering toes and preserves a slightly “S” shaped impression of the middle toe. Identifiable theropod trackways preserve prints that are slightly “pigeon-toed” having an inward rotation of the feet. However, many other tracks and trackways do not exhibit such features. Although clearly made by two-legged dinosaurs, these less well-defined prints may have been made by a different type of dinosaur such as a plant-eating ornithomimid. In many cases, it is impossible to identify the trackmaker as to ornithomimid or theropod. Interestingly, most of the identifiable trackways go in the same south-southwesterly direction. This could indicate herding or migratory animal behavior, or presence of a physically constrained pathway (such as a tidal flat or beach next to an open body of water). One interpretation would be that the dinosaurs might have been moving parallel to the shoreline. However, the shape and direction of ripples indicate that relatively deeper water conditions existed to the southwest. Therefore, it appears that dinosaurs were moving perpendicular to the shoreline and not parallel, so they were likely moving toward the water.

The tracks were preserved through a combination of biological and physical processes. The dinosaurs walked in limy mud held together by a film of algae that stabilized the tracks. The dry, hot air caused the surface to dry rapidly, forming salt crystals in the track layer. Subsequently, rising sea levels buried them with another layer of mud. The age of the tracks is believed to be 167 Ma. This was determined by dating a

volcanic ash layer just above the track-bearing surface, and by the paleontological evidence from fossil oysters (*Gryphaea*) and ammonites.



Figure 98. A dinosaur's footprint at Red Gulch Dinosaur Tracksite.

## **Acknowledgments**

We would like to acknowledge the Storke Memorial Fund that made this trip possible, and to thank Professor Steve Goldstein and Professor David Walker for accepting the trip proposal. We are very grateful to the trip leader Professor Mark Anders for expert guidance in the field and limitless scientific insights into geologic history and structure of the Western US. Mark's extensive field experience and superb knowledge of the area were invaluable at all stages of the trip planning and execution. Special thanks also go to our student leaders: Rafael Almeida, Anna Foster and Amelia Paukert for preparing the proposal and for organizing the trip. A million thanks go to Mark's Aunt Fluorine whose warm hospitality in hosting us for two nights at her house was truly admirable. We also thank Mike Koski from Stillwater mine for an insightful tour of the complex, and Jill VanTongeren for helping to organize it. Finally, many thanks go to all participants of the trip, and especially for all drivers, for making our Wyoming field trip a fun and interesting experience.

## **Appendix 1. Trip Participants.**

Mark Anders, *Associate Professor, Lamont-Doherty Earth Observatory*  
*PhD students, Department of Earth and Environmental Sciences:*

Guleed Ali

Rafael Almeida

Claire Bendersky

Julius Busecke

Ellen Crapster-Pregont

Cathleen Doherty

Anna Foster

Ge Jin

Jason Jweda

Alexander Lloyd

Pritwiraj Moulik

Amelia Paukert

John Tempelton

Marc Vankeuren

Jill VanTongeren

Michael Wolovick

Yang Zha

Natalia Zakharova

## Appendix 2. Trip costs.

|                        |                    |
|------------------------|--------------------|
| Airfare                | \$6,726.80         |
| Airport Trans          | \$246.80           |
| Van Rentals            | \$3,220.99         |
| Gasoline               | \$2,005.43         |
| Food                   | \$1,451.83         |
| Lodging                | \$479.16           |
| Miscellaneous          | \$1,138.56         |
| <b>TOTAL COST</b>      | <b>\$15,269.57</b> |
| Students contribution  | -\$4,800.00        |
| <b>TOTAL DEES COST</b> | <b>\$10,469.57</b> |